AMERICAN UNIVERSITY OF BEIRUT

UNRAVELING THE MOLECULAR SIGNATURE OF *BCR-ABL*^{P210} AND *BCR-ABL*^{T315I} *IN* THE *DROSOPHILA MELANOGASTER* CML MODEL

by
AMRO SALIM BAASSIRI

A dissertation
submitted in partial fulfillment of the requirements
for the degree of Doctor of Philosophy
to the Department of Anatomy, Cell Biology and Physiological Sciences
of the Faculty of Medicine
at the American University of Beirut

Beirut, Lebanon
September 2022

AMERICAN UNIVERSITY OF BEIRUT

UNRAVELING THE MOLECULAR SIGNATURE OF *BCR-ABL*^{P210} AND *BCR-ABL*^{T315I} *IN* THE *DROSOPHILA MELANOGASTER* CML MODEL

by
AMRO SALIM BAASSIRI

Approved by:

Dr. Rihab Nasr, Professor ______________________
Department of Anatomy, Cell Biology and Physiological Sciences Advisor

Dr. Nadine Darwiche, Professor ______________________
Chair of Committee

Dr. Margret Shirinian, Assistant Professor ______________________
Co-Advisor

Dr. Elias Rahal, Associate Professor ______________________
Member of Committee

Dr. Laure El Chami, Associate Professor ______________________
Member of Committee

Dr. Ehab Atallah, Professor ______________________
Member of Committee

Date of dissertation defense: SEPTEMBER 2, 2022

AMERICAN UNIVERSITY OF BEIRUT

DISSERTATION RELEASE FORM

Student Name: ___BAASSIRI________AMRO______ SALIM__________
Last First Middle

I authorize the American University of Beirut, to: (a) reproduce hard or electronic copies of my dissertation; (b) include such copies in the archives and digital repositories of the University; and (c) make freely available such copies to third parties for research or educational purposes:

☐ As of the date of submission

☐ One year from the date of submission of my dissertation.

☐ Two years from the date of submission of my dissertation.

✓ Three years from the date of submission of my dissertation.

_Amro Baassiri______________September 15, 2022_______________

Signature Date

ACKNOWLEDGEMENTS

I dedicate this work to my two angels; my angel in the sky, my dad, and my angel on Earth, my mom. No words will ever do you justice for the amount of love and support you have provided me with throughout the years. I owe you everything. I would like to thank my brother as well, Abdul Rahman, for being a steadfast constant in my life offering much love and support. I love you all with every fiber of my being. Thank you!

Dr. Rihab Nasr, I daresay that you have been a motherly figure to me throughout this journey. This journey started even before joining your lab but since our work in Amalouna years prior. It has been my utmost privilege to have been under your tutelage. You have been a role model wherein I have learned what it means to be a great scientist and still be more humble than ever. Your thirst for knowledge and love for science is contagious and I will take with me wherever I go the memories of the most riveting and exhilarating scientific discussions I've ever had. Moreover, many may know you as a great scientist, but I've been lucky to have met the great human that you are. Thank you for being "human"! You have a bright mind but also a radiant heart of gold. Thank you!

Dr. Margret Shirinian, with open arms you have welcomed me and introduced me to a whole new dimension of this scientific world, the *Drosophila*. I would like to thank you for the guidance, support, and most importantly your patience in unraveling this model to me. Once more, I have been lucky throughout my life to meet genuine, warm, and kind-hearted people and you are a further testament of that. Thank you for all the times you have been understanding throughout these rough times. You have been a constant force pushing me forward in spite of everything and for that I am truly thankful. Thank you!

Ali Ghais, you have been a great companion and I am genuinely glad to have worked along your side. This work is the fruit of your work just as much as it is mine. It is our work. I am very proud of the growth that you have had as a scientist. I have also learned a lot from you as well through your inquisitive nature which took us into some fascinating and fervent scientific discussions. Moreover, I believe that with your assiduous nature and keen mind that you will do great things as a future physician and scientist. Keep that fire alive. Thank you!

Abdallah Kurdi, single-handedly and in a brief amount of time, you have enriched my journey through meeting the amazing human being that you are and you augmented my scientific knowledge Log2FC. I will never be able to thank you enough for guiding me through the world of bioinformatics which is undoubtedly the future of science. Our interaction is proof that it's not necessarily the amount of time you spend with someone to leave an impact on others but by the quality of time spent. The scientific discussions we had were the most thrilling of all, since you opened my eyes to the spellbinding potential of bioinformatics. If it were up to me, some discussions could have continued for hours on end without feeling the passage of time. Thank you!

My dear lab family (Dr. Nasr and Dr. Shirinian Lab members), if I want to thank each and every one of you, then I would have to type out an entire thesis on this matter alone. Even if I do not name you one by one, know that each one of you has a dear place in my heart. It is one thing to love what you do, but it means a whole lot more when you love the people you work, eat, and hangout with. You were the light throughout the dark and the beacon of hope at every downfall. I will never forget your support and love. I am thrilled to see your bright futures and marvelous journeys that are about to unfold. Our story does not end with my PhD journey. We are friends for life and our paths will cross again soon because there are a lot of places to travel and things to discover in this lifetime and the only way to do this right is by your side. Thank you!

My PhD partners in crime, we are undoubtedly, statistically significant with a p-value of <0.0001, the BEST PhD gang to EVER exist. I am so blessed and grateful to have you as my PhD family. The memories, laughter, and love that we shared are beyond what words can describe. My love for you can never be contained within my physical being. Thus, I will keep sharing some of it around with others everywhere I go because I would like to propagate that happy feeling I get whenever you cross my mind. Thank you!

Dr. Nadine Darwiche, I would like to end this section with you because you truly have been with me on this journey from the very beginning since my undergraduate studies and it would only be appropriate to end this journey with you. I remember that day in our genetics course class when you introduced to us Gleevec. You were filled with excitement since you understood the implications of such a drug and how it can transform people’s lives. Your enthusiasm was contagious and that drive is still motivating me to this day. Is it a coincidence that I ended up working on CML? It certainly was not planned, perhaps destiny had a hand in it. In any event, I can’t start to share how grateful I am that destiny has made our paths cross. I genuinely mean it. It was such an honor and a privilege to be your student and your assistant teaching the molecular biology of cancer course. You have taught me so much about science and more importantly about life; for that I will be forever grateful. Thank you!

Finally, my mom and dad taught me that the true meaning and value of this life lies in touching other people’s lives. And to that I say, may our touch be gentle filled with kindness and our impact be filled with hope. So let us use science to help as many people as we can.

ABSTRACT
OF THE DISSERTATION OF

Amro Salim Baassiri for Doctor of Philosophy
Major: Cell Biology of Cancer

Title: Unraveling the Molecular Signature of *BCR-ABL*^{P210} and *BCR-ABL*^{T315I} in the *Drosophila Melanogaster* CML Model

Background: Chronic Myeloid Leukemia (CML) is a myeloproliferative neoplasm characterized by the Philadelphia chromosome, a reciprocal t (9;22) chromosomal translocation leading to the fusion of the *BCR* gene on chromosome 22 and the *ABL* gene on chromosome 9, and resulting in the formation of the *BCR-ABL1* fusion gene. This gene encodes for the BCR-ABL1 oncoprotein that drives the uncontrolled cell proliferation via its constitutively active tyrosine kinase domain in the ABL1 region. Tyrosine kinase inhibitors (TKIs) were established as targeted therapies and are currently the standard first-line treatment for patients with CML. However, *BCR-ABL1* mutations have been a major mechanism of resistance. Patients with *BCR-ABL*^{T315I} gatekeeper point mutation, a Threonine to Isoleucine substitution at position 315 in the ATP-binding region of the ABL1 kinase domain, are resistant to first and second generation TKIs. Currently, the only FDA approved drugs which patients with this mutation respond to are the third generation TKI, ponatinib, and the first allosteric inhibitor, asciminib. However, these drugs have severe side effects which affect compliance and their efficacy is majorly in chronic phase CML patients. Therefore, the main aim of this study is to find novel potential targets against *BCR-ABL*^{T315I} to aid in this unmet clinical need. However, our approach will allow us to identify common targets against *BCR-ABL*^{p210} and *BCR-ABL*^{T315I} mutant should they arise.

Methods: We will express *BCR-ABL*^{p210} and *BCR-ABL*^{T315I} in the hemolymph system of the *Drosophila melanogaster* utilizing the Hml Δ driver to test if their expression in this system will result in a phenotype be it an increased hemocyte count, disruption in the sessile hemocyte banding pattern, or a dysregulation in the humoral arm of the innate immunity. The effect on the innate immunity will be studied via RT-PCR quantification of downstream AMPs of the Toll, Imd, and JAK/STAT pathway namely *Drosomycin*, *Diptericin A,* and *TotA* in the hemolymph, respectively. As such, hemolymph will be collected from third-instar larva, RNA will be extracted, cDNA will be synthesized, then RT-PCR will be performed. We will also collect hemolymph for RNA sequencing in order to determine differentially expressed genes (DEGs) between groups to identify potential targets. As such, Hml Δ-Gal4; UAS-GFP flies will be crossed with *w1118 (wt)*, *UAS-BCR-ABL*^{P210}, and *UAS-BCR-ABL*^{T315I} flies for these experiments. For the RNA sequencing, we will utilize the Illumina NovaSeq6000 and perform RNA sequencing with a 100bp paired-end read and 40 million reads per sample. We will also generate screening lines harboring the Hml Δ driver and the *BCR-ABL*^{p210} and *BCR-ABL*^{T315I} transgenes which will be validated by immunofluorescence since the *BCR-ABL1* genes are tagged with Myc as a reporter. DEGs will be cross-

referenced with transcriptome of CML patients and those patients with the *BCR-ABL^{T315I}* mutation specifically if available. Selected genes will be validated via RT-PCR. In case we identify upregulated screening genes, then we will cross our screening lines with flies harboring the RNAi system specifically for the target genes. Then we will check hemocyte count and banding pattern to check for partial or total rescue of the phenotype.

Results: Upon the expression of *BCR-ABL^{p210}* and *BCR-ABL^{T315I}*, there was an increase in hemocyte count and a disruption in the sessile banding pattern. An exacerbated version of the phenotypes was noted in the *BCR-ABL^{T315I}* mutant. The hemocyte count in *BCR-ABL^{p210}* flies was significantly higher than the control and the *BCR-ABL^{T315I}* flies had an even higher hemocyte count as compared to *BCR-ABL^{p210}* flies. Moreover, the disruption in the sessile pattern was partial in the *BCR-ABL^{p210}* flies when compared to the control while it was total in the *BCR-ABL^{T315I}* flies. Furthermore, we identified dysregulation in the Toll, Imd, and JAK/STAT pathways at the mRNA level in both the 3rd instar larva and adult stage via measuring, *Drosomycin, Diptericin A,* and *TotA*, respectively. Transcriptomic analysis showed us similar molecular signatures for *BCR-ABL^{p210}* and *BCR-ABL^{T315I}* but they were very distinctive than that of the *wt* control. After cross-referencing upregulated genes against adult, pediatric CML patient samples and *BCR-ABL^{T315I}* mutant mice, a total of six genes were chosen (*Rapgap1, CG9265, meltrin, sprint (spri), wing blister (wb),* and *zasp52).* Knockdown of *Rapgap1* partially rescued the hemocyte count in *BCR-ABL^{p210}* and *BCR-ABL^{T315I}* flies. Knockdown of *spri* and *CG9265* partially rescued the hemocyte count in *BCR-ABL^{T315I}* flies whereby their count decreased to levels comparable to the less aggressive wild type *BCR-ABL^{p210}*. However, knockdown of *spri* increased the hemocyte count in *BCR-ABL^{p210}* flies. Moreover, knockdown of meltrin partially rescued the sessile hemocyte banding pattern in *BCR-ABL^{p210}* and *BCR-ABL^{T315I}* flies; however, it increased their hemocyte counts so it also had an oncogenic effect. *wb* RNAi increased the hemocyte count in *BCR-ABL^{P210}* and *BCR-ABL^{T315I}* flies while *spri* RNAi and zasp52 RNAi had no effect.

Conclusion: We expressed *BCR-ABL^{P210}* and *BCR-ABL^{T315I}* in *Drosophila melanogaster* hematopoietic system that resulted in phenotypic consequences such as increasing circulating hemocyte count and disruption in the sessile hemocytes' banding pattern. In addition, their expression dysregulated the humoral Toll, Imd, and JAK/STAT pathways at the mRNA level in both the 3rd instar larva and adult stage. The *BCR-ABL^{T315I}* mutant demonstrated a more complex oncogenic effect than that of the wild type *BCR-ABL^{P210}* by presenting with more severe phenotypes and a higher deviation in humoral dysregulation. Furthermore, we unraveled the transcriptome of our hematopoietic *BCR-ABL^{P210}* and *BCR-ABL^{T315I}* CML *Drosophila* models whereby their molecular signatures were very similar to each other but distinctly different than that of *wt* control. In addition, we identified four potential target genes that had a rescue effect on both the *BCR-ABL^{p210}* and *BCR-ABL^{T315I}* flies namely, *Rapgap1, spri, CG9265,* and *meltrin*. The validity of this hematopoietic CML model is strengthened by the fact that upon cross-referencing our genes with adult, pediatric CML patient samples, and *BCR-ABL^{T315I}* mouse model, several genes were found to be differentially expressed when compared to *wt* control and they were differentially expressed in the same direction be it over or under expressed. The novelty in this study lies in the power of this hematopoietic *Drosophila* CML model. It allowed us to target some genes that were not highlighted before in the literature pertaining to leukemia. We have identified targets that are common to both *BCR-ABL*^{p210} and *BCR-ABL*^{T315I} which are worth pursuing since CML patients with and without the T315I mutation can benefit alike. There are still more upregulated genes to be screened for in the pipeline and many more taking into account the down regulated genes.

TABLE OF CONTENTS

ILLUSTRATIONS

Figure

TABLES

Table

ABBREVIATIONS

ABL1	Abelson murine leukemia
ADAM	A disintegrin and metalloproteinase domain
AMP	Antimicrobial peptide
BCR	Breakpoint Cluster Region
BomS2	Bomanin Short 2
CML	Chronic myeloid leukemia
CP	Chronic phase
CZ	Cortical zone
DEG	Differentially expressed gene
DREDD	Death-related ced-3/Nedd2-like protein
ECM	Extracellular matrix
Eig	Ecdysone-induced gene
FAK	Focal adhesion kinase
Fon	Fondue
GABA	Gamma-aminobutyric acid
GAP	GTPase activating protein
GEF	Guanine nucleotide exchange
GMR	Glass multiple reporter
Hml Δ	Hemolectin delta
Idgf5	Imaginal disc growth factor 5
IKK	IkappaB kinase
ILK	Integrin-linked kinase
IRIS	International randomized study of interferon and cytarabine versus STI571
JAK/STAT	Janus-activated kinase/Signal Transducer and activator of transcription
JNK	c-Jun N-terminal kinase
Log2FC	log2 fold change
M-bcr	Major breakpoint cluster region
MZ	Medullary zone
NGS	Normal goat serum
PBS	Phosphate Buffered Saline
PBST	PBS-0.3% Triton
PCA	Principle component analysis
PI3K/Akt	Phosphoinositide 3-kinase/AKT
PO	Phenoloxidase
PPO	Prophenoloxidase
PSC	Posterior signaling center
Ras/MEK	Ras-mitogen-activated protein kinase/MEK
ROS	Reactive oxygen species
RP49	Ribosomal protein 49
RPL11	Ribosomal protein 11
Spri	Sprint
STI571	Signal transduction inhibitor 571
TGF	Transforming growth factor
Tie	Tie-like receptor tyrosine kinase

TK	Tyrosine kinase
TKI	Tyrosine kinase inhibitors
TNF	Tumor necrosis factor
TotA	Turandot A
UAS	Upstream activating sequence
VDRC	Vienna Drosophila Resource Center
wb	Wing blister
wt	W^{1118} (wild-type) flies

CHAPTER I

INTRODUCTION

A. Chronic myeloid leukemia (CML)

1. Molecular biology

CML is a myeloproliferative neoplasm characterized by a reciprocal t(9;22) chromosomal translocation leading to the Philadelphia chromosome and the fusion of the *Breakpoint Cluster Region* (*BCR)* gene on chromosome 22 and the *Abelson* murine leukemia (*ABL)* gene on chromosome 9, and resulting in the formation of the *BCR-ABL1* fusion gene. Depending on where the breakpoint occurs in the *BCR* segment, the resulting fusion gene may encode for BCR-ABL1 isoform oncoproteins of 210 KD, 190 KD, or 230 KD [1]; p210 is mostly encountered in CML while p190 in B-cell acute lymphoblastic leukemia and p230 in neutrophilic-CML (figure 1)[2]. Concerning the nomenclature of the *BCR-ABL1* transcripts, a specific breakpoint cluster region (bcr) was identified at first whereby the exons within this region (exons 12-16) were referred to as b1-b5 [3]. Future studies showed that there are more breakpoint regions specific to CML that were located upstream of the previously identified bcr. This new larger region which included the old bcr and the new additional breakpoints was referred to as the major breakpoint cluster region (M-bcr) [4]. As such, it is preferred now to name the transcript in reference to its exon number now rather than b1-b5 as they did historically. Moreover, due to alternative splicing, even one genomic breakpoint can produce several transcripts. Therefore, the p210 *BCR-ABL1* can comprise of exon 13 (e13) or exon 14 (e14) which were previously referred to as b2 and b3, respectively. Since this translocation is always occurring at the *ABL* exon 2 so it is annotated as a2. To sum up, the p210 *BCR-ABL1* transcripts can be either e13a2 (previously b2a2) or e14a2 (previously b3a2) (figure 1).

The BCR-ABL1 oncoprotein drives the uncontrolled cell proliferation via myriad of ways. For instance, BCR's N-terminal coiled-coil motif increases its tyrosine kinase (TK) activity and allows ABL1 to bind F-actin[5]. In addition, BCR can activate signaling pathways mediated normally by ABL1's TK via its own serine-threonine kinase domain [6]. Moreover, it constitutively activates TK domain in the ABL1 region. Normally, ABL1 has a myristate group at its N-terminal, SH1 domain (a non-receptor TK that conducts its phosphorylation activity) with a myristoylation site, SH2 and SH3 domains[2, 7]. Upon binding of the myristate to the myristoylation site of the SH1 domain, it undergoes a conformational change that creates a docking site for the SH2 domain resulting in the autoinhibition of the TK. However, upon the fusion of *BCR* upstream of *ABL1*, the latter loses its upstream control element namely, its N-terminal myristate group (figure 2)[8]. Consequently, the resulting BCR-ABL1 protein is constitutively activating several effector pathways, primarily the Janus-activated kinase/Signal Transducer and activator of transcription (JAK/STAT), phosphoinositide 3-kinase/AKT (PI3K/Akt), and Ras-mitogen-activated protein kinase/MEK (Ras/MEK), via phosphorylation of downstream proteins[9]. Its phosphorylated substrates alter stromal adhesion, inhibit apoptosis and autophagy, impair differentiation and genomic surveillance while promoting cell proliferation and growth factor independence (figure 3)[10].

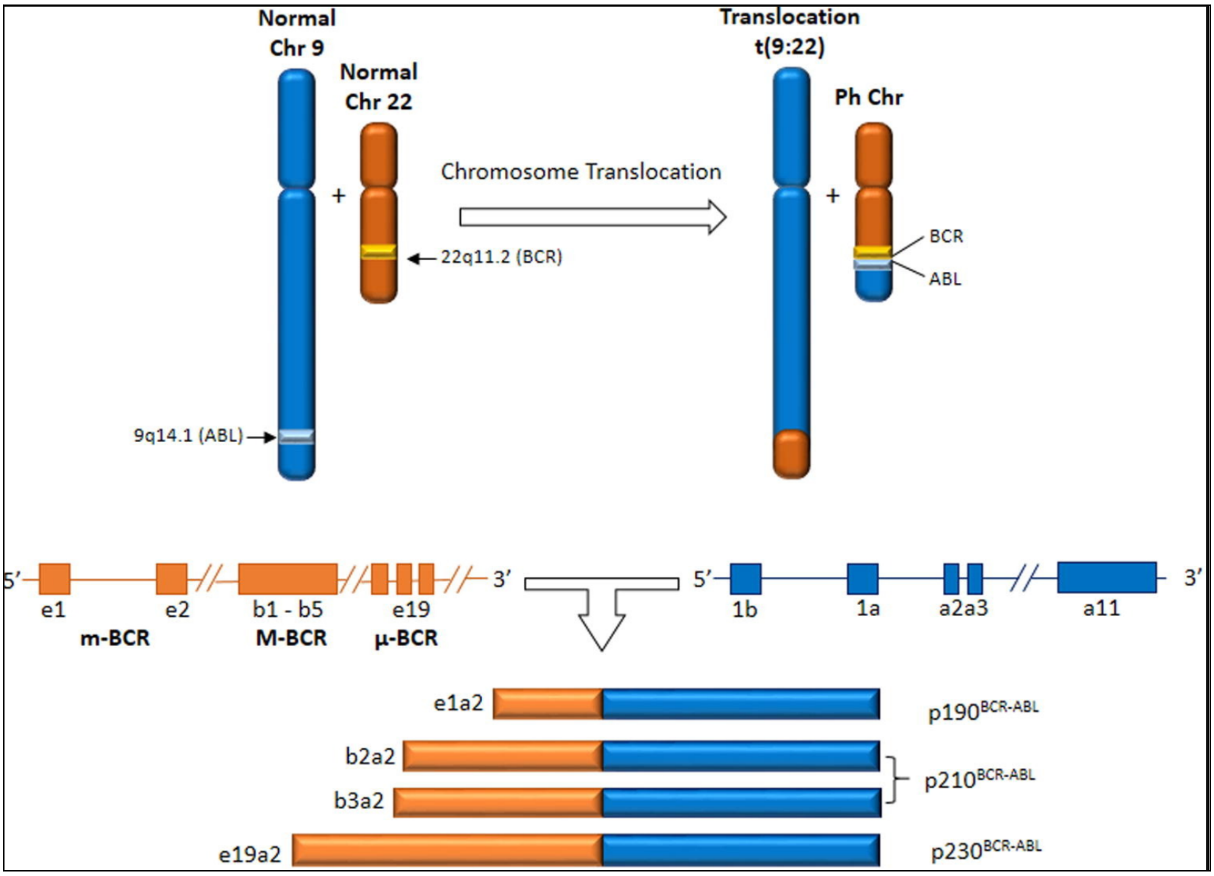

Figure 1. Formation of the BCR-ABL1 fusion gene.

Translocation (9;22) and BCR/ABL transcripts associated to CML at different breakpoints (adapted from Avelino et al. 2017) [11]

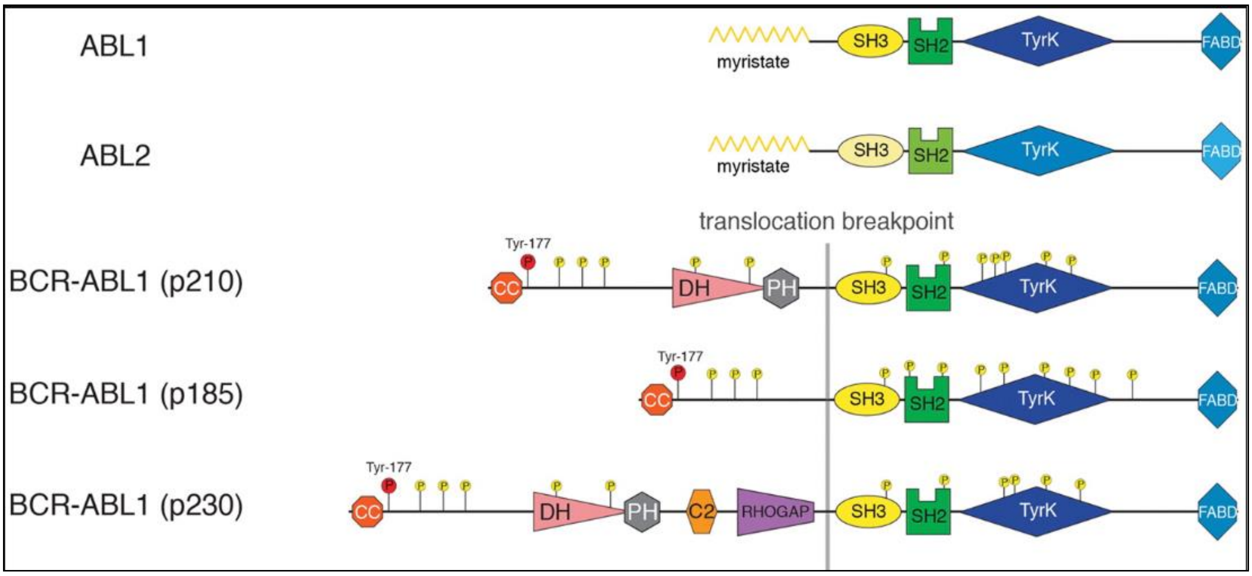

Figure 2. Loss of ABL1 N-terminal myristate group upon *BCR-ABL1* fusion. Schematic domain representation of ABL1 and ABL2 proteins as well as the BCR-*ABL1* fusion gene products which arise from reciprocal t(9;22) chromosomal translocation. Known phosphorylation sites are indicated. Domain abbreviations are as follows: TyrK, tyrosine kinase; FABD, F-actin binding; CC, coiled-coil; DH, Dbl-homolgy; PH, Pleckstrin-homology; RHOGAP, Rho GTPase-activating protein (adapted from Hantschel *et al.* 2012)

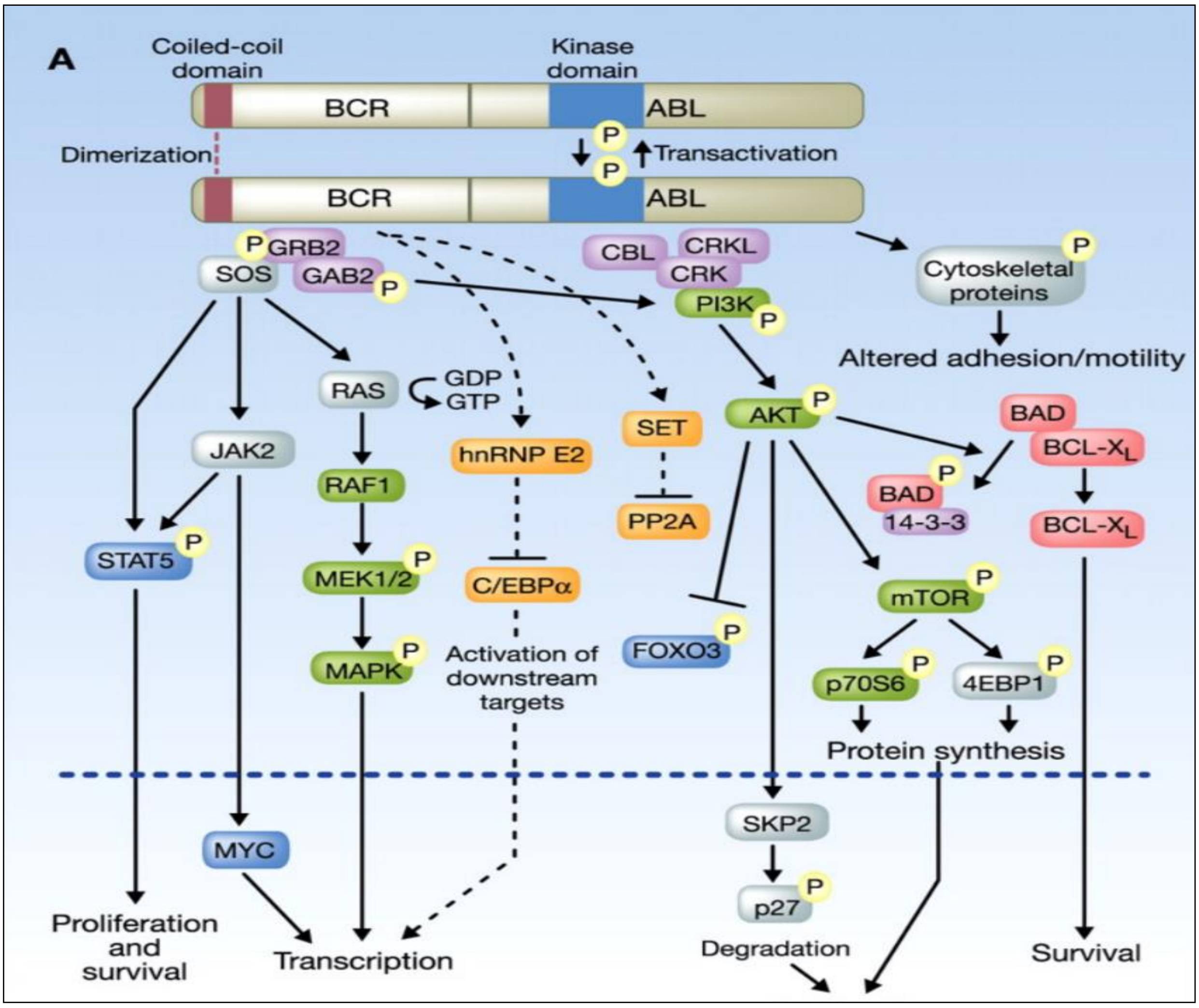

Figure 3. BCR-ABL1 signaling network in CML.
Dimerization of *BCR-ABL1* triggers phosphorylation events that activate multiple pathways that promote cell proliferation, growth factor independence, alter stromal adhesion, and inhibit apoptosis (adapted from O'Hare *et al.* 2011) [12]

2. Treatment

CML is usually diagnosed at the chronic phase (CP) that if left untreated, it may progress to an accelerated or blast phase[13]. The only curative therapy is the allogeneic stem cell transplant. However, this is not a viable option in most cases due to the lack of a suitable stem-cell donor or the ineligibility of the patient due to their elderly age since they will not be able to tolerate the serious side effects[14]. Currently, tyrosine kinase inhibitors (TKIs) remain the first-line therapy for newly diagnosed patients with CML while allogeneic stem transplant is reserved for patients who have failed multiple TKIs [13, 15]. There are six FDA approved TKIs in use; one first generation (imatinib), three second generation (nilotinib, dasatinib, and bosutinib), one third generation TKI (Ponatinib), and a first-in-class allosteric inhibitor of BCR-ABL1 kinase activity (asciminib)[13, 16]. All TKIs mentioned bind to the ATP-binding pocket of the kinase domain in the BCR-ABL1 protein except for asciminib that targets the ABL1 myristoyl pocket[17, 18]. TKIs are highly effective since they result in high progression-free and overall survival associated with a low risk of disease progression [19-22]. However, a major resistance mechanism is point mutations in the BCR-ABL1 kinase domain which are associated with poor prognosis and higher risk of disease progression compared to the wild type *BCR-ABL1*[22-26]; the most common mutations include T315I/A, V299L, Y253H, G250E, E255K/V, F317L/I/V/C, and F359V/C[13, 27].

Imatinib (Gleevec®) formerly known as signal transduction inhibitor 571 (STI571) was first presented in 1996 by Druker and colleagues who showed that it was effective against CML cell lines[28]. It is an ATP-competitor, which means the SH1 domain of BCR-ABL1 can still bind to substrate molecules however; it will not be able to phosphorylate them. The phase 1 study that followed showed that it induced cytogenetic response in addition to controlling blood counts and restoration of the chronic phase[28]. The phase 2 study along with the IRIS (international randomized study of interferon and cytarabine versus STI571) study revolutionized the management of CML since they showed high rate of complete cytogenetic remission in chronic phase patients who did not respond to interferon α[29, 30]. Nevertheless, upon years of follow up, it was noticed that several patients for various reasons would be removed off imatinib[7]. Some BCR-ABL1-dependent resistance includes amplification of the *BCR-ABL1* gene while loss of efficacy because of BCR-ABL1-independent resistance can be due to either a decrease in activity of the drug influx transporter or overexpression of the multidrug resistant P-glycoprotein (MDR1)[31-35]. A third problem was patient intolerance. However, the most frequent reason was point mutation development in the ABL1 kinase domain that decreased the binding of imatinib since it binds to the kinase domain via six hydrogen bonds, one of which is disrupted by the T315I point mutation[35].

The resistance to imatinib triggered the interest in developing second generation TKIs effective against kinase specific mutations. Phase 1 study of Dasatinib showed complete cytogenetic remission in 35% of imatinib resistant patients in chronic and accelerated phase while only temporary cytogenetic and hematological responses in similar patients in blast crisis phase. However, patients with the T315I mutation remained resistant[36]. Moreover, a serious side effect making patient selection a priority is its pleuro-pulmonary toxicity[37]. Likewise, nilotinib had similar results as dasatinib only with a different toxicity that is cardiovascular[37, 38]. Furthermore, bosutinib demonstrated complete cytogenetic remission in 24% of patients unresponsive to 2-3 previous TKIs and it was specifically tested in imatinib resistant patients whereby 47% achieved complete cytogenetic remission [39, 40].

Patients with the notorious T315I (*BCR-ABL*^{T315I}) gatekeeper point mutation are completely resistant to first and second generation TKIs [41, 42]. Currently, the only available drugs that patients with *BCR-ABL*^{T315I} respond to are the third generation TKI and the allosteric inhibitor ponatinib and asciminib, respectively [43, 44]. Clinical efficacy against T315I was confirmed in ponatinib phase 1 and 2 studies with 63% and 46% patients carrying *BCR-ABL*^{T315I} in chronic phase achieving complete cytogenetic remission, respectively[45, 46]. However, premature data in phase 2 demonstrated an increased incidence of arterial thrombotic events in patients in the ponatinib arm[46]. Ponatinib is associated with hepatotoxicity and serious cardiovascular events such as vascular occlusion and heart failure [44, 47, 48]. As for asciminib, some frequent adverse events reported include gastrointestinal, pancreatic, and hepatotoxicity, myelosuppression, thrombocytopenia, leukopenia, and hemorrhage [43]. Nevertheless, high dose asciminib has shown to be equally effective when it comes to patients with *BCR-ABL*^{T315I} [49]. Interestingly, *in vitro* studies demonstrate a synergy between ponatinib and asciminib whereby ponatinib stabilizes asciminib's binding to the myristoyl pocket by docking in the ATP-binding pocket[50].

3. Resistant BCR-ABL^{T315I} ***mutant***

The T315I mutation accounts for 15-20% of mutations in CML patients [24, 51]. Patients with *BCR-ABL*^{T315I} demonstrate a more rapid clinical course associated with a poorer prognosis than those with wild type *BCR-ABL*^{p210} [24, 27, 52].This challenging mutation is not limited to patients with pre-existing resistant subclones prior to treatment, but studies have shown that resistant mutations can emerge during treatment that are detected at relapse. Moreover, patients with existing mutations are more likely to acquire compound mutations that exacerbate their prognosis [53].

CML cells harboring *BCR-ABL*^{T315I} have demonstrated to have several different characteristics than those of the wild type *BCR-ABL*^{p210} that may play a role in its oncogenic severity. For instance, the phagocytic activity of *BCR-ABL*$^{T315I+}$ myeloid cells is significantly reduced compared to that of *BCR-ABL*$^{p210+}$ [54]. Interestingly, despite *BCR-ABL*^{T315I} presenting with a 10-20% increased potency to transform myeloid cells, however, it exhibits a reduced kinase activity when compared to the wild type. One explanation was that the kinase domain recognizes novel substrates that increase its potency while its reduced kinase activity is a result of not recognizing the classical ABL1 substrates. This altered substrate recognition was supported by identifying a unique phsophosubstrate signature in *BCR-ABL*^{T315I} whereby an increased Tyr257 phosphorylation in the ATP binding loop [55, 56].

Furthermore, there is a difference in *BCR-ABL*$^{T315I+}$ cell interaction with the bone marrow microenvironment and its remodeling. This is primarily mediated via the fibronectin/integrin β3/Integrin-linked kinase-signaling pathway [54]. The focal adhesion protein FAK, involved in cytoskeletal stability and actin polymerization, usually presents as punctate which reflects an intact focal adhesosome [54, 57, 58]. Wild type cells present with reduced punctae; however, *BCR-ABL*$^{T315I+}$ cells present additionally with complete dispersion and granularity reflecting the complete disarray in the actin cytoskeleton polymerization [54]. In addition, integrin β3 is significantly overexpressed in *BCR-ABL*$^{T315I+}$ cells compared to wild type that is probably influencing progression since it has been shown that AML leukemic progression is dependent on integrin β3 signaling [54, 59]. Moreover, *BCR-ABL*$^{T315I+}$ fibroblasts deposit less fibronectin that affects the communication between the cells and its microenvironment. Finally, it has been revealed that there is an impairment in the binding of integrin β3 and integrin-linked kinase, a RAF-like kinase involved in fibronectin deposition and integrin-mediated signal transduction, in *BCR-ABL*$^{T315I+}$ cells [54, 60-62].

B. Drosophila melanogaster

1. A model organism

Drosophila melanogaster, commonly known as the fruit fly, has several remarkable features that make it a common model organism to study various disciplines. Some advantages include small size, ease of handling, cheap to maintain and manipulate, a relatively rapid life cycle (figure 4), hundreds of genetically identical offspring from a single fertile mating pair within 2 weeks at 25ºC, well defined external developmental stages, and a plethora of mutant and transgenic fly lines that can be acquired from fly stock centers [63-65].

In the past decade, there has been an exponential increase in publications in its utilization as a cancer model that signifies its relevance to cancer research [66]. Its genome is 60% homologous to that of humans with homologs present for 75% of genes involved in human diseases [67]. Most cell growth and invasion signaling pathways in mammals have a conserved function in the fruit fly [68]. Several studies have demonstrated a highly conserved hematopoietic system between humans and *Drosophila* [69, 70]. Moreover, several genes that play a role in blood cell development with a potential involvement in human leukemia have been studied via this model [66, 71]. A highly notorious gene was identified to play a significant role in human leukemia via the JAK/STAT pathway namely *hopscotch* which encodes the *Drosophila* homologue of JAK kinase [72]. Furthermore, a rapid functional characterization of conserved oncogenes and tumor suppressor genes is possible due to the combination of genetic screens associated with efficient recombination techniques [73]. One useful genetic tool is the generation of balancer chromosomes for they are chromosomes with one or more inversions that prevent recombination. In addition, they carry recessive mutations and dominant markers that makes homozygosity of balancer chromosomes lethal and identification of rare recombinants for screening purposes possible, respectively. Consequently, we conserve the balancer and balanced chromosomes in this population [65]. Another tool is the *UAS-GAL4* targeted expression system in *Drosophila* that provides a relatively easy method to express or knockdown specific genes. GAL4 is a yeast galactose-responsive transcription factor that allows the spatial and temporal expression of target genes; they can drive or knockdown expression at a specific developmental stage, in specific cells and tissues. The construct of this system is as follows: the first component is a tissue-specific promoter upstream of GAL4 and the second component is a GAL4-binding upstream-activating sequence (UAS) in front of the gene or RNAi of interest. When the promoter is activated in the specific tissue of interest, GAL4 protein is produced which then binds the UAS resulting in the expression of the gene of interest or production of an RNAi (figure 5) [74].

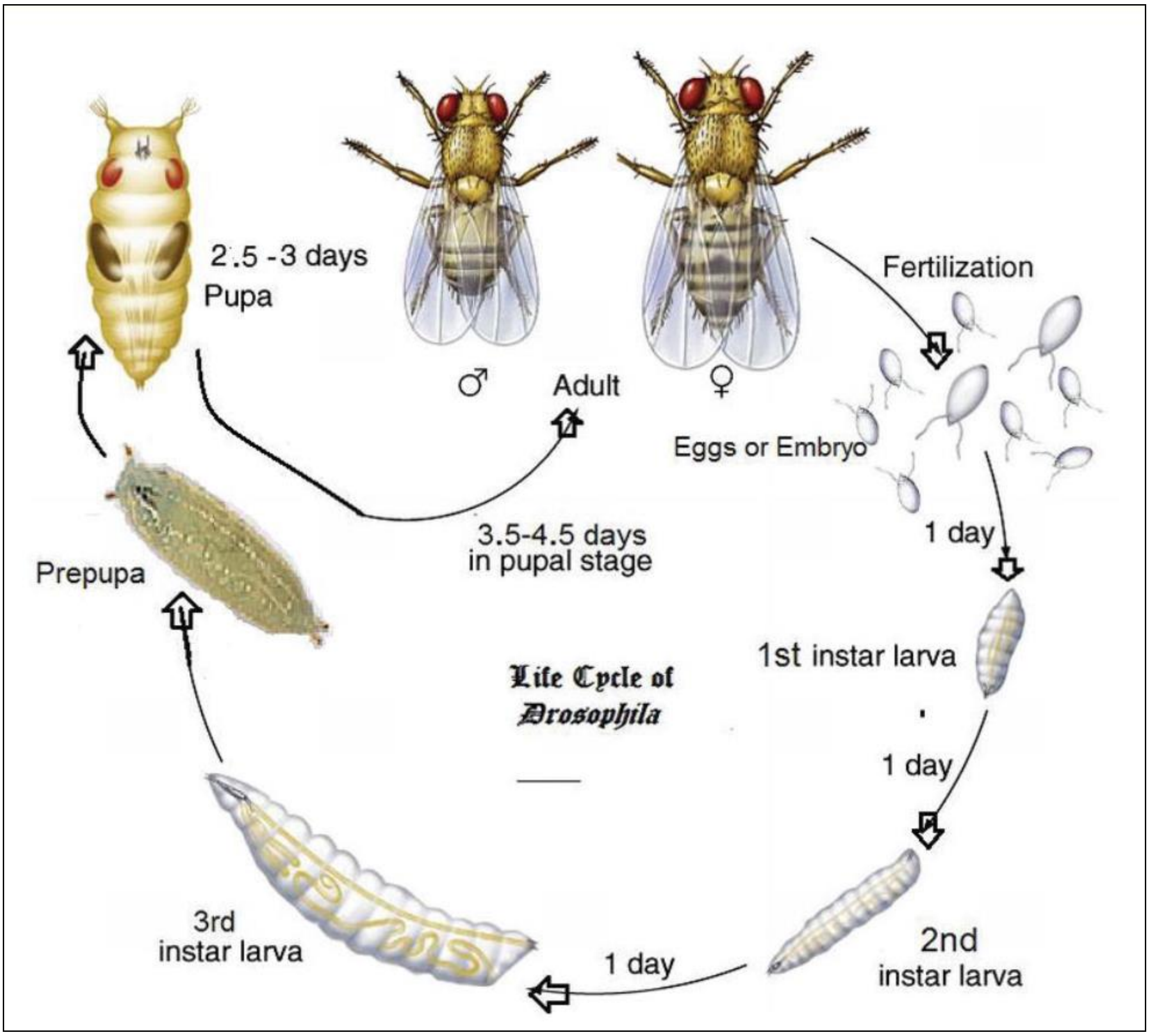

Figure 4. *Drosophila melanogaster* lifecycle.

Involves three larval stages followed by a pupal stage before reaching adulthood. . The *Drosophila* lifecycle typically takes 9-10 days at 25°C (adapted from Perveen et al. 2018) [75]

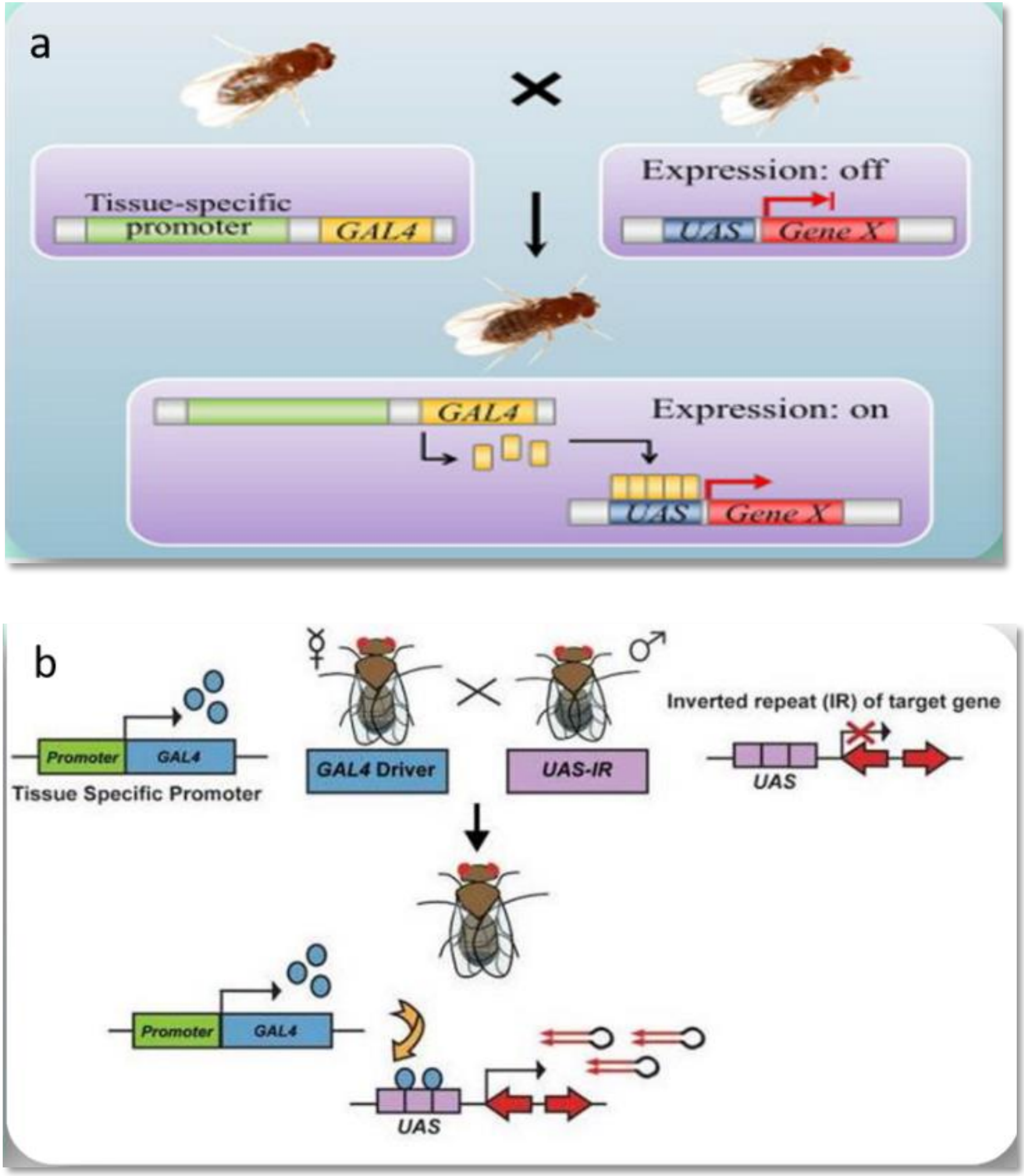

Figure 5. A schematic diagram of the UAS-GAL4 system.
In a specific tissue of interest, we can (a) induce the expression of the gene of interest X or (b) knockdown via RNAi (adapted from Cho *et al.* 2014 and Blake *et al.* 2017). [76, 77]

2. *Haematopoietic system*

Prohemocytes are multipotent hematopoietic progenitor cells that give rise to four types of blood cells referred to as hemocytes. These hemocytes are plasmatocytes, crystal cells, lamellocytes, and primocytes (figure 6) [78]. In a third-instar larva, the majority of hemocytes (90-95%) are plasmatocytes that are relatively small with a granular cytoplasm [79]. They have phagocytic, antimicrobial, and homeostatic functions. They phagocytose bacteria and initiate the encapsulation of larger parasites [78]. They are involved in several homeostatic functions including, but not limited to, aid during embryonic development and metamorphosis via secreting the required extracellular matrix components, wound healing, and glucose metabolism regulation [78, 80, 81]. Crystal cells make up the remaining 5-10% of hemocytes [78]. They are involved in melanization since they contain prophenoloxidase (PPO); a zymogen when activated turns into phenoloxidase (PO) which is an enzyme that produces melanin [78]. They facilitate wound healing, hypoxic response, and innate immunity [82]. Upon injury, the crystal cell ruptures induced by the c-Jun N-terminal kinase (JNK) pathway and Eiger, the tumor necrosis factor (TNF) homolog that results in PPO release. In turn, the zymogens become activated by a proteolytic cascade into PO that catalyzes the production of quinones that result in a melanin plug once polymerized. In addition, as by products, reactive oxygen species (ROS) are produced which aid in pathogen elimination [83-86]. Lamellocytes are produced in response to parasitoid wasp infections [78].

Primocytes, a new class of hemocytes, were identified that seem to be related to the cells in the posterior signaling center (PSC). The PSC region is located in the posterior tip of the primary lobe of the lymph gland that contains a group of cells that may act on the differentiated hemocytes or intermediate progenitors to control balance of blood cell differentiation. Their relation to the cells within the PSC region lies in the expression of similar markers namely, the *Antennapedia* and *Knot* markers [78]. The primocytes were called several names by different authors amongst which include PL-ImpL2 and PM11 [87, 88]. They are relatively rare since they represent only about 0.3% of all peripheral hemocytes [87, 89]. One gene is preferentially expressed, in primocytes, *CG15550* which encodes for a small predicted transmembrane protein of unknown function [78]. Furthermore, they seem to play a role in the immune system since *ImpL2* is another enriched gene in primocytes that encodes a secreted insulin antagonist which induces adipose tissue to release carbohydrates and lipoproteins which are used by the activated immune system [90-92].

Hemocytes are produced in two waves during development [93]. The first wave of cells originate from the head mesoderm in the embryo. They produce embryonic plasmatocytes and crystal cells that are not circulating freely in the embryo but they are motile. Those same cells are the founders of the circulating and sessile hemocytes in the larval stage. They also contribute to the latter two stages namely, the pupal and adult stages. The second wave of cells originate from the thoracic mesoderm that develops into the lymph gland. These cells contribute to the pupal and adult stages since they are released in the prepupal stage [78]. The formation of the lymph gland begins in the late embryo stage whereby a single pair of anterior lobes form along the dorsal vessel/cardiac tube. Towards the end of the first-instar larval stage, a pair of posterior lobes appear which increase in number by the third-instar larval stage whereby they become several smaller pairs of posterior lobes separated by pericardial cells. The anterior lobes are composed of three zones having the progenitor cells in the inner/medullary zone, their mature counterparts in the outer/cortical zone, and intermediate progenitors in between which lack markers of both prohemocytes and mature blood cells. In addition, as noted prior, the posterior tip of the primary lobe has the PSC region. The posterior lobes constitute of prohemocytes and recently detected primocyte-like cells (figure 7) [78, 93-97].

During the larval stage, about half of the hemocytes present are circulating in the hemocoel while the other half are sessile in epidermal-muscular pockets (figure 6) [78, 98]. The sessile cells begin by forming lateral patches that develop into dorsal stripes. This sessile pattern is dependent on three main factors namely hemocytes' homing to the pockets, adhesion, and lateral migration. Homing is induced by the innervation of peripheral neurons to these pockets that provide transforming growth factor (TGF-b) signals which play a dual role of promoting adhesion and proliferation [98, 99]. Moreover, sessile hemocytes depend on the interaction between the collagen Multiplexin in the extracellular matrix and the hemocyte's membrane protein Eater [100, 101].

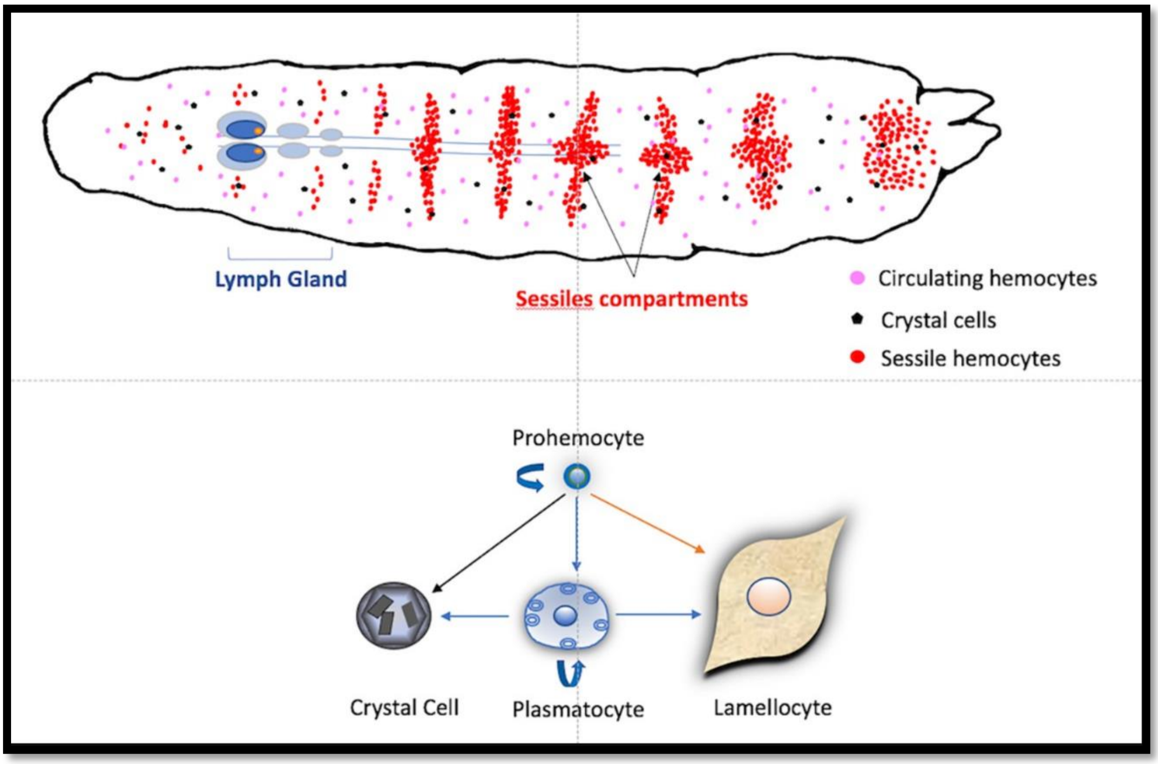

Figure 6. Hematopoiesis in *Drosophila melanogaster*.
Prohemocyte cells give rise to the plasmatocytes, crystal cells, and lamellocytes. Hemocytes form sessile banding patterns in the larval stage (adapted from Kim-Jo *et al.* 2019) [102]

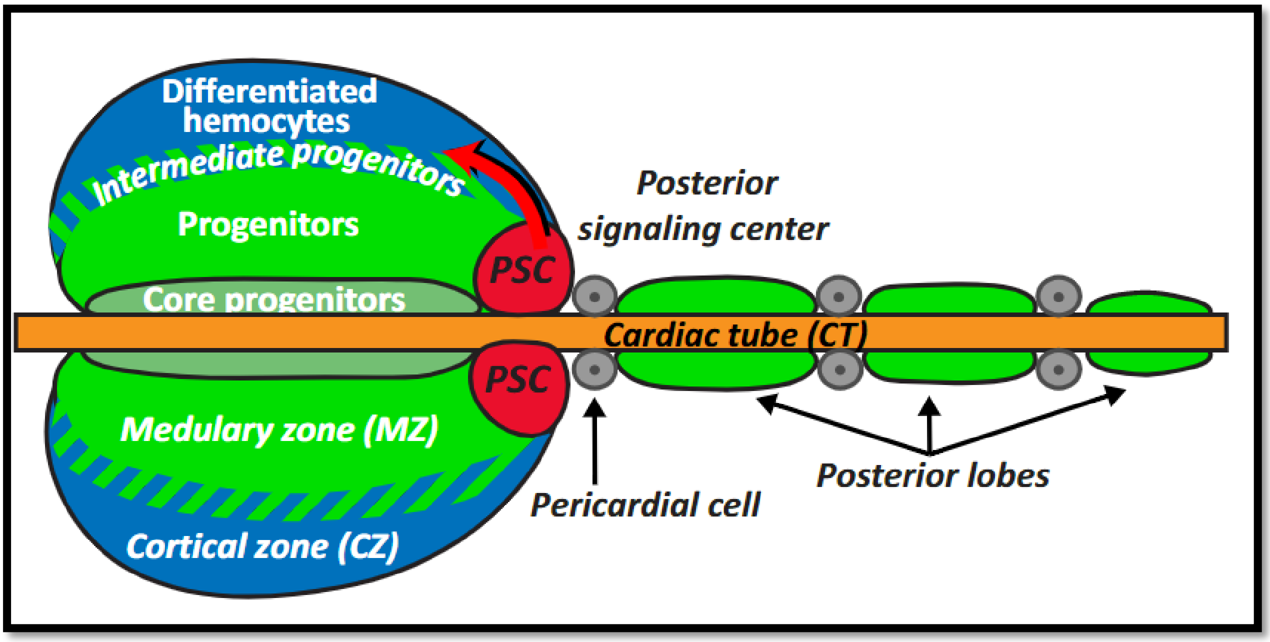

Figure 7. *Drosophila* lymph gland organization in the third instar larval stage.

The primary lobes comprise of the posterior signaling center (PSC, in red), the cortical zone (CZ, in blue), the medullary zone (MZ, in green), and the intermediate progenitors (striped green/blue) which are between the CZ and MZ. The posterior lobes composed of prohemocytes (adapted from Letourneau et al. 2016).

3. Immune system

Drosophila melanogaster lacks an adaptive immune system; however, it has an innate immune system that is divided into cellular and humoral. The immune responses include epithelial barriers, clotting, humoral response which involves the fat body releasing antimicrobial peptides (AMPs), and cellular phagocytosis of pathogens [103]. Epithelia are the first line of defense whereby AMPs are expressed on their surface [104]. Moreover, they have numerous and diverse AMPs. There are antifungal AMPs (drosomycin, metchnikowin), anti-Gram positive AMPs (defensin), and anti-Gram negative AMPs (diptericin, drosocin, attacins, and cecropins) [105].

The three main pathways are Toll, Imd, and JAK/STAT. The first two are two distinct NF-κB pathways. The Toll pathway protects against Gram-positive bacterial and fungal infections. The Toll receptor is activated via binding of the cleaved ligand Spatzle. This will in turn assemble the MyD88, Tube and the Pelle kinase complex that will result in the degradation of IκB protein Cactus. Thereafter, Dorsal and Dif are free to localize to the nucleus. The main antifungal peptide in this pathway is drosomycin [103, 106]. As for the Imd pathway, it protects against Gram-negative bacteria [105]. Activation of its main receptor peptidoglycan recognition protein-LC (PGRP-LC) results in the formation of the IKK complex that phosphorylates Relish. When phosphorylated, relish is cleaved by DREDD that releases the Rel domain to translocate to the nucleus and transcribe *Diptericin* [103, 107]. Finally, the JAK/STAT pathway protects against viruses with one of its main target stress-related humoral factor is TotA. Once one of the Unpaired, Unpaired 2 or 3 binds to the Domeless receptor, it will initiate signaling downstream whereby its associated receptor JAK tyrosine kinase Hopscotch will phosphorylate itself and the cytoplasmic tail of the Domeless receptor.

This will result in the creation of docking sites for STAT92E proteins that will become phosphorylated, dimerize, and translocate to the nucleus in order to induce gene expression [103, 108-113].

4. *A CML model*

Incorporating the *BCR-ABL1* transgene into the *Drosophila* across several systems has demonstrated the suitability of the *Drosophila melanogaster* as a model to study this chromosomal translocation. Outa *et al*. validated transgenic CML fly models expressing *BCR-ABL*^{p210} and *BCR-ABL*^{T315I} in the eye utilizing the glass multiple reporter (GMR) driver. Expression of the *BCR-ABL*^{T315I} mutant demonstrated an exacerbated phenotype than that of *BCR-ABL*^{p210} whereby adult flies' eyes were not only rough but also had a larger surface area distortion of the ommatidial architecture. The severity was temperature dependent whereby it increased with higher temperatures (figures 8&9). Furthermore, this model was validated by demonstrating the rescue of ommatidial loss consequently restoring the posterior eye defect in the *BCR-ABL*^{p210} flies via intake of dasatinib and ponatinib [114].

Bernardoni *et al*. observed similar findings upon usage of the same driver and they demonstrated the impairment this transgene has on *Drosophila* blood homeostasis when expressed under the domeless driver [115]. Another study expressed *BCR-ABL*^{p210}and *BCR-ABL*^{p185} in the developing nervous system whereby it rescued *Abl* mutant flies from pupal lethality demonstrating that the transgenic ABL1 can substitute for *Drosophila* Abl. In addition, increased levels of phosphorylated *Drosophila* Abl demonstrated that it is a substrate for the transgenic BCR-ABL1 that means we can study the transgenic functionality namely its signal transduction in this model [116].

Furthermore, transgenic CML flies were utilized to identify putative candidate genes that could be targeted for rescue. A novel finding was that a tight connection between Rab family members and BCR-ABL1 was identified and it was successfully validated in CML patients [117]. Another study additionally validated the utilization of *Drosophila* as a screening tool for drug libraries targeting wild type and *BCR-ABL*^{T315I} mutant [118]. Finally, Stevens *et al.* demonstrated the effective utilization of the *Drosophila* model to study the effect of ABL1 in morphogenesis that may aid in better understanding the biological functions pertaining to *BCR-ABL1* [119].

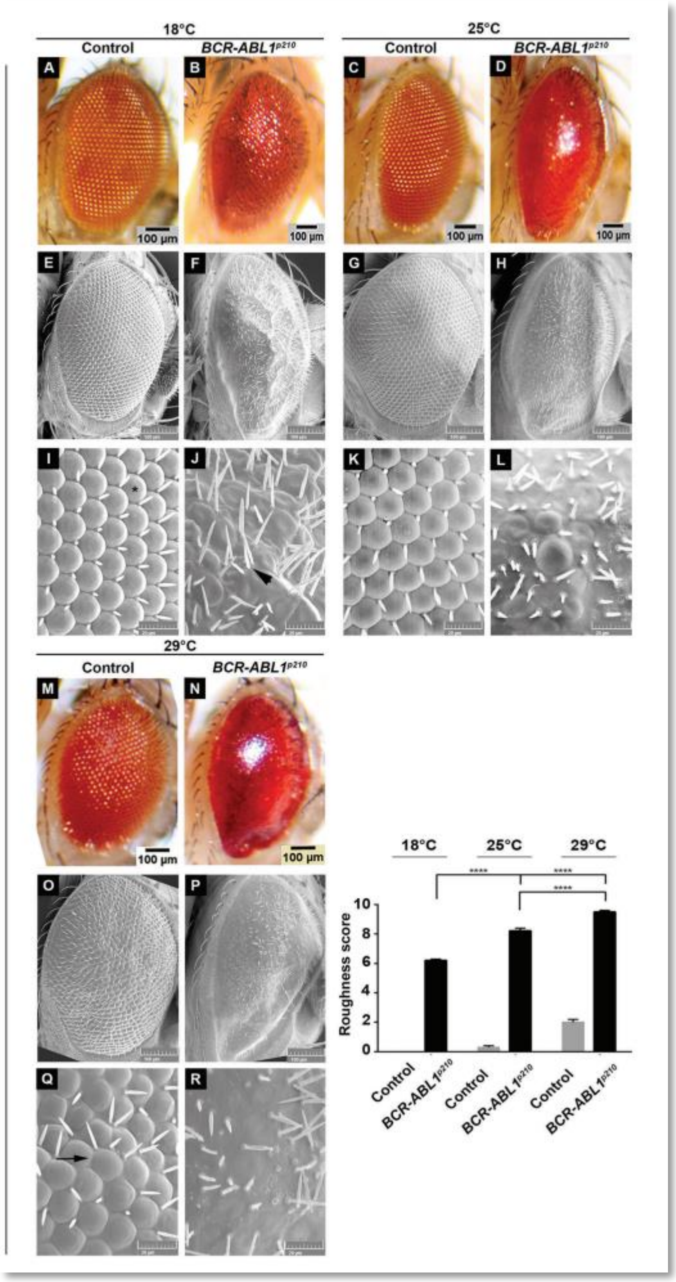

Figure 8. Rough eye phenotype induced by overexpression of human BCR-ABL^{p210}.

Light (A-D, M-N) and scanning electron (E-L, O-R) micrographs of adult *Drosophila* compound eyes expressing BCR-ABL^{p210} under the control of the eye specific promoter GMR-GAL4. Flies were raised on 18°C (A, B, E, F, I, J), 25°C (C, D, G, H, K, L) or 29°C (MR). I-L and Q-R are high magnifications of the centermost region of E-H and O-P respectively (1,370x). Ommatidial facets are depicted in (I) by (*), misplaced mechanosensory bristles in (J) depicted by arrowheads and ommatidial fusions in (Q) are shown by arrow. Data represents mean ± SEM. ****, P<0.0001 (adapted from Al Outa et al. 2020).

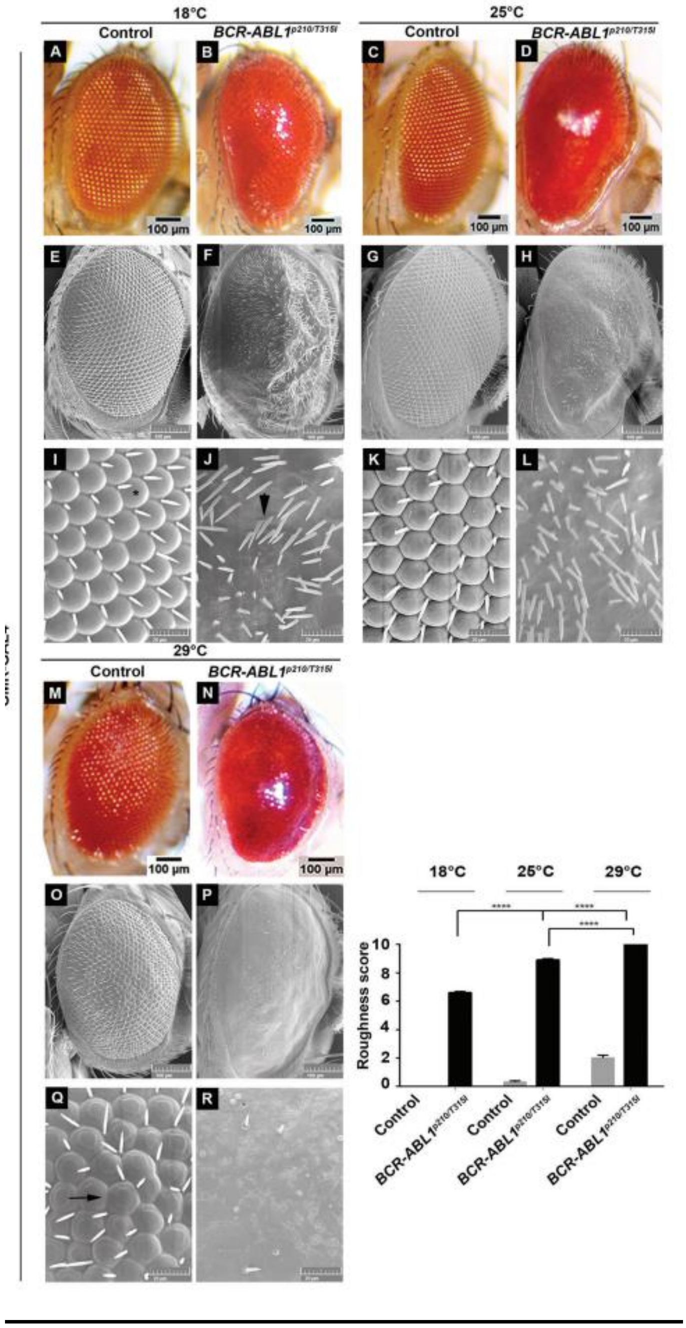

Figure 9. Rough eye phenotype induced by overexpression of human BCR-ABL$^{p210/T315I}$ (referred to in this text as BCR-ABL^{T315I}).

Light (A-D, MN) and scanning electron (E-L, O-R) micrographs of adult *Drosophila* compound eyes expressing BCR-ABL$^{p210/T315I}$ under the control of the eye specific promoter GMR-GAL4. Flies were raised on 18°C (A, B, E, F, I, J), 25°C (C, D, G, H, K, L) or 29°C (MR). I-L and Q-R are high magnifications of the centermost region of E-H and O-P respectively (1,370x). Ommatidial facets are depicted in (I) by (*), misplaced mechanosensory bristles in (J) depicted by arrowheads (adapted from Al Outa et al. 2020).

CHAPTER II

AIMS

CML is a myeloproliferative neoplasm characterized by the Philadelphia chromosome that results in the formation of the *BCR-ABL1* fusion gene [1]. TKIs are the first-line therapy for newly diagnosed patients with CML [2]. Patients with the notorious *BCR-ABL*^{T315I} gatekeeper point mutation renders them completely resistant to first and second generation TKIs [3, 4]. Currently, the only available drugs that patients with *BCR-ABL*^{T315I} respond to are the third generation TKI and the allosteric inhibitor ponatinib and asciminib, respectively [43, 44]. Despite demonstrating a promising efficacy in chronic-phase CML patients with *BCR-ABL*^{T315I}, both drugs have less than a 50% response rate in accelerated-phase and blast-phase CML patients with *BCR-ABL*^{T315I} [43, 45, 46]. Moreover, Ponatinib is associated with hepatotoxicity and serious cardiovascular events such as vascular occlusion and heart failure [44, 47, 48]. Some frequent adverse events reported with asciminib include gastrointestinal, pancreatic, and hepatotoxicity, myelosuppression, thrombocytopenia, leukopenia, and hemorrhage [43]. Therefore, **the main objective of this study is to find novel potential targets against *BCR-ABL*^{T315I} to aid in this unmet clinical need**. Unfortunately, most of the literature on *BCR-ABL*^{T315I} is of clinical studies in the context of whether patients with this mutation are responding or not to novel treatment. The literature lacks in understanding the molecular and pathophysiological differences between the mutant and the wild type. This is a major disadvantage for those aiming to find novel effective treatments. Hence, in this study we intend on unraveling the molecular signatures of *BCR-ABL*^{T315I} and *BCR-ABL*^{p210}. Should the mutant have a unique signature then it may be possible to identify a target specific for it. However, if it is very similar to that of the wild type, then we might be looking at identifying targets that may be common to both hopefully with a higher efficacy against the mutant than that of the drugs available today.

Aim 1: Identify whether significant phenotypic differences result from the expression of the human wild type *BCR-ABL*^{P210} and *BCR-ABL*^{T315I} mutant in the hematopoietic system of *Drosophila*.

Rationale: Phenotypic differences give us a visual and/or measurable variable that could be documented, analyzed, and further assessed when we target candidate genes by documenting phenotypic reversal.

- Aim 1a: Investigate if there is a change in hemocyte count
- Aim 1b: Investigate if there is a change in sessile banding pattern

Aim 2: Profile the transcriptome of *BCR-ABL*^{P210} and *BCR-ABL*^{T315I} expressing hemocytes

Rationale: Transcriptomic data may provide us with target genes that turn out to be significantly differentially expressed whether compared to the control or between *BCR-ABL*^{P210} and *BCR-ABL*^{T315I}

Aim 3: Validate candidate genes either by overexpressing down-regulated genes or by knocking down overexpressed genes in *Drosophila melanogaster*.

- Aim 3a: Create a screening line for each genotype carrying the Hml Δ driver via the utilization of balancer chromosomes

-Aim 3b: validate selected target genes via RT-PCR

- Aim 3c: Cross screening line with RNAi flies (in case of overexpressed gene of interest) OR cross screening line with UAS-GAL4 X (in case of underexpressed gene of interest) and check for hemocyte count or sessile banding pattern rescue.

CHAPTER III

EXPRESSION OF CHRONIC MYELOID LEUKEMIA ONCOGENES *BCR-ABL*^{P210} AND *BCR-ABL*^{T315I} AFFECT CELLULAR AND HUMORAL INNATE IMMUNITY IN *DROSOPHILA MELANOGASTER*

Dana Abubaker[1,2*], Amro Baassiri[3*], Mirna Ghannam[1,2,] Amani Al Outa[3], Ali Ghais[1], Elias Rahal[1,2], Rihab Nasr[3*] and Margret Shirinian[1,2*]
Published: *Micropublication Biology, 2022.*

A. *Abstract*

Chronic myeloid leukemia (CML) is a myeloproliferative neoplasm that results from a chromosomal translocation between chromosome 9 and chromosome 22. The resulting fusion gene (*BCR-ABL*) encodes a constitutively active BCR-ABL tyrosine kinase. Some mutations of this oncogene, especially the Threonine 315 to Isoleucine substitution of the ABL kinase is resistant to first and second-generation tyrosine kinase inhibitors (TKIs) conventionally used in CML therapy. We have previously validated a CML fruit fly model for drug screening using the adult fly compound eye. Here we expressed wild-type *BCR-ABL*^{P210} and mutated *BCR-ABL*^{T315I} in *Drosophila melanogaster* hematopoietic system to understand the phenotypic consequences of this expression and its impact on innate immune pathways. Flies expressing both wild-type *BCR-ABL*$^{\mathrm{P210}}$ and mutant *BCR-ABL*$^{\mathrm{T315I}}$ showed increased number of circulating hemocytes, disruption in sessile patterning of resident hemocytes, dysregulation in the humoral Toll, Imd, and JAK/STAT pathways at the mRNA level in both the 3rd instar larva and adult stage. Of note, *BCR-ABL*$^{\mathrm{T315I}}$ flies presented more severe phenotypes and a higher deviation in humoral

dysregulation than BCR-*ABL*^{P210} flies pointing towards more complex oncogenic effect of this mutant which requires further investigation.

B. Introduction

Chronic Myeloid Leukemia (CML) is a myeloproliferative neoplasm resulting from the BCR-ABL1 fusion protein coded by the Philadelphia chromosome which results from a reciprocal translocation between the *Abelson* murine leukemia gene (*ABL*) on chromosome 9 and *Breakpoint Cluster Region* gene (*BCR*) on chromosome 22 [120-122]. This translocation creates the *BCR-ABL1* oncogene which codes for the BCR-ABL1 fusion protein; a constitutively active tyrosine kinase [123]. Tyrosine kinase inhibitors (TKIs) are considered the gold standard treatment for CML patients [124]. Despite the advancement offered by the first and second-generation TKIs, there are certain resistant BCR-ABL1 mutant leukemic clones. For instance, the T315I mutation which results from the substitution of Threonine with Isoleucine at the 315th position of ABL imparts resistance to first and second generation TKIs [12, 125]. One TKI that showed efficacy against the T315I mutation is ponatinib [126, 127]. However, due to its pan-activity on different kinases, ponatinib has severe side effects and high toxicity and is now administered to patients with precaution [128]. Despite the extensive research on BCR-ABL1, the molecular mechanisms and functional interactors in wild-type P210 and T315I mutant background are yet to be fully understood. Conservation between *Drosophila melanogaster* and mammalian genes [129], in addition to the shared homology in proteins that interact with BCR-ABL1 [116, 130], suggest that a fly model can be used to understand BCR-ABL1 genetic interactors [117]. We previously validated a CML *Drosophila* model for drug screening using TKIs. We expressed *BCR-ABL*^{P210} and *BCR-*

ABL^{T315I} in *Drosophila* eyes and observed a rough eye phenotype which was more severe in T315I mutants. Furthermore, we used this eye model to test the efficacy of clinically administered TKIs [114]. Bernardoni *et al.* showed similar rough eye phenotypes upon expression of *BCR-ABL*^{P210} through interaction with endogenous *Drosophila* Abl (Ena) indicating a conserved signal transduction pathway between humans and flies. In addition, *BCR-ABL1* expression in the hematopoietic precursor cells of the lymph gland affected *Drosophila* blood cell homeostasis by increasing the number of circulating blood cells [115]. Nevertheless, the impact of *BCR-ABL1* oncogene on innate immunity is yet to be understood. Fruit flies possess two forms of innate immune responses, cellular and humoral. The cellular response is mediated by *Drosophila* hemocytes which can be either circulating or sessile. Circulating hemocytes are present in the hemolymph while sessile hemocytes are found in pockets between the epidermis and muscular layers in the larvae [131, 132]. Circulating hemocytes can be of three types, macrophage-like plasmatocytes, crystal cells and lamellocytes. Plasmatocytes phagocytose bacteria and apoptotic debris while crystal cells are involved in melanization process; the latter is analogous to wound healing. Lamellocytes, the largest in size among circulating hemocytes, are very low in number and differentiate only upon parasitic infection [133, 134]. The humoral response on the other hand results in the synthesis of antimicrobial peptides (AMPs) and hemolymph coagulation and melanization. Humoral pathways help *Drosophila melanogaster* discriminate between pathogens based on their surface molecules such that, either one of the NF-κB transcription factors can be activated; Dorsal/Dif or Relish, which are representative of the Toll or Imd pathway, respectively. The JAK/STAT pathway on the other hand was shown to be involved in viral infection whereby Domeless activates the transcription factors Hopscotch and STAT92E, consequently activating the expression of immune and stress-responsive genes such as *Tep1* and *Tot A [104, 135]*. Therefore, the *Drosophila's* reductionist hematopoietic and immune system would aid in understanding the role of *BCR-ABL1* expression on the immune response and hematopoiesis in general.

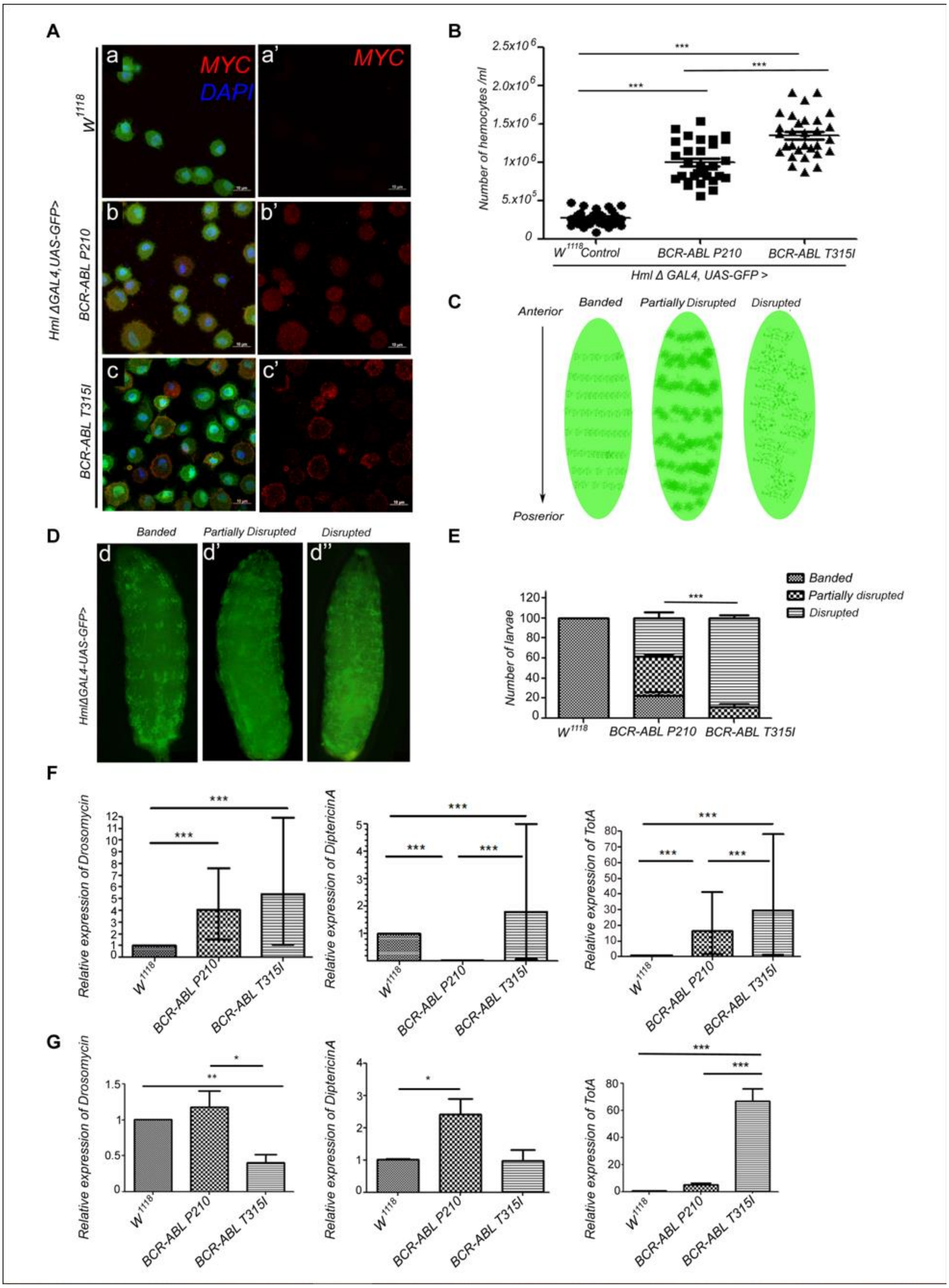

Figure 10. Expression of BCR-ABL^{P210} and BCR-ABL^{T315I} in *Drosophila melanogaster* hematopoietic system results in an increase in hemocyte count, disruption in the patterning of the sessile hemocytes, and TotA overexpression which persists from 3rd instar larval to adult stage in *BCR-ABL^{T315I}* flies:

(A) Maximum intensity projection at 100X magnification showing absence of MYC (tag present at the N-terminus of both BCR-ABL^{P210} and BCR-ABL^{T315I} flies) staining in GFP-positive control hemocytes (a, a'), MYC expression in GFP-positive hemocytes indicating expression of BCR-ABL^{P210} (b, b') and BCR-ABL^{T315I} (c, c'). Scale bar is 10 µm. (B) A significant increase in hemocyte count in BCR-ABL^{P210} and BCR-ABL^{T315I} expressing larval bleed when compared to control flies and to each other. (C, D) Sketch Diagram and representative images of disruption in sessile hemocyte patterning in BCR-ABL^{P210} and BCR-ABL^{T315I} flies. Green fluorescence indicates GFP expressed in lymph gland and circulating hemocytes under Hml Δ-Gal4; UAS-GFP driver. Regular banding of sessile patterning of hemocytes in third-instar control larva (d), partial disruption of sessile hemocyte in BCR-ABL^{P210} third-instar larva (d'), and complete disrupted patterning of sessile hemocytes in BCR-ABL^{T315I} third-instar larva (d''). (E) Enumeration of banded, partially disrupted, and disrupted patterning in control, BCR-ABL^{P210} and BCR-ABL^{T315I} larva demonstrating the disruptive phenotype in BCR-ABL^{P210} and BCR-ABL^{T315I} larva with a significant exacerbated phenotype in the latter. (F) Drosomycin, Diptericin A, and TotA relative expressions normalized to RP49 in control, BCR-ABL^{P210} and BCR-ABL^{T315I} larva hemolymph. A significant increase of all expressions in BCR-ABL^{P210} and BCR-ABL^{T315I} larva when compared to control flies except Diptericin A which is under expressed in BCR-ABL^{P210} larva. A significant increase of Diptericin A and TotA in BCR-ABL^{T315I} larva when compared to BCR-ABL^{P210} larva. (G) Drosomycin, Diptericin A, and TotA relative expressions normalized to RPL11 in control, BCR-ABL^{P210} and BCR-ABL^{T315I} adult flies. A significant decrease of Drosomycin expression in BCR-ABL^{T315I} adult flies when compared to control flies and BCR-ABL^{P210}. Diptericin A is overexpressed in BCR-ABL^{P210} adult flies compared to control adult flies. TotA is overexpressed in BCR-ABL^{T315I} adult flies compared to BCR-ABL^{P210} and control adult flies. Error bars represent S.E.M B,D,E: n = 30 triplicates tested. F: n = 50 triplicates tested. G: n= 25 triplicates tested. One-way ANOVA with Tukey's posthoc test (B), Chi-square test (E), and unpaired T-test (F,G) were performed to test statistical significance (*, $p<0.05$; **, $p<0.01$; ***, $p<0.001$).

C. Methods

1. Fly stocks

Fly stocks used were *w1118 (wt)* (BDSC #3605), Hml Δ-Gal4; UAS-GFP (BDSC #30140), *UAS-BCR-ABL^{P210}* (p210)[114] and *UAS-BCR-ABL^{T315I} (T315I)* [114]. Fly crosses were performed at 29˚C.

2. Immunofluorescence

For hemocyte staining, late wandering third instar were bled in 10 µl of 1X-PBS in a 12 well plate using a modified protocol [136]. Then the bleed was transferred to slides and left to attach for 30 minutes in a humidified chamber. The bleed was washed with 1X PBS- 0.3% Triton (PBST) twice for 5 minutes, samples were then blocked in 5% Normal Goat Serum (NGS) in PBST (Dako, Santa Clara, CA) for 2 hours. Anti-Myc antibody (9E-10 kind gift from Bengt Hallberg) 1:300 was used on hemocytes overnight. Samples were washed with PBST 2x5 minutes. Samples were incubated with secondary antibody Alexa-594 1:500 in 5%NGS PBST (Abcam, Cambridge, UK). Samples were washed with PBST 2x5 minutes. Then Fluor shield Mounting Medium with DAPI (Abcam) was added and samples were then imaged using a laser scanning confocal microscope (Carl Zeiss Laser Scanning Microscopy 710, Jena, Germany).

3. Hemocyte bleed and count

Late wandering third-instar larvae were picked from the walls of the food vial with a pair of forceps and cleaned from food and debris by placing them in a 1X PBS containing petri plate before being transferred to a tissue paper to dry them. The larvae were kept in the petri plate on ice throughout the bleed process to minimize their movement. The larvae were placed in 13 µl of 1X-PBS that was placed on parafilm strip under a light microscope. Using two pair of forceps the larval cuticle was pierced and hemolymph was released. The larva was left to bleed for 30 seconds. The larva was removed with one side of the forceps not to lose a greater volume of the bleed. The hemolymph bleed was mixed thoroughly with a pipette before taking 10 µl of the bleed and placing it in a Neubauer chamber (Buerker-Turk, Marienfeld, Germany) with a coverslip attached. The Neubauer chamber was placed under an Axiostar plus light microscope (Zeiss, Oberkochen, Germany) and number of cells in each of the four quadrants was noted down. Hemocyte number was then reported as hemocytes per milliliter of bleed. The average number of hemocytes was obtained from three different biological replicates (N=3) with ten third-instar larvae for each replicate. Total number of larvae used in each condition is (n=30).

4. Larvae handling and imaging for sessile patterns

Late wandering third-instar larvae were picked from the walls of the food vial with a pair of forceps and cleaned from food and debris by placing them in a petri plate containing 1X Phosphate Buffered Saline (PBS) (Sigma Aldrich, St. Louis, MO). After drying with a tissue paper, the larvae were placed in an Eppendorf at -80ºC for one and a half minute. The Eppendorf was then placed on a plate on ice. The larvae were then imaged for sessile patterning using an SZX2-ILLT GFP Olympus microscope (Olympus, Tokyo, Japan) while submerged in a drop of 50% glycerol (Sigma-Aldrich, St. Louis, MO) This is a modified protocol [137]. Performed on three different biological replicates (N=3) with thirty third-instar larvae for each replicate. Total number of larvae used in each condition is (n=90).

5. *RNA extraction*

a. Third-instar larva:

50 larvae were bled in 20-60 microliter PBS then put in 1 milliliter of Trizol (TRI reagent, Sigma Aldrich). Centrifugated at 12,000g for 15 mins at 4ºC. Then 200 microliters of chloroform (Sigma-Aldrich) were added. Tubes were shaken well then centrifugated at 12,000g for 15 mins at 4ºC. Upper layer was transferred to another Eppendorf and added to it 0.7V of isopropanol 100%. Kept at room temperature for 10mins. Then centrifugated for 30 mins max speed at 4ºC. Isopropanol was removed then RNA pellet was washed with 1 milliliter ethanol 70% (Sigma-Aldrich) which was centrifugated at max speed for 10 mins at 4ºC. Ethanol was removed and Eppendorf was set to air dry for 10 mins under hood. Pellet was resuspended in 20 microliter Nuclease free water (Autoclaved milli-Q water). Performed on three different biological replicates (N=3) with fifty third-instar larvae for each replicate. Total number of larvae used in each condition is (n=150).

b. Adult flies:

Total RNA was extracted using Trizol from 25 adult flies (3 days old). After adding 150µl of Trizol, flies were grinded using a pestle while working on ice. The pestle was washed with additional 150 µl of Trizol. The samples were left to incubate for 5 minutes at room temperature under the fume hood then centrifuged at (14,000 g) at 4˚C for 5 minutes. All centrifugations were done at 4˚C at maximum speed (14,000 g). Chloroform was added to the Trizol in a ratio of 1:5 (Chloroform: Trizol). The sample were mixed and incubated for 1 minute and centrifuged for 10 minutes. The upper layer was transferred, and isopropanol was added. The mixture was incubated at room temperature for 10 minutes and then centrifuged for 30 minutes. Samples were then washed with 70% ethanol twice and centrifuged for 10 minutes. the pellet was air-dried and resuspended in 30 µl Nuclease free water. Performed on three different biological replicates (N=3) with 25 adult flies for each replicate. Total number of larvae used in each condition is (n=75).

6. RT- PCR

Real time PCR was performed using SYBR green (Bio-Rad). Each sample was run in triplicates. Bio-RAD CFX96 Real time system was used for real time analysis. Relative gene expression was analyzed using the Livak and Schmittegn system [138]. The assessment was repeated for three biological replicates where each biological group included 50 third-instar larva/25 adult flies. In the case of the larva, expression levels were normalized against the housekeeping gene *Ribosomal protein 49* (*Rp49*). While in the case of the adult flies, expression levels were normalized against the housekeeping gene *Ribosomal protein L11* (*RpL11*). The Forward and Reverse primers (Macrogen, Seoul, South Korea) sequences used all have an annealing temperature of 57 °C. Sequences are reported in the Reagents section. Targets tested were *Drosomycin*, *Diptericin A* and *TotA*.

7. *Statistical Analysis Results*

These statistical analyses were performed on a GraphPad Prism 6.0 program. P-values lower than 0.05 were considered statistically significant.

Table 1. Statistical analyses results

Figure Panels	**Statistical Test**		**P value**
B	ANOVA		<0.0001
B	Tukey’s post-hoc test	wt vs. BCR-ABL^{P210}	<0.0001
B	Tukey’s post-hoc test	wt vs. BCR-ABL^{T315I}	<0.0001
B	Tukey’s post-hoc test	BCR-ABL^{P210} vs. BCR-ABL^{T315I}	<0.0001
E	Chi-square test	Banded: wt vs. BCR-ABL^{P210}	<0.0001
E	Chi-square test	Banded: wt vs. BCR-ABL^{T315I}	<0.0001
E	Chi-square test	Banded: BCR-ABL^{P210} vs. BCR-ABL^{T315I}	<0.001
E	Chi-square test	Partially: wt vs. BCR-ABL^{P210}	<0.0001
E	Chi-square test	Partially: wt vs. BCR-ABL^{T315I}	0.0115
E	Chi-square test	Partially: BCR-ABL^{P210} vs. BCR-ABL^{T315I}	0.0018
E	Chi-square test	Disrupted: wt vs. BCR-ABL^{P210}	<0.0001
E	Chi-square test	Disrupted: wt vs. BCR-ABL^{T315I}	<0.0001
E	Chi-square test	Disrupted: BCR-ABL^{P210} vs. BCR-ABL^{T315I}	<0.0001
F	Unpaired T-test	*Drosomycin*: wt vs. BCR-ABL^{P210}	<0.001
F	Unpaired T-test	*Drosomycin:* wt vs. BCR-ABL^{T315I}	<0.001
F	Unpaired T-test	*Drosomycin:* BCR-ABL^{P210} vs. BCR-ABL^{T315I}	0.47
F	Unpaired T-test	*Diptericin A:* wt vs. BCR-ABL^{P210}	<0.001
F	Unpaired T-test	*Diptericin A:* wt vs. BCR-ABL^{T315I}	<0.001

F	Unpaired T-test	*Diptericin A:* BCR-ABL^{P210} vs. BCR-ABL^{T315I}	<0.001
F	Unpaired T-test	*TotA:* wt vs. BCR-ABL^{P210}	<0.001
F	Unpaired T-test	*TotA:* wt vs. BCR-ABL^{T315I}	<0.001
F	Unpaired T-test	*TotA:* BCR-ABL^{P210} vs. BCR-ABL^{T315I}	<0.001
G	Unpaired T-test	*Drosomycin*: wt vs. BCR-ABL^{P210}	0.47
G	Unpaired T-test	*Drosomycin:* wt vs. BCR-ABL^{T315I}	0.0068
G	Unpaired T-test	*Drosomycin:* BCR-ABL^{P210} vs. BCR-ABL^{T315I}	0.0365
G	Unpaired T-test	*Diptericin A:* wt vs. BCR-ABL^{P210}	0.0442
G	Unpaired T-test	*Diptericin A:* wt vs. BCR-ABL^{T315I}	0.9008
G	Unpaired T-test	*Diptericin A:* BCR-ABL^{P210} vs. BCR-ABL^{T315I}	0.0713
G	Unpaired T-test	*TotA:* wt vs. BCR-ABL^{P210}	0.0578
G	Unpaired T-test	*TotA:* wt vs. BCR-ABL^{T315I}	0.0022
G	Unpaired T-test	*TotA:* BCR-ABL^{P210} vs. BCR-ABL^{T315I}	0.0030

8. Reagents

Table 2. *Drosophila melanogaster* stocks used

	Genotype	Source	Stock #
w1118 (wt)	w[1118]	Bloomington *Drosophila* Stock Center	3605
Hml Δ-Gal4; UAS-GFP	w[1118]; P{w[+mC]=Hml-GAL4.Delta}2, P{w[+mC]=UAS-2xEGFP}AH2	Bloomington *Drosophila* Stock Center	30140
UAS-BCR-ABL^{P210}	*UAS-BCR-ABL^{P210}*	[114]	FBtp0141454
UAS-BCR-ABL^{T315I}	*UAS-BCR-ABL^{T315I}*	[114]	FBtp0141455

Table 3. Primers used for RT-PCR

Target Gene	Primer	Sequence (5' to 3')
Drosomycin	Forward	TACTTGTTCGCCCTCTTCG
	Reverse	GTATCTTCCGGACAGGCAGT
Diptericin A	Forward	AAGTGGGAAGCACCTACACCTACA
	Reverse	GTATCTTCCGGACAGGCAGT
TotA	Forward	CCCAGTTTGACCCCTGAG
	Reverse	GCCCTTCACACCTGGAGA
RP49	Forward	CGGATCGATATGCTAAGCTGT
	Reverse	GCGCTTGTTCGATCCGTA
RPL11	Forward	CGATCCCTCCATCGGTATCT
	Reverse	GCCCTTCACACCTGGAGA

D. Results

First, we validated the expression of *BCR-ABL*^{P210} and *BCR-ABL*^{T315I} in the hemocytes. We utilized the UAS-Gal4 system to drive oncogene expression in circulating hemocytes and the cortical zone of the lymph gland using *Hml Δ-Gal4;UAS-GFP [139]*. Upon larval bleed, the expression of GFP was visualized in hemocytes **(Figure 10A a,b,c)**. Control hemocytes lacking transgene expression **(Figure 10A a,a')** whilst the expression of the *BCR-ABL*^{P210} **(Figure 10A b,b')** and *BCR-ABL*^{T315I} **(Figure 10A c,c')** were visualized in most of the GFP expressing hemocytes merged images (**Figure 10A b,c**)

Next, we assessed the effect of expression of both oncogenes on circulating hemocytes (n=30 triplicates). Expression of both *BCR-ABL*^{P210} and *BCR-ABL*^{T315I} in hemocytes resulted in a significant increase in circulating hemocyte number compared to control. The average number of circulating hemocytes in control flies was 2.7×10^5 cells/ml, compared to 9.9×10^5 cells/ml in *BCR-ABL*^{P210} and 13.4×10^5 cells/ml in *BCR-ABL*^{T315I} expressing flies. Notably, *BCR-ABL*^{T315I} exhibited a significantly higher hemocyte number compared to *BCR-ABL*^{P210} **(Figure 10B)**.

Furthermore, we assessed sessile hemocyte mobilization since it is one of the key-indicators of the immune burden in *Drosophila melanogaster* (n=30 triplicates) [140, 141]. In addition, the defects observed in circulating hemocyte number by *BCR-ABL*^{P210} or *BCR-ABL*^{T315I} expression may also be reflected phenotypically affecting the regular banded pattern of the sessile hemocytes in third-instar larvae. Three phenotypic criteria were used to categorize the degree of sessile hemocyte disruption; banded, partially disrupted, and disrupted **(Figure 10C, D)**. The expression of *BCR-ABL*^{P210} and *BCR-ABL*^{T315I} resulted in disruption of sessile hemocyte patterning. All control larvae showed normal sessile patterning (100%). The patterning was disrupted in *BCR-ABL*^{P210}; with

40% exhibiting partial banding and 40% showing complete disruption. Interestingly, 90% of the *BCR-ABL*^{T315I} larvae showed complete disruption with merely 10% with partial banding. The increased disruption in *BCR-ABL*^{T315I} sessile patterning was highly significant compared to *BCR-ABL*^{P210} and was consistent with the higher increase in circulating hemocytes **(Figure 10E)**.

Given the phenotypic defects observed in the cellular arm of innate immunity in *BCR-ABL*^{P210} and *BCR-ABL*^{T315I} expressing larvae, we further examined the status of humoral Toll, Imd, and JAK/STAT pathways at the mRNA level by quantifying downstream effectors such as *Drosomycin*, *Diptericin A* and *Turandot A* (*TotA)* at the 3rd-instar larval (n=50 triplicates) and adult stages (n=25 triplicates). At the 3rd-instar larval stage, expression of *BCR-ABL*^{P210} and *BCR-ABL*^{T315I} resulted in dysregulation of all pathways. There was a significant increase in *Drosomycin* and *TotA* expression in *BCR-ABL*^{P210} and *BCR-ABL*^{T315I} larva when compared to the control; a mean of 4 and 5-fold increase in *Drosomycin* and a mean of 15 and 30-fold increase in *TotA* expression in *BCR-ABL*^{P210} and *BCR-ABL*^{T315I} larva, respectively. Notably, the overexpression of *TotA* in *BCR-ABL*^{T315I} larva was significant when compared to that of *BCR-ABL*^{P210} larva. As for *Diptericin A*, a significant under expression in *BCR-ABL*^{P210} larva was detected while *BCR-ABL*^{T315I} larva had a mean of 2-fold increase when compared to the control **(Figure 10F).** Likewise, at the adult stage, expression of *BCR-ABL*^{T315I} resulted in dysregulation of all pathways. We detected a significant down regulation in *Drosomycin* expression in *BCR-ABL*^{T315I} flies compared to control. However, there was no significant difference in *Drosomycin* expression when comparing BCR-*ABL*^{P210} to control. In addition, there was a 2.5-fold increase in *Diptericin A* expression in *BCR-ABL*^{P210} flies when compared to the control flies. Furthermore, there was a significant difference in *TotA* relative expression between control flies and *BCR-ABL*$^{\mathrm{T315I}}$. *BCR-ABL*^{T315I} expressing flies showed a 66.7-fold increase compared to *BCR-ABL*$^{\mathrm{P210}}$ which showed 5.1-fold increase compared to control (**Figure 10G**).

E. Discussion

Utilizing an established *Drosophila melanogaster* CML model [115], this study demonstrated transformative phenotypes in the hemolymph upon the expression of BCR-*ABL*$^{\mathrm{P210}}$ and *BCR-ABL*$^{\mathrm{T315I}}$ which were represented by an increase in hemocyte count and sessile hemocyte patterning disruption when compared to control flies. Moreover, these phenotypic defects in the cellular arm of innate immunity were associated with dysregulation in the humoral Toll, Imd, and JAK/STAT pathways at the mRNA level in both the 3$^{\mathrm{rd}}$ instar larval and adult stages. Interestingly, *BCR-ABL*$^{\mathrm{T315I}}$ flies presented more severe phenotypes and a higher deviation in humoral dysregulation than BCR-*ABL*$^{\mathrm{P210}}$ flies when compared to the control; there were significant differences even between BCR-*ABL*$^{\mathrm{P210}}$ and *BCR-ABL*$^{\mathrm{T315I}}$ flies.

The higher number of hemocytes exhibited in *BCR-ABL*$^{\mathrm{T315I}}$ flies when compared to wild-type *BCR-ABL*$^{\mathrm{P210}}$ flies indicates a more prominent effect of the *BCR-ABL*$^{\mathrm{T315I}}$ mutant on hemocyte homeostasis. The importance of this finding stems from the role hemocytes play as a primary line of defense in *Drosophila melanogaster*. A similar increase in the hemocyte number was observed in another study when *BCR-ABL*$^{\mathrm{P210}}$ was expressed in the lymph gland [142]. Furthermore, since the presence of a stressor such as expression of oncogenes might result in the recruitment of hemocytes from sessile compartments to the hemolymph [141], we examined whether *BCR-ABL1* expression presents an immune burden and if *BCR-ABL*$^{\mathrm{P210}}$ mobilizes the sessile hemocytes differently from *BCR-ABL*^{T315I}. We observed more prominent sessile patterning disruption in *BCR-ABL*^{T315I}. This could highlight differential interaction of *BCR-ABL*^{T315I} with the extracellular matrix (ECM) that controls hemocyte migration. For instance, Kumar *et al.*, suggested that *BCR-ABL*^{T315I} varies from wild-type *BCR-ABL*^{P210} in its interaction with the ECM. Particularly, the integrin β3/ILK-mediated signaling pathway affects leukemia progression in *BCR-ABL*^{T315I} distinctly compared to wild-type *BCR-ABL*^{P210}. *BCR-ABL*^{T315I} showed lower phosphorylation of focal adhesion kinase (FAK) and integrin-linked kinase (ILK) as well as lower disposition of Fibronectin [54]. Furthermore, Moreira *et al*. showed that *zyxin* knockdown (involved in the formation of adhesion sites that connect the ECM to the cellular cytoskeleton) resulted in a significant increase in cell speed and migration [143]. Therefore, one possible explanation for the severe disruption in sessile patterning in *BCR-ABL*^{T315I} could be its involvement in activating integrins and adhesion complexes which are required for migration of the sessile hemocytes.

The effect of *BCR-ABL1* on the cellular immunity consequently directed us to assess the status of humoral immune pathways upon oncogene expression. The Toll pathway for example, is an important regulator of hemocyte number in the hemolymph and their proliferation in the lymph gland [104, 144]. Toll pathway activation results in *Drosomycin* and *Metchikowin* activation [145, 146]. When assessing the Toll pathway, there was a significant upregulation in *Drosomycin* transcript level in BCR-*ABL*^{P210} and *BCR-ABL*^{T315I} flies during 3rd instar larval stage which is maintained in adult flies of the former genotype while the latter is significantly downregulated in the adult stage. Meanwhile, concerning the Imd pathway, *Diptericin A* levels are usually first observed at the 3rd instar larval stage which peak at the pupal stage only to decrease once again at the adult stage to levels lower than that of 3rd instar larva [147]. This pattern was observed in the *BCR-ABL*^{T315I} flies whereby they had a significantly higher expression at the 3rd instar larval stage when compared to the control, only to return to comparable levels once more at the adult stage. However, interestingly BCR-*ABL*^{P210} flies shifted from having a significant under expression at the 3rd instar larval stage to a significant over expression at the adult stage when compared to control flies.

As for the JAK/STAT pathway, the *TotA* gene is expressed during the third-instar larval stage, maintained throughout the entire pupal period, then expressed little to none during the adult life only to increase gradually once more 3-4 weeks after eclosure. However, it is induced in adults under stressful conditions such as high temperatures and bacterial challenge [148, 149]. As such, we anticipated an increase in *TotA* expression in all flies at 29ºC. Interestingly, there was a significant increase in *TotA* expression in BCR-*ABL*^{T315I} flies which was maintained from the 3rd instar larval stage into the adult stage while BCR-*ABL*^{P210} flies demonstrated an overexpression only in the 3rd instar larval stage only to return to control fly levels during the adult stage. This suggests that the *BCR-ABL*^{T315I} mutant is more stress tolerant. This may be associated with an increased expression of heat shock proteins, stress induced MAP kinase cascades, NF-κB signal transduction, and/or JAK/STAT pathway signaling events; all of which could contribute to resistance in CML patients with this mutation against TKIs. In fact, the JAK/ STAT pathway has been studied extensively in CML. STAT5 was shown to maintain the survival and growth of CML cells and JAK2 has been correlated with increased LSC persistence in a TKI background [150]. Therefore, any of these stress-response signaling elements could be therapeutic targets for a combined therapy with current FDA approved TKIs. In fact, clinical trials utilizing pegylated interferon (IFN) in combination with second generation TKIs are already underway [151]. Lastly, due to the significant increase in JAK/STAT pathway in *BCR-ABL*^{T315I}, reflected in the increase of *Tot A* maintained from 3rd instar larval to adult stage, associated with the significant decrease in *Drosomycin* during the adult stage echoed the findings by Kim *et al.* which showed that overexpression of the JAK/STAT pathway could decrease *Drosomycin* via the Jra/Stat92E/Dsp1 repressosome complex [152]. As such, it would be interesting to conduct bacterial challenge assays examining the JAK/STAT pathway, which might elucidate the etiology behind resistance to TKI treatment experienced by CML patients with mutant BCR-*ABL*^{T315I} and whether this strong stress response perpetuated by JAK-STAT pathway may result in suppression of other critical immune pathways which might affect response to treatment.

CHAPTER IV

UNRAVELING THE MOLECULAR SIGNATURE OF *BCR-ABL*^{P210} AND *BCR-ABL*^{T315I} *IN* THE *DROSOPHILA MELANOGASTER* CML MODEL

Amro Baassiri, Ali Ghais, Abdallah Kurdi, Elias Rahal, Rihab Nasr*, and Margret Shirinian* to be submitted

A. *Abstract*

Chronic myeloid leukemia (CML) is a clonal hematopoietic stem cell disorder resulting from a balanced translocation namely the Philadelphia chromosome. It produces the *BCR-ABL1* oncogene that encodes for the BCR-ABL1 fusion protein that demonstrates an increased activity in its tyrosine kinase. Despite the development of Tyrosine kinase inhibitors (TKIs), the notorious T315I (*BCR-ABL*^{T315I}) gatekeeper point mutation remains elusive. The available options ponatinib and asciminib have some serious side effects and they have promising results in chronic phase patients only. We utilized our validated *Drosophila* CML models to find novel potential targets. We have previously reported an increased hemocyte count and disruption in sessile hemocyte banding patterns upon expression of both *BCR-ABL*^{p210} and *BCR-ABL*^{T315I} in the hemolymph, these phenotypes were more prominent and exacerbated in *BCR-ABL*^{T315I} flies. To understand the mechanism behind these phenotypes and assess whether there exists a gene signature that differentiates *BCR-ABL*^{p210} and *BCR-ABL*^{T315I} we opted to perform RNA sequencing to unravel their transcriptome. Their molecular signatures turned out to be very similar and allowed us to identify 6 upregulated genes which were cross-referenced and validated in adult, pediatric CML patients, and *BCR-ABL*^{T315I}

mice. We discovered 3 potential targets that partially rescued hemocyte count, 2 of which rescued both genotypes upon their knock down namely, *Rapgap1*and *CG9265*, while *spri* partially rescued *BCR-ABL*^{T315I} flies and increased hemocyte count in *BCR-ABL*^{p210} flies. *Meltrin* is another gene whose knockdown partially rescued the sessile hemocyte banding pattern; however, it along with *wing blister* had an oncogenic effect on hemocyte count. We have identified targets that are common to both BCR-ABL^{p210} and BCR-ABL^{T315I} which are worth pursuing since CML patients with and without the T315I mutation can benefit alike.

B. Introduction

The hallmark of chronic myeloid leukemia (CML), a clonal hematopoietic stem cell disorder, is the Philadelphia chromosome which is a balanced translocation between chromosomes 9 and 22 [153]. It results in the *BCR-ABL1* oncogene that encodes for the *BCR-ABL1* fusion protein which demonstrates an increased activity in its tyrosine kinase [123]. The development of tyrosine kinase inhibitors (TKIs) has changed the natural course of this disease. Nowadays, patients with CML who respond well to treatment are expected to have a relatively normal life expectancy [154, 155]. However, the notorious T315I (*BCR-ABL*^{T315I}) gatekeeper point mutation remains elusive to a great extent since it is completely resistant to first and second generation TKIs [41, 42]. Currently, the only available drugs that patients with *BCR-ABL*^{T315I} respond to are the third generation TKI and the allosteric inhibitor ponatinib and asciminib, respectively [43, 44]. However, ponatinib is associated with hepatotoxicity and serious cardiovascular events such as vascular occlusion and heart failure [44, 47, 48]. Some frequent adverse events reported with asciminib include gastrointestinal, pancreatic, and hepatotoxicity, myelosuppression, thrombocytopenia, leukopenia, and hemorrhage [43]. Despite demonstrating a promising efficacy in chronic-phase CML patients with *BCR-ABL*^{T315I}, both drugs have less than a 50% response rate in accelerated and blast-phase CML patients with *BCR-ABL*^{T315I} [43, 45, 46]. Therefore, there is a critical unmet clinical need to find novel potential targets against *BCR-ABL*^{T315I}.

We previously validated transgenic CML fly models expressing *BCR-ABL*^{p210} and *BCR-ABL*^{T315I} in the eye and hemolymph utilizing the glass multiple reporter (GMR) and hemolectin delta (Hml Δ) drivers, respectively [114, 156]. Upon the expression in the eye, flies presented with rough eyes and architectural distortion in their ommatidia[114]. The expression in the hemolymph resulted in an increased hemocyte count along with a disruption in the sessile hemocytes' banding pattern [156]. Moreover, in both models, expression of the *BCR-ABL*^{T315I} mutant demonstrated an exacerbated phenotype than that of *BCR-ABL*^{p210} [114, 156]. The highly conserved hematopoietic system between humans and *Drosophila* associated with the observed phenotypic changes in our CML hematopoietic model demonstrate potential to identify novel targets against the wild type *BCR-ABL*^{p210} and *BCR-ABL*^{T315I} mutant should we unravel the molecular signatures of our *BCR-ABL*^{p210} and *BCR-ABL*^{T315I} CML models, respectively [69, 70]. In fact, several genes that play a role in blood cell development with a potential involvement in human leukemia have been studied via this model [28-30]. A highly notorious gene was identified to play a significant role in human leukemia via the JAK/STAT pathway namely *hopscotch* which encodes the *Drosophila* homologue of JAK kinase [72]. As such, we extracted the hemolymph from our hematopoietic CML *Drosophila* models and unraveled their transcriptome. Furthermore, to validate our data, we cross-referenced them with the transcriptome of adult, pediatric patients with CML, and mice harboring the *BCR-ABL*^{T315I} mutation. As a first step, in this study we targeted the cross-referenced genes that were overexpressed when compared to control utilizing RNAi flies with the end-point of total or partial rescue of hemocyte count and/or sessile banding pattern in the attempt to find novel potential targets for the wild type *BCR-ABL*^{p210} and *BCR-ABL*^{T315I} mutant.

C. Methods

1. Fly stocks

Fly stocks used were *w1118* (*wt*) (BDSC #3605), IF/CyO; TM3sb/TM6tb (gift from Dr. Zakaria Kambris), Hml Δ-Gal4; UAS-GFP (BDSC #30140), *UAS-BCR-ABL*^{P210} (p210) (FBtp0141454) [114] and *UAS-BCR-ABL*^{T315I} (T315I) (FBtp0141455) [114]. *BCR-ABL*^{p210} and *BCR-ABL*$^{P210/T315I}$ were inserted into pUAST-attB *Drosophila* expression vector (Custom DNA cloning). 1x Myc tag (MEQKLISEEDL) with its own start codon was added at the N-terminus before the transcription start site of BCR (EcorI-and combined speI-xbaI sites). pUAST-attB-myc *BCR-ABL*^{p210} and pUAST-attB-myc *BCR-ABL*$^{p210/T315I}$ were injected into y1 w67c23;P {CaryP} ABLattP2 (8622 BDSC) embryos to generate transgenic flies (BestGene Inc, Chino Hills, CA). RNAi flies were obtained from Vienna Drosophila Resource Center (VDRC): *Rapgap1*-RNAi (VDRC #26721), *Spri*-RNAi (VDRC # 101164), *CG9265*-RNAi (VDRC #102456), *meltrin*-RNAi (VDRC #3702), *wing blister* (*wb*)-RNAi (VDRC #3141), *Zasp52*-RNAi (VDRC #102456). The screening lines generated: Hml Δ-Gal4/CyO; *BCR-ABL*^{p210}/ TM6tb and Hml Δ-Gal4/CyO; *BCR-ABL*^{T315I} / TM6tb (Fig 1. A-F). All crosses were performed at 29˚C.

2. *Crosses performed*

Hml Δ-Gal4; UAS-GFP flies were crossed with *wt*, *UAS-BCR-ABL*^{P210}, and *UAS-BCR-ABL*^{T315I} for hemolymph collection, RNA extraction, RNA-sequencing, and RT-PCR. Screening lines were crossed with RNAi flies whereby the selected progeny collected were green fluorescent and non-tubby (without TM6tb) since the genotype desired was either Hml Δ-Gal4/+; *BCR-ABL*^{p210}/ RNAi X or Hml Δ-Gal4/RNAi X; *BCR-ABL*^{p210}/ + (same case for *UAS-BCR-ABL*^{T315I}) depending on which chromosome the RNAi was. These underwent banding and hemocyte enumeration. Workflow and screening line generation are depicted in Figure 11.

3. *RNA extraction*

For RNA-seq samples, 300 larvae were bled in 240-300 microliter PBS then put in 700-760 microliter of Trizol (TRI reagent, Sigma Aldrich). For the RT-PCR, 150 larva were bled in 120-160 microliter PBS then put in 840-880 microliter of Trizol,centrifuged at 12,000g for 15 mins at 4ºC. Then 200 microliters of chloroform (Sigma-Aldrich) were added. Tubes were shaken well then centrifuged at 12,000g for 15 mins at 4ºC. Upper layer was transferred to another tube and added to it 0.1V 3M sodium acetate, 0.7V of isopropanol 100%, and 2 µl of glycoblue (Invitrogen), kept at room temperature for 10mins, then centrifuged for 30 mins max speed at 4ºC. Isopropanol was removed then RNA pellet was washed with 1 milliliter cold ethanol 70% (Sigma-Aldrich) which was centrifugated at max speed for 10 mins at 4ºC. Ethanol was removed and the pellet was set to air dry for 10 mins under the hood. Pellet was resuspended in 20 microliter Nuclease free water (Autoclaved milli-Q water) and theneft on heat block at 55°C for 10 mins. The above was performed on three different biological replicates (N=3) with 300 third-instar larvae for each replicate for RNA-seq, and 150 third-instar larvae for RT-PCR. Total number of larvae used in each condition is n=900 and n=450 for RNA-seq and RT-PCR, respectively.

4. *Hemocyte bleed and count*

Late wandering third-instar larvae were picked from the walls of the food vial with a pair of forceps and cleaned from food and debris by placing them in a 1X PBS containing petri plate before being transferred to a tissue paper to dry them. The larvae were placed in 10 microliter of 1X-PBS that was placed on parafilm strip under a light microscope. Using two pair of forceps the larval cuticle was pierced and hemolymph was released. The larva was left to bleed for 20 secs. The larva was removed with one side of the forceps not to lose a greater volume of the bleed. The hemolymph bleed was pipetted and mixed with an equal volume of trypan blue. A total of 10 microliter of the mix was placed in a Neubauer chamber (Buerker-Turk, Marienfeld, Germany) with a coverslip attached. The Neubauer chamber was placed under an Axiostar plus light microscope (Zeiss, Oberkochen, Germany) and number of cells in each of the four quadrants was noted down. Hemocyte number was then reported as hemocytes per milliliter of bleed. The average number of hemocytes was obtained from three different biological replicates (N=3) with ten third-instar larvae for each replicate. Total number of larvae used in each condition is (n=30).

5. *Immunofluorescence*

We performed hemocyte staining, to validate our screening lines. Late wandering third instar were bled in 10 microliter of 1X-PBS in a 12 well plate using a modified protocol [136]. Then the bleed was transferred to slides and left to attach for 30 mins in a humidified chamber. The bleed was washed with 1X PBS- 0.3% Triton (PBST) twice for 5 mins and samples were then blocked in 5% Normal Goat Serum (NGS) in PBST (Dako, Santa Clara, CA) for 2 hours. Anti-Myc antibody (9E-10 kind gift from Bengt Hallberg) 1:300 was used on hemocytes overnight. Samples were washed with PBST 2x5 mins and incubated with secondary antibody Alexa-594 1:500 in 5%NGS PBST (Abcam, Cambridge, UK). Then, after 2 washes with PBST, Fluor shield Mounting Medium with DAPI (Abcam) was added and samples were then imaged using a laser scanning confocal microscope (Carl Zeiss Laser Scanning Microscopy 710, Jena, Germany)(Fig 18).

6. Larvae handling and imaging for sessile patterns

Late wandering third-instar larvae were picked from the walls of the food vial with a pair of forceps and cleaned from food and debris by placing them in a petri plate containing 1X Phosphate Buffered Saline (PBS) (Sigma Aldrich, St. Louis, MO). After drying with a tissue paper, the larvae were placed on a plate and kept at -20ºC for 30-60secs. The larvae were then imaged for sessile patterning using an SZX2-ILLT GFP Olympus microscope (Olympus, Tokyo, Japan) (modified protocol from Anderl et al. 2016). The above was performed on three different biological replicates (N=3) with ten third-instar larvae for each replicate. Total number of larvae used in each condition is (n=30).

7. Quantitative RT-PCR

Real time PCR was performed using SYBR green (Bio-Rad). Each sample was run in triplicates. Bio-RAD CFX96 Real time system was used for real time analysis. Relative gene expression was analyzed using the Livak and Schmittegn system (Livak and Schmittgen 2001). The assessment was repeated for three biological replicates where each biological group included 150 third-instar larvae. Expression levels were normalized against the housekeeping gene *Ribosomal protein 49* (*Rp49*). The Forward and Reverse primer (Macrogen, Seoul, South Korea) sequences were as follow: *Diptericin A,* 5'-ACGCCACGAGATTGGACTG-3', 5'-CAGCTCGGTTCTGAGTTGC-3'; *Diptericin B,* 5'-CTATTCATTGGACTGGCTTGTGC-3', 5'- ATCGAATCCTTGCTTTGGGCT-3'; *ADGF-D,* 5'-GTGGTTTCTAGGTGCTTTGGT-3', 5'-CTCCCTCAGTGTTTCATAGGGT-3'; *Rapgap1,* 5'-CTACGATGCGAGAGGAAATCC-3', 5'-TCCTGTAGCACTTGGCCGTAT-3'; *meltrin,* 5'-TTCCATCAGTCGGAAGGAGAA-3', 5'-CGGTCGTATCACAGTGTAAGTTG-3'; *Spri,* 5'-GTGCGTCATCTCGACCGTAT-3', 5'-GGCTCCCCATTAAGCAGTGT-3'; *wb,* 5'-ATCGGATTGCGATAAGCGAAC-3', 5'-CGCCGTGAGATTCCAGTGAC-3'; *zasp52,* 5'-GGCGTGAAGAGCATTGTCAA-3', 5'-ATCGCTGTAAATGCCAACCG-3'; *Rp49,* 5'-CGCTTCAAGGGACAGTATCTG-3', 5'-AAACGCGGTTCTGCATGA-3'.

8. *RNA sequencing and data analysis*

Utilizing the Illumina NovaSeq6000, we performed RNA sequencing with a 100bp paired-end read and 40 million reads per sample. Raw fastq files were uploaded to Galaxy US server and were subjected to quality checks using FastQC [157]. Sequence alignment to dm6 reference genome was performed using HISAT2 [158]. Alignment BAM files were sorted and indexed using SAMtools [159]. Raw read count over genomic features was done using featureCounts [160] and annotation GTF file from FlyBase release 6.45 with parameters (-t gene -g gene_symbol -s 2 -p -B). Differential expression analysis was performed using DESeq2 [161] and genes with an absolute log2 fold change (Log2FC) > 1 and a p-adjusted < 0.05 were considered differentially expressed. Over-representation analysis of the differentially expressed genes was done using pathfindR [162]. We cross-referenced the upregulated genes in *BCR-ABL*^{p210}and *BCR-ABL*^{T315I} against adult and pediatric CML patient samples (PRJNA687184) as well as *BCR-ABL*^{T315I} mutant mice (PRJNA812502). Heatmap, volcano plots and PCA plot were generated using pheatmap, ggplot2, and ggfortify R packages, respectively.

9. *Statistical Analysis*

Statistical analyses were performed on a GraphPad Prism 6.0 program. RT-PCR results were tested via an unpaired T-test. Hemocyte counts were compared through one-way ANOVA followed by Tukey's post-hoc test and banding patterns were tested via Chi-square test. P-values lower than 0.05 were considered statistically significant.

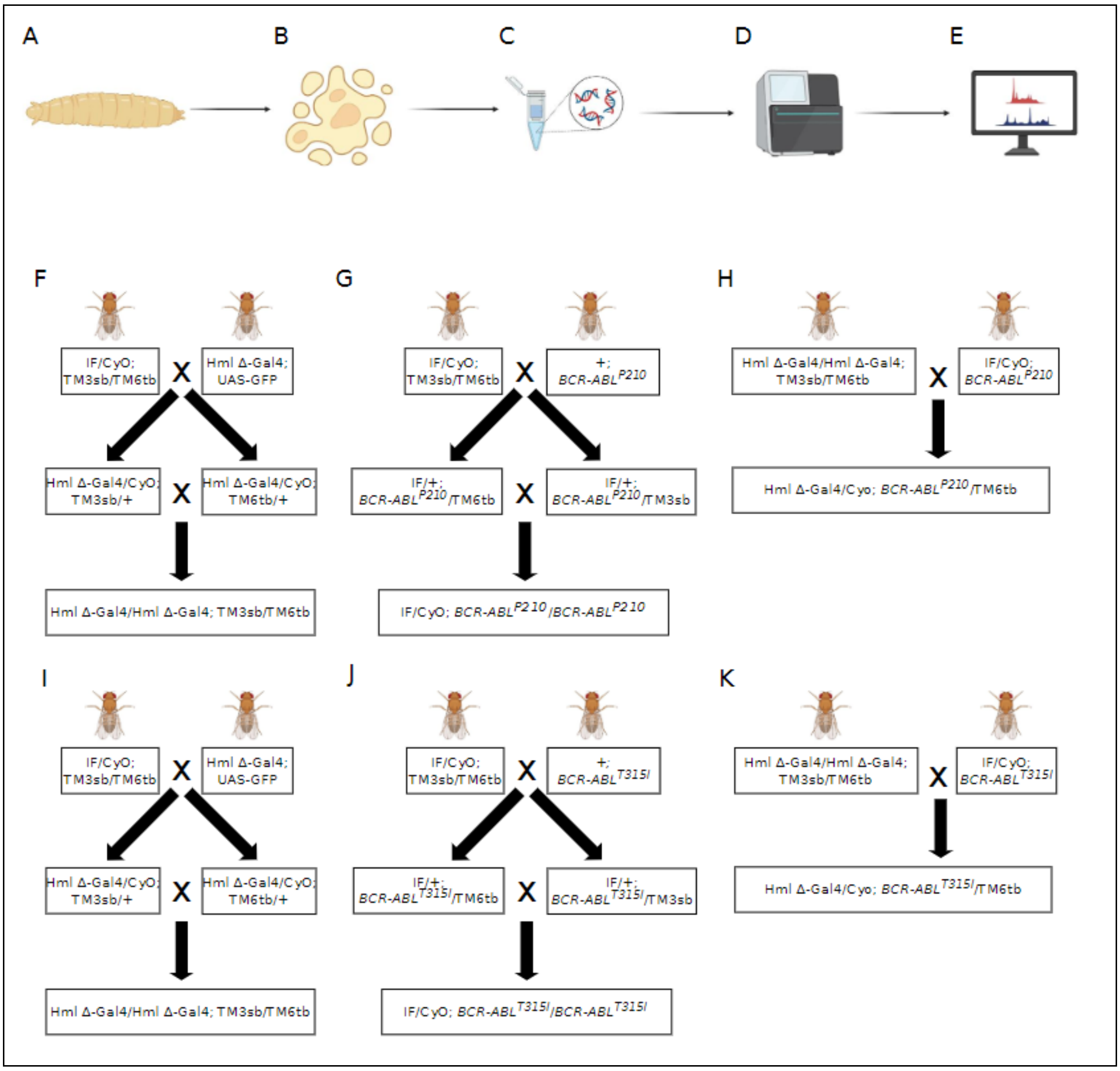

Figure 11. A workflow schematic.

(A) Third-instar larva were collected then (B) bled to collect their hemolymph. (C) RNA extracted from hemolymph that (D) underwent RNA-sequencing. (E) Transcriptomic data was analyzed. As for generating the screening lines, (F-H) these were the crosses performed to obtain the *BCR-ABL*^{P210} and (I-K) *BCR-ABL*^{T315I} screening lines.

D. Results

1. *The molecular signatures of BCR-ABL^{p210} and BCR-ABL^{T315I} are similar while distinctly different from that of wt control.*

The principle component analysis (PCA) plot reflects how similar the *BCR-ABL*^{p210} and *BCR-ABL*^{T315I} samples are within the same group and between each other (Fig 12A). This was further confirmed through the generated heat map (Fig 12B) that displayed striking distinct molecular signatures for the *BCR-ABL*^{p210} and *BCR-ABL*^{T315I} that stood out against *wt* control. Transcriptomic analysis reflected this as well whereby, for the condition of p-adjusted value <0.05 and absolute Log2FC >1, *BCR-ABL*^{p210} and *BCR-ABL*^{T315I} had a total of 3651 (789 upregulated vs. 2862 downregulated) and 3254 (622 upregulated vs. 2632 downregulated) differentially expressed genes (DEGs) compared to *wt* control (Fig 12C). Meanwhile, *BCR-ABL*^{T315I} has only a total of 35 (12 upregulated vs. 23 downregulated) DEGs when compared to *BCR-ABL*^{p210}.

The top 10 downregulated genes in *BCR-ABL*^{p210} compared to *wt* control in descending order were *lncRNA:CR44909, CG4151, CG3397, Eig71Ed, lncRNA:CR43835, lncRNA:CR40469, Eig71Ec, CG17105, fon,* and *Idgf5*. Meanwhile the top 10 downregulated genes in *BCR-ABL*^{T315I} compared to *wt* control in descending order were *lncRNA:CR44909, lncRNA:CR45347, Amy-d, Eig71Ed, CG34244, CG42500, CG4367, CG17105, DptB,* and *CG13606*.

The top 10 upregulated genes in *BCR-ABL*^{p210} compared to *wt* control in descending order were *dpr4, Ca-beta, tRNA:Leu-CAG-1-4, CG6553, CG10553, SPR, BomS2, CG5955, Tie,* and *ChLD3*. Whereas, the top 10 upregulated genes in *BCR-ABL*^{T315I} compared to *wt* control in descending order were *lncRNA:CR45650, SPR, yellow-g2, zye, sano, CG33462, CG16826, CG15370, CG3906,* and *CG16710*.

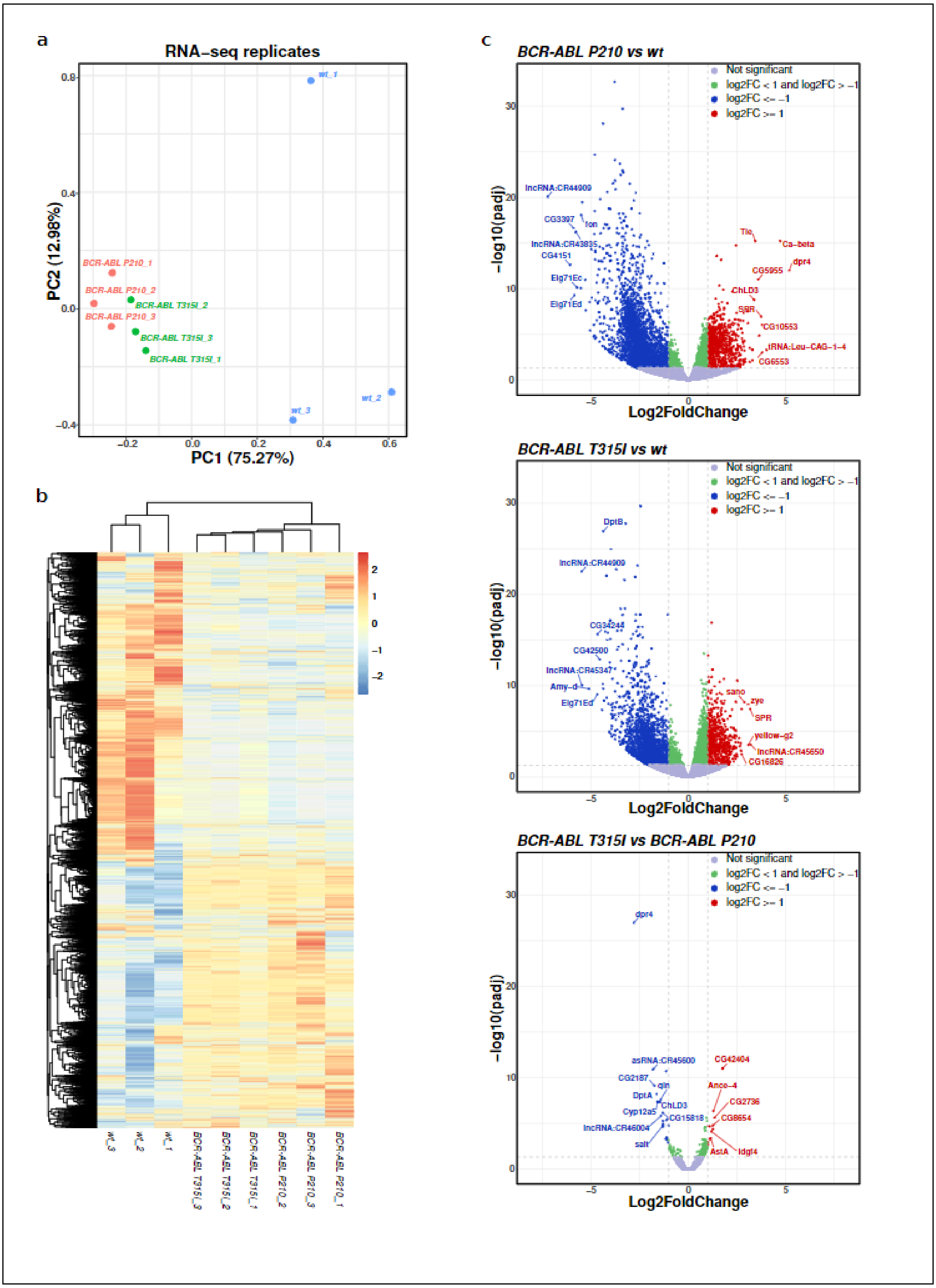

Figure 12. The molecular signatures of wt control, BCR-ABL^{P210}, and BCR-ABL^{T315I} hemolymph samples.

(a) Principal component analysis (PCA) of 9 distinct RNA-seq samples (3 samples from each genotype) highlighting the similarity between biological replicates of the same genotype and the difference between different genotypes. Markedly, the BCR-ABL^{P210} and BCR-ABL^{T315I} samples are relatively like each other compared to wt control. (b) A hierarchical clustering of all genes in the samples based on similarity of their gene expression profiles (columns) and their corresponding gene specific expression values (rows). The heat map generated displays similar gene profiles of BCR-ABL^{P210} and BCR-ABL^{T315I} samples and their differences compared to wt control. Red: relatively high expression; Blue: relatively low expression. The ratio values normalized by row. (c) Volcano plots showing differentially expressed genes (DEGs) in each comparison between genotypes. Upregulated genes (Log2FC≥1), down regulated genes (Log2FC≤ -1), and genes with -1< Log2FC >1 are represented by red, blue, and green dots, respectively. The gray dotted line represents the significant cutoff (p-adj value ≤ 0.05)

2. ***Integrating transcriptomic data from Drosophila BCR-ABL^{P210} and BCR-ABL^{T315I} with CML patient samples and mouse model reveals six potential common genes.***

We cross-referenced the upregulated genes in 2 separate analyses; once *Drosophila BCR-ABL^{p210}* and *BCR-ABL^{T315I}* against adult and pediatric CML patient samples, while another was against the adult CML patient samples and *BCR-ABL^{T315I}* mutant mice [163, 164]; we identified 16 and 11 common upregulated genes, respectively (Fig 13A). The first analysis was meant to identify potential targets against CML wild type while the second was to identify potential targets against the mutant type. Only six genes made the cut since they were common for both genotypes, had VDRC RNAi flies available in stock, and seemed promising based on our literature review. The genes were *Rapgap1, CG9265, meltrin, sprint (spri), wing blister (wb),* and *zasp52* (Fig 13B). Moreover, the overexpression of *meltrin* (p=0.0086), *spri* (p <0.0001), and *zasp52* (p <0.0001) in *BCR-ABL^{p210}* and *BCR-ABL^{T315I}* when compared to *wt* control were validated as well (Fig 14 A-E).

3. *Gene ontology biological process analysis comparing Drosophila BCR-ABL^{P210} and BCR-ABL^{T315I} transcriptome shows enrichment of the Toll/Imd signaling and purine metabolism pathways*

Upon gene ontology biological process analysis between *Drosophila BCR-ABL*^{p210} and *BCR-ABL*^{T315I} transcriptome, two pathways were enriched namely the Toll/Imd signaling pathway and purine metabolism pathway with the involvement of the *Diptericin A, Diptericin B,* and *ADGF-D*, respectively. *Diptericin A* and *Diptericin B* were downregulated in *BCR-ABL*^{T315I} when compared to *BCR-ABL*^{p210} with Log2FC values of -1.62 and -1.1, respectively. *ADGF-D* was overexpressed in *BCR-ABL*^{T315I} when compared to *BCR-ABL*^{p210} with Log2FC value of 1.26. However, these three genes were downregulated in the *BCR-ABL*^{p210} and *BCR-ABL*^{T315I} flies when compared to *wt* control. Although the relationship of *Diptericin A, Diptericin B,* and *ADGF-D* between *BCR-ABL*^{p210} and *BCR-ABL*^{T315I} were not validated, nevertheless these genes' underexpression with respect to *wt* control was validated by RT-PCR ($p < 0.0001$) (Fig 14 F-H).

A

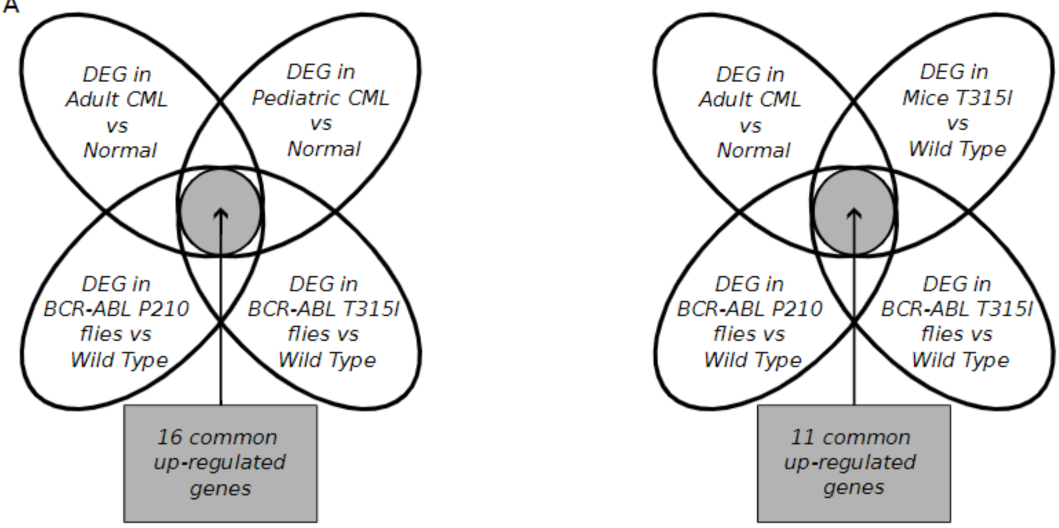

B

Fly gene	human orthologue	Function	Log2 (FC) fly *BCR-ABL*^{P210} vs wt	p-adjusted value	Log2 (FC) fly *BCR-ABL*^{T315I} vs wt	p-adjusted value	Log2 (FC) adult CML vs normal	p-adjusted value	Log2 (FC) *BCR-ABL*^{T315I} mice vs wt	p-adjusted value
Rapgap1	Rap1GAP	A GTPase activating protein (GAP); a major player in receptor-linked signaling pathways involved in cell growth and differentiation. [159]	2.15456727	0.0001009	1.976452157	0.0002	3.312886643	6.95E-05	0.976990485	0.0405220
Spri	RIN1	A Ras binding protein. Involved in multiple signal transduction pathways.[160]	1.24532425	8.17E-06	1.14004763	9.91E-07	2.00098681	0.0114862	1.511362722	0.0080466
wb	LAMA5	Encodes for lamnin, a major constituent of the basement membrane. Involved in cell adhesion, migration, and differentiation.[161]	1.45379183	0.0010979	1.448088447	0.000489	1.780538463	0.0011433	1.768025205	1.44E-08
Meltrin	ADAM8	A disintegrin and metalloprotease. involved in cell-cell and cell-matrix interactions[162]	1.84263429	4.47E-05	1.710346948	8.03E-05	1.35811921	0.0231167	3.749742363	6.17E-12
CG9265	DHRS3	A short chain hydrogenase/reductase. oxidixes and reduces a variety of substrates.[163]	1.07348834	0.0049110	1.10690467	0.003249	1.319264384	0.0231406	2.041389272	0.0038596
ZASP52	PDLIM5	A PDZ-LIM family member. A scaffold protein. Regulates cell structure and gene transcription.[164]	1.78623536	2.33E-05	1.706767887	1.43E-07	1.039877362	0.0216591	1.436912333	0.0003417

Figure 13. Cross-referencing transcriptomic data to validate and identify relevant targets.

(A) We had a total of 16 upregulated genes common to adult and pediatric patients with CML, while 11 upregulated genes common to adult patients with CML and *BCR-ABL*^{T315I} mutant mice. (B) We identified 6 potential upregulated targets namely, *Rapgap1*, *CG9265*, *meltrin*, *spri*, *wb*, and *zasp52* [165-170].

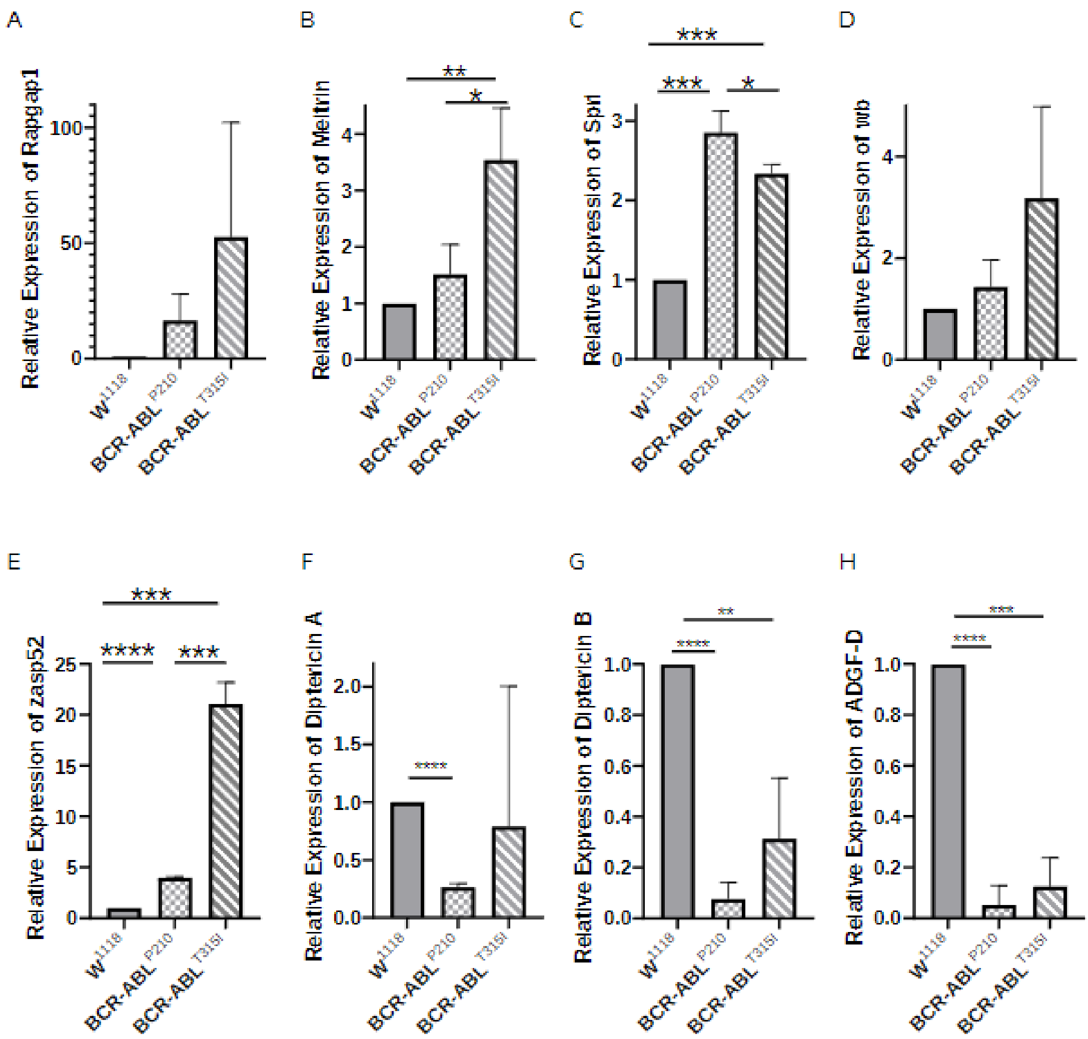

Figure 14. RT-PCR validation of transcriptomic data.

(A-E) *Rapgap1*, *meltrin*, *spri*, *wb*, and *zasp52* are overexpressed in *BCR-ABL*^{P210}, and *BCR-ABL*^{T315I} larva when compared to the *wt* control. (F-H) *Diptericin A*, *Diptericin B*, and *ADGF-D* are underexpressed in *BCR-ABL*^{P210}, and *BCR-ABL*^{T315I} larva when compared to *wt* control. All genes were normalized to *RP49.* Error bars represent standard deviation. P-values (*, p<0.05; **, p <0.01; ***, p<0.001; ****, p<0.0001).

.

4. ***Downregulation of Rapgap1, spri, and CG9265 had a partial rescue effect on hemocyte count and downregulation of meltrin had a partial rescue effect on the sessile banding pattern.***

RNAi flies for the six selected upregulated genes were crossed with the *BCR-ABL*^{P210} and *BCR-ABL*^{T315I} screening lines to see if any would rescue the hemocyte count and/or sessile banding pattern phenotypes. *Rapgap1* RNAi partially rescued *BCR-ABL*^{P210} ($p < 0.0001$), and *BCR-ABL*^{T315I} flies ($p < 0.0001$), by reducing their hemocyte counts from an average of $1.16\text{x}10^6$ cells to $7.61\text{x}10^5$ and $1.94\text{x}10^6$ cells to $6.52\text{x}10^5$, respectively. *Spri* RNAi and *CG9265* RNAi partially rescued *BCR-ABL*^{T315I} by decreasing their hemocyte counts to *BCR-ABL*^{p210} levels ($p < 0.0001$), from an average of $1.94\text{x}10^6$ cells to $1.22\text{x}10^6$. However, *Spri* RNAi increased the hemocyte count in *BCR-ABL*^{P210} flies ($p = 0.0019$) from an average of $1.16\text{x}10^6$ cells to $1.39\text{x}10^6$. In addition, *Meltrin* RNAi and *wb* RNAi increased hemocyte count in *BCR-ABL*^{P210} ($p < 0.0001$) and *BCR-ABL*^{T315I} flies ($p < 0.0001$). *Meltrin* RNAi increased the hemocyte count in *BCR-ABL*^{P210} and *BCR-ABL*^{T315I} flies from an average of $1.16\text{x}10^6$ cells to $2.71\text{x}10^6$ and $1.94\text{x}10^6$ cells to $3.94\text{x}10^6$, respectively. While *wb* RNAi increased the hemocyte count in *BCR-ABL*^{P210} and *BCR-ABL*^{T315I} flies from an average of $1.16\text{x}10^6$ cells to $1.58\text{x}10^6$ and $1.94\text{x}10^6$ cells to $2.69\text{x}10^6$, respectively. *Zasp52* RNAi had no effect on either genotype (Fig 15). Concerning the sessile banding pattern, *meltrin* RNAi was the only RNAi to have an effect whereby it partially rescued the banding pattern in *BCR-ABL*^{P210} ($p = 0.0175$), and *BCR-ABL*^{T315I} flies ($p = 0.0195$). *BCR-ABL*^{P210} ratio of partial banding pattern increased from 3/30 baseline to 11/30 and *BCR-ABL*^{T315I} ratio of partial banding pattern increased from 0/30 baseline to 5/30 (Fig 16 & 17).

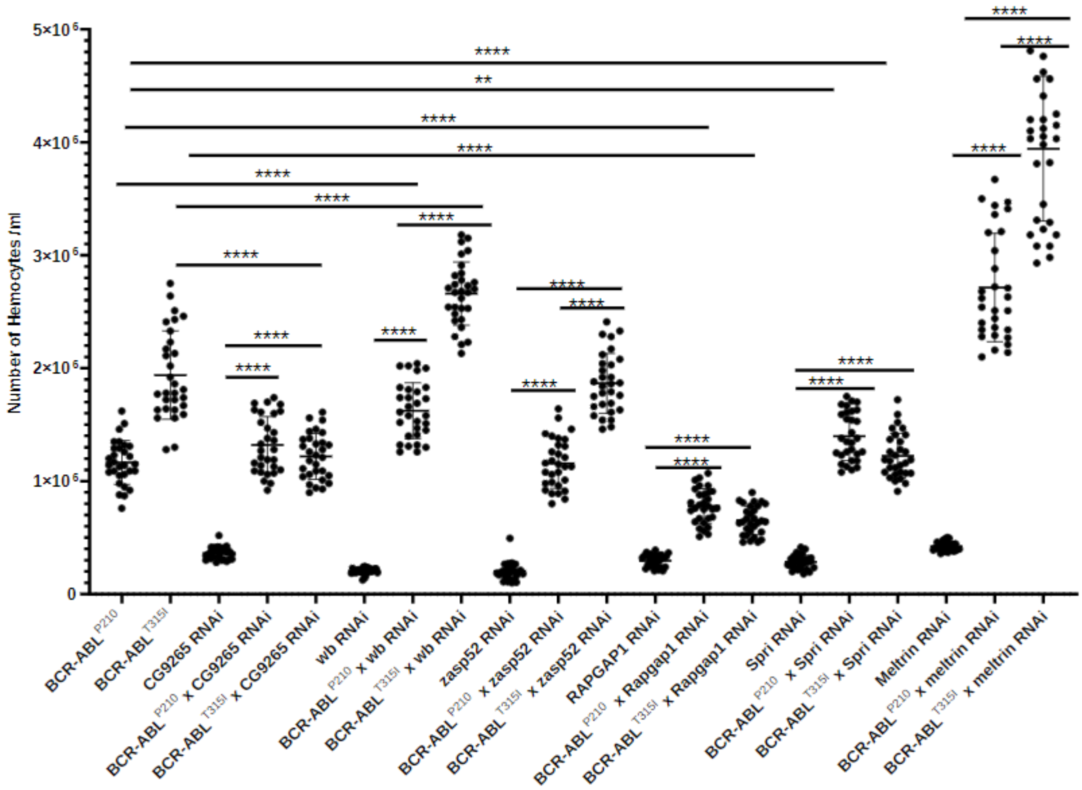

Figure 15. Enumeration of hemocytes in larva (n=30 triplicates).

Rapgap1 RNAi partially rescued *BCR-ABL^{P210}* and *BCR-ABL^{T315I}* flies while *Spri* RNAi and *CG9265* RNAi partially rescued *BCR-ABL^{T315I}*. *Spri* RNAi increased hemocyte count in *BCR-ABL^{P210}* whereas *Meltrin* RNAi and *wb* RNAi increased hemocyte count in *BCR-ABL^{P210}* and *BCR-ABL^{T315I}* flies. Error bars represent standard deviation. P-values: ; **, p <0.01; ****, p<0.0001.

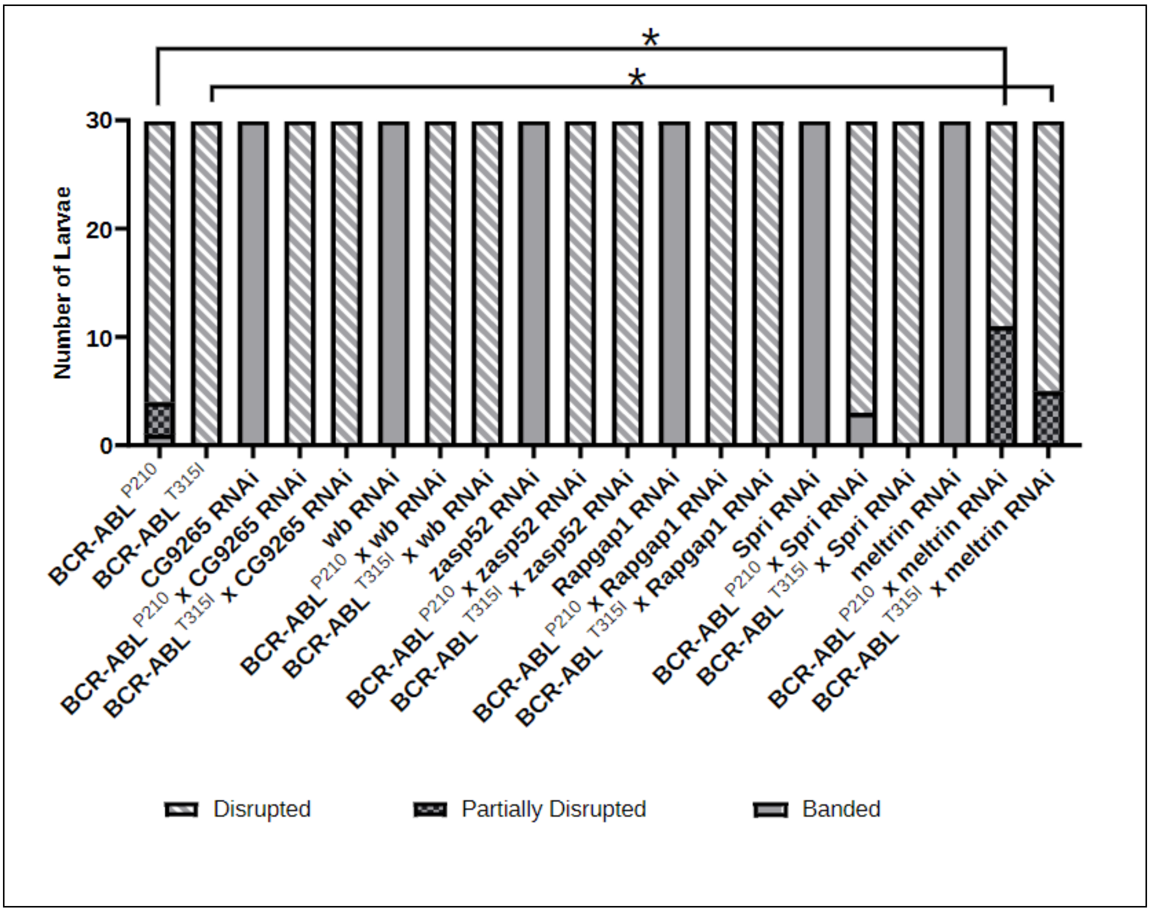

Figure 16. Enumeration of banded, partially disrupted, and disrupted hemocyte sessile patterning in larva (n=30 triplicates).

Meltrin RNAi partially rescued banding in *BCR-ABL*^{P210} and *BCR-ABL*^{T315I} larva. P-value: *, $p<0.05$

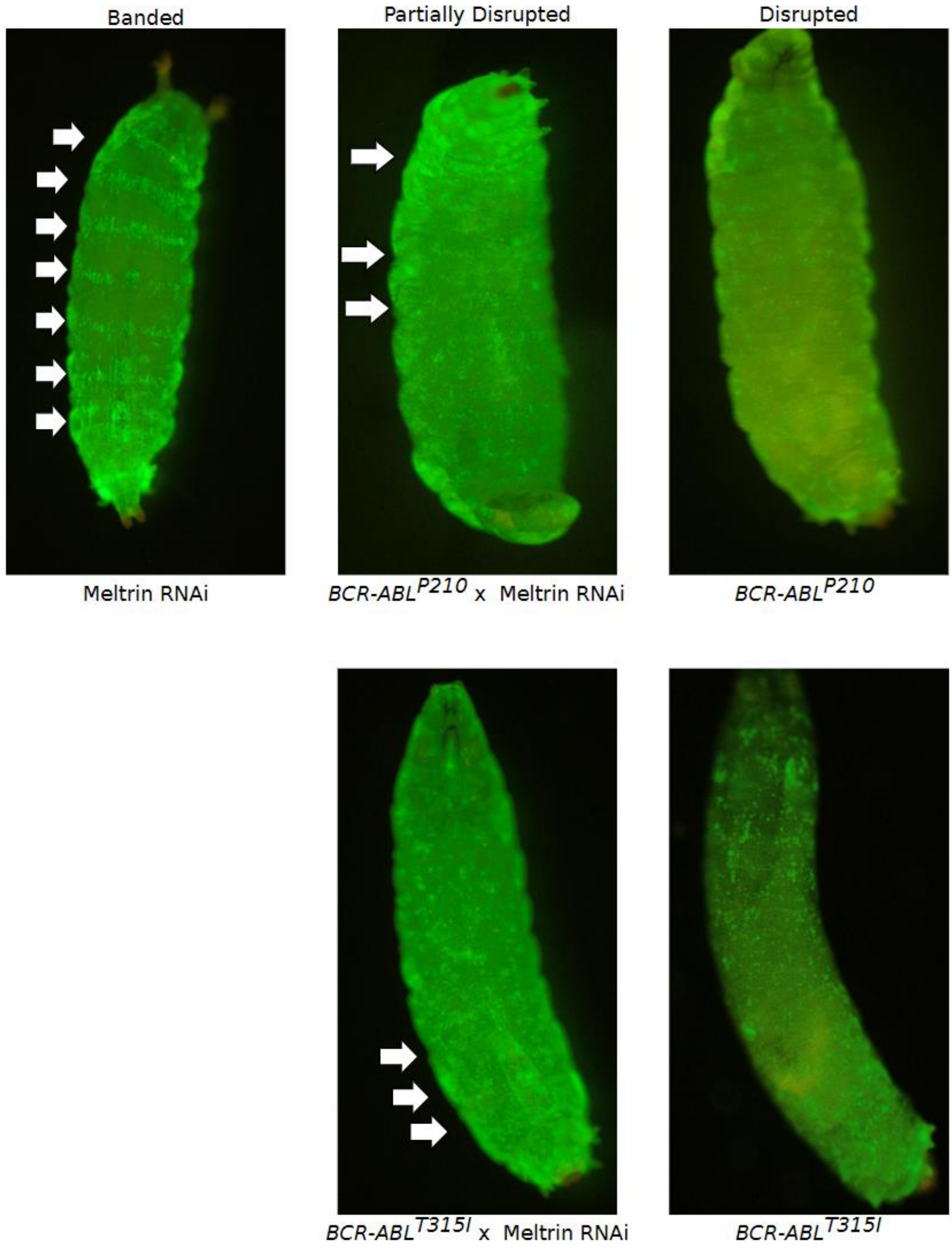

Figure 17. Meltrin knockdown partially rescued banding pattern.

Meltrin knockdown partially rescued banding patterns of *BCR-ABL*^{P210} and *BCR-ABL*^{T315I} larva from total disruption to partial disruption phenotype.

E. Discussion

In this study, we demonstrate the utilization of a *Drosophila* CML model to identify novel potential targets via unraveling its transcriptome. The validation of several genes as they were cross-referenced with transcriptomic data from adult and pediatric patients with CML reaffirms the relevance of this model in leukemia and other human diseases alike. The top 10 downregulated genes in *BCR-ABL*^{p210} compared to *wt* control include three long non-coding genes all of which currently have an unknown molecular function and biological processes. There are also 3 uncategorized proteins, 2 of which have unknown functions, while *CG3397* is predicted to be involved in dehydro-D-arabinono-1,4-lactone biosynthetic process. Two ecdysone-induced genes (Eigs), one of which is involved in metamorphosis (*Eig71Ed*) while *Eig71Ec* is predicted to be involved in defense response to bacterium. The last two were Fondue (fon) which is produced by the fat body and is involved in clotting reaction and the Imaginal disc growth factor 5 (*Idgf*5) which stimulate the proliferation and motility of the imaginal disk cells. The top 10 downregulated genes in *BCR-ABL*^{T315I} compared to *wt* control include two long non-coding genes both of which have an unknown molecular function and biological processes. There are also 5 uncategorized proteins, 4 of which have unknown functions, while *CG42500* is predicted to be involved in defense response. It also includes *Eig71Ed* and *Diptericin B*, the latter which is involved in the Imd pathway. Finally, the Amylase distal (*Amy-d*) which encodes an amylase enzyme. It is worth noting that *lncRNA:cr44909*, *Eig71Ed*, and *CG17105* are common genes between *BCR-ABL*^{p210} and *BCR-ABL*^{T315I} in their top 10 under expressed genes when compared to the *wt* control [171].

The top 10 upregulated genes in *BCR-ABL*^{p210} compared to *wt* control include 3 uncategorized proteins, one of which who's function is unknown, whereas *CG6553* is predicted to be active in the plasma membrane, and *CG5955* is predicted to be involved in threonine catabolic process. The other genes are involved in myriads functions, including synapse organization (*dpr4*), Calcium ion transmembrane transport (*Ca-beta*), translation (*tRNA:Leu-CAG-1-4*), regulating sleep behavior and reproductive behaviors (*SPR*), and chitin binding activity (*ChLD3*). In addition, the Bomanin Short 2 (*BomS2*) is a Toll signaling peptide. Interestingly, the tie-like receptor tyrosine kinase (*Tie*) is upregulated as well which is a predicted transmembrane tyrosine kinase receptor involved in cell survival and migration. The top 10 upregulated genes in *BCR-ABL*^{T315I} compared to *wt* control include 5 uncategorized proteins, three of which who's function is unknown, whereas *CG33462* and *CG16710* are predicted to enable serine-type endopeptidase activity. In addition, it has a long non-coding gene with an unknown function. The rest of the genes have a myriad of activities including female specific role in egg development (*yellow-g2*), a structural component of chitin-based cuticle so it is involved in cell-matrix adhesion (*zye*), and a cytosolic protein which contributes to trachea development (*sano*). *SPR* is the only common gene between *BCR-ABL*^{p210} and *BCR-ABL*^{T315I} in their top 10 overexpressed genes when compared to the *wt* control [171].

Concerning the screened potential targets, the knockdown of *Rapgap1* and *meltrin* partially rescued hemocyte count and sessile banding pattern, respectively, in *BCR-ABL*^{P210} and *BCR-ABL*^{T315I} flies, while the knockdown of *CG9265* partially rescued the hemcoyte count in *BCR-ABL*^{T315I} flies. In addition, knockdown of *meltrin* and *wb* resulted in an oncogenic effect by increasing the hemocyte count in *BCR-ABL*^{P210} and *BCR-ABL*^{T315I} flies.

Rapgap1 is an interesting target since its downregulation was able to partially rescue both the wild type *BCR-ABL*^{p210} as well as the *BCR-ABL*^{T315I} mutant. Rapgap1, a homologue of the human Rap1GAP, is a GTPase activating protein (GAP) that negatively regulates Rap1 which is involved in ERK signaling pathway which regulates cell growth [172]. It is usually considered to be a tumor suppressor whereby it is often downregulated in cancers. In fact, its upregulation would inhibit proliferation and would induce cell differentiation [173]. However, it was found to be upregulated in our CML model. Studies have already demonstrated that Rapgap1 can sometimes act as a tumor promoter. For instance, Rapgap1 reduces the coupling of the adherens junctions to the actin cytoskeleton via inhibiting Rap1 which results in increasing mobility of the cell to regulate the extent of epithelial invagination in the *Drosophila* [174]. Moreover, upregulation of Rap1GAP has shown to promote leukemic and squamous cell carcinoma invasion via the secretion of metalloprotease MMP9 [165, 175]. Interestingly, it seems to act on tumor invasiveness rather than cell proliferation. Therefore, we can hypothesize that the reduction in hemocyte count via Rapgap1 knockdown may have been a result of decreasing the mobility of the cells rather than an absolute decrease in cell proliferation. However, we would expect the sessile banding pattern to have been restored or partially rescued which was not the case. Another hypothesis could be that the depletion of Rapgap1 restored the expression of Rap1 which in turn could inhibit mTORC1 activation used by tumor cells as a means of regulating autophagy and prolonging their survival [176-178]. Therefore, we can consider monitoring phosphorylation status of mTORC1 substrates in the hemolymph of *BCR-ABL*^{p210} and *BCR-ABL*^{T315I} flies and comparing them to those crossed with *Rapgap1* RNAi flies. A decrease in mTORC1 substrate phosphorylation would be supportive of this hypothesis.

Concerning CG9265, it is an uncharacterized protein predicted to enable NAD-retinol dehydrogenase activity [179]. Its human ortholog is DHRS3 which is a short-chain dehydrogenases/reductases involved in the oxidation of steroids and retinol to retinaldehyde [180]. Despite the antitumor effects of retinoid therapy in several cancers including acute promyelocytic leukemia [181]; however, DHRS3 has also been shown to be amplified and be negatively associated with various cancers including triple-negative breast cancer and papillary thyroid carcinomas, [182-184] Likewise, *CG9265* was overexpressed in our samples and *CG9265* RNAi partially rescued *BCR-ABL*^{T315I} flies but had no effect on the *BCR-ABL*^{P210} flies. Despite not having a possible explanation for our findings, but a partial rescue was observed which shows that CG9265 does play a role and is a potential target which needs to be understood better. More studies are required to understand its mechanism of action and its pathway in the context of *BCR-ABL*^{T315I} since knocking down *CG9265* only had an effect in the T315I mutant and not the wild type *BCR-ABL*^{P210}.

Meltrin is a disintegrin and metalloprotease which happens to have its human ortholog to be ADAM8 [185]. ADAMs are usually involved in tumors via regulating integrin function and growth factor activities. ADAM 8 is an extracellular matrix degrading proteinase. Just like in our case, ADAMs tend to be overexpressed in cancers. ADAM 8 has shown to increase invasiveness since it promotes migration [186]. Interestingly, it has been noted that ADAM8 specifically is a culprit in TKI-resistant CML cells. Once their expression was inhibited, the cells became sensitive once again to TKIs [187]. This echoes our findings here as well since *meltrin* was found to be upregulated in BCR-ABL^{P210} and *BCR-ABL*^{T315I} flies. Upon knockdown of *meltrin* via its RNAi, the sessile banding pattern was partially rescued in BCR-ABL^{P210} and *BCR-ABL*^{T315I} flies which reflects the disability of these cells to migrate as they used to be uninhibited. However, it increased the hemocyte count for both genotypes. We can hypothesize that the increase of hemocyte production can be related to its response to a stressful state. During embryonic development, meltrin is usually detected in neuroblasts suggestive of a role it has in the development of the nervous system [185]. In the *Drosophila*, there are examples in which a defect in the neural system can induce a response of hemocyte production as we hypothesize in our case. For instance, during homeostasis, certain levels of odorant ligands in the larval's surroundings maintain Gamma-aminobutyric acid (GABA) levels in blood circulating that signal favorable conditions for the lymph gland's medullary zone cells to be maintained in their progenitor phase during development. Should the larvae lose its sense of smell, a strong immune response will ensue since the balance between GABA and cytosolic calcium in the medullary zone has been distorted. This will make the quiescent cells in the medullary zone lose their quiescence and differentiate [82]. Likewise, should the knockdown of *meltrin* be significant enough to affect the development of the nervous system, then maybe the fly is in distress and this "immune response" maybe is its reaction.

Wing blister encodes laminin α chains, an extracellular matrix component associated with the basement membrane that are involved in cell adhesion via their interaction with integrins. Its human ortholog LAMA5 is usually upregulated in cancers whereby it promotes angiogenesis, metastasis, and resistance to certain cancer treatments [188, 189]. It was upregulated in BCR-*ABL*^{P210} and *BCR-ABL*^{T315I} flies. Interestingly, its RNAi resulted in an increase in hemocyte count. Given the whole picture beginning from the fact that it is involved in cell adhesion, an increase in hemocyte associated with total loss of sessile banding pattern; those cells maybe the very same hemocytes that are supposed to be attached to the wall in the epidermal-muscular pockets; however, the RNAi which knocked down this laminin may have affected cell adhesion and not cell proliferation.

Spri functions as a guanine nucleotide exchange (GEF) so it is a Ras effector; its human ortholog is RIN1[190]. It regulates *BCR-ABL1* so it is highly associated with it. Upon its overexpression, it potentiates the expression of *BCR-ABL1*. Moreover, silencing of *RIN1* has shown to increase sensitivity to TKIs [191, 192]. Given the strong association of this protein with *BCR-ABL1,* it explains *spri* RNAi effect on *BCR-ABL*^{T315I} flies which resulted in a partial rescue of hemocyte count; however, we could not explain the increase of hemocyte count observed in BCR-*ABL*^{P210} flies.

Finally, zasp 52 is a scaffold protein involved in muscle attachment. Its human ortholog is PDLIM5 [193]. *PDLIM5* is usually upregulated in cancers whereby it promotes cell differentiation and migration [194]. Similarly, it was upregulated in BCR-*ABL*^{P210} and *BCR-ABL*^{T315I} flies; however, knocking it down did not have any observable effect.

F. Conclusion

We unraveled the transcriptome of our hematopoietic CML *Drosophila* models expressing *BCR-ABL*^{p210} and *BCR-ABL*^{T315I} in their hemolymph. Their molecular signatures were very similar to each other but distinctly different than that of *wt* control.

Six genes were chosen from the cross-referenced upregulated genes. They were validated in adult, pediatric CML patients, and *BCR-ABL*^{T315I} mice. We discovered 3 potential targets, upon their knockdown, *Rapgap1* partially rescued hemocyte count in both genotypes while *spri* and *CG9265* partially rescued hemocyte count in *BCR-ABL*^{T315I} flies. However, knockdown of *spri* in *BCR-ABL*^{p210} flies resulted in increase of hemocyte count. In addition, we identified another gene that partially rescued the sessile hemocyte banding pattern that is *meltrin*; however, it did increase hemocyte count. Moreover, knocking down of *wb* turned out to have an oncogenic effect on hemocyte count as well while *spri* and *zasp52* had no effect on either phenotypes. We have identified targets that are common to both *BCR-ABL*^{p210} and *BCR-ABL*^{T315I} which are worth pursuing since CML patients with and without the T315I mutation can benefit alike. Also, future studies should address the pathways of the identified targets to understand how they result in the leukemic phenotype especially since they are dysregulated in the opposite direction of literature findings in other cancers. Finally, the partial rescue of the *BCR-ABL*^{T315I} phenotype upon the knockdown of the uncharacterized protein CG9265 has made it more pertinent to study it and characterize it.

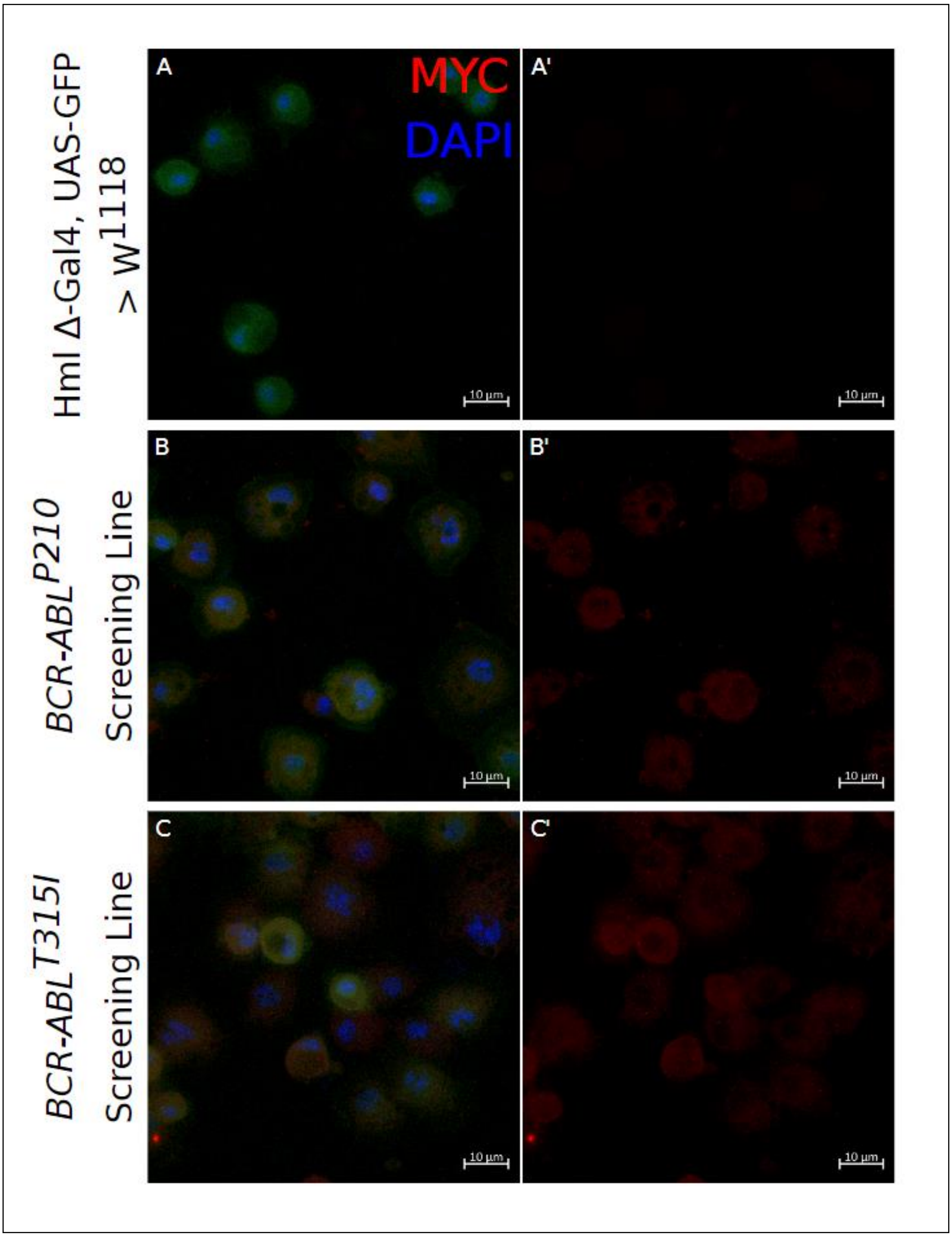

Figure 18. BCR-ABL^{P210} and BCR-ABL^{T315I} expression in screening lines.

Maximum intensity projection at 100X magnification showing absence of MYC staining in GFP-positive control hemocytes (a,a’), MYC expression in GFP-positive hemcoytes indicating expression of (b,b’) *BCR-ABL^{P210}* and (c,c’) *BCR-ABL^{T315I}* screening lines, respectively. Scale bar is 10μm.

CHAPTER V

CONCLUSION

The main aim of this study is to find novel potential targets against *BCR-ABL*^{T315I} to aid in this unmet clinical need. Nevertheless, our approach allowed us to identify targets that were effective against the wild type *BCR-ABL*^{p210} and *BCR-ABL*^{T315I} mutant. We had already validated a *Drosophila* CML model that expressed *BCR-ABL*^{p210} and *BCR-ABL*^{T315I} in the eye. Some observed phenotypes were rough eyes and ommatidial distortion that were present when compared to the control. However, we were also able to identify an exacerbated phenotype in the *BCR-ABL*^{T315I} flies when compared to the wild type *BCR-ABL*^{p210} flies [114]. This was a promising start for our CML model since observable phenotypes could aid us in identifying an effective target by observing a partial or total rescue of phenotype. Based on these findings, we embarked on expressing *BCR-ABL*^{p210} and *BCR-ABL*^{T315I} in the hemolymph system under the Hml Δ driver since it would be the ideal system to study CML. Our first objective was to see whether observable phenotypes would show up. The two phenotypes that were observed were an increase in hemocyte count and a disruption in the sessile banding pattern. Once again, an exacerbated version of the phenotypes was noted in the *BCR-ABL*^{T315I} mutant. The hemocyte count in *BCR-ABL*^{p210} flies was higher than the control and the *BCR-ABL*^{T315I} flies had an even higher hemocyte count. Moreover, the disruption in the sessile pattern was partial in the *BCR-ABL*^{p210} flies when compared to the control while it was total in the *BCR-ABL*^{T315I} flies. Since the cellular arm of the *Drosophila*'s innate immunity was affected, we were curious to see whether the humoral arm would be affected as well. We identified dysregulation in the Toll, Imd, and JAK/STAT pathways at the mRNA level in both the 3rd instar larva and adult stage via measuring the major AMP of each pathway namely, *Drosomycin, Diptericin A,* and *TotA*, respectively [156].

Since the expression of *BCR-ABL^{p210}* and *BCR-ABL^{T315I}* in the hematopoietic system presented with phenotypes when compared to control flies, the next objective was to collect their hemolymph, extract the RNA, and pass it on to RNA-sequencing then analyze the transcriptomic data in order to detect the DEGs and identify potential genes from that pool. Meanwhile, we generated a screening line for *BCR-ABL^{p210}* and *BCR-ABL^{T315I}* that were validated by immunofluorescence whereby the *BCR-ABL1* genes were tagged with Myc as a reporter that was visualized in the hemocytes of each screening line. Transcriptomic analysis showed us similar molecular signatures for *BCR-ABL^{p210}* and *BCR-ABL^{T315I}* but they were very distinctive than that of the *wt* control. After transcriptomic analysis, we cross-referenced the upregulated DEGs against adult and pediatric CML patient samples to identify potential genes that may be targets for wild type and T315I mutant (16 genes identified). Moreover, we cross-referenced them again against adult CML patient samples and *BCR-ABL^{T315I}* mice to narrow down potential targets against the T315I mutant (11 genes identified). They were narrowed down to a total of six genes that were promising based on our literature review (*Rapgap1, CG9265, meltrin, spri, wb,* and *zasp52).* We crossed the screening lines with RNAi flies for these genes. We discovered a total of 4 potential targets. *Rapgap1* RNAi partially rescued the hemocyte count in *BCR-ABL^{p210}* and *BCR-ABL^{T315I}* flies. *Spri* RNAi and *CG9265* RNAi partially rescued the hemocyte count in *BCR-ABL^{T315I}* flies whereby their count decreased to levels comparable to the less aggressive wild type *BCR-ABL^{p210}*. *Meltrin* RNAi partially rescued the sessile hemocyte banding pattern in *BCR-ABL^{p210}* and *BCR-ABL^{T315I}* flies; however, it increased their hemocyte counts so it also had an oncogenic effect. Finally, we would like to emphasize the validity of this hematopoietic CML model is strengthened by the fact that upon cross-referencing our data, several genes were found to be differentially expressed when compared to control and they were differentially expressed in the same direction be it over or under expressed.

We targeted some genes that were not highlighted before in the literature pertaining to leukemia. Interestingly, although some genes were upregulated similarly to the cross-referenced data, yet they were not previously studied in leukemia. This is probably since some upregulated genes were dysregulated in the opposite direction that what was expected from the literature in other cancers. However, we observed partial rescue of the leukemic phenotypes upon their knockdown. Therefore, we have opened the gates to several future studies. First, this study encourages the screening of all genes that are cross-referenced in this model. Second, we need to study the pathways of the identified targets to understand how they result in the leukemic phenotype especially those which were dysregulated in the opposite direction of literature findings in other cancers, namely Rapgap1 and CG9265. Third, the partial rescue of the *BCR-ABL*^{T315I} phenotype upon the knockdown of the uncharacterized protein CG9265 has made it more pertinent to study it and characterize it. Fourth, future studies can inhibit ADAM8 using any of its inhibitors GW280264, FC387, FC143, or BB94 (Bastimastat) in CML cell lines and in CML mouse models in particular in mice models with the *BCR-ABL*^{T315I} mutant such as the one described by Huang *et al.* [164, 195]. It would be interesting to see the effect it would have especially since they are not targeted therapies. Nevertheless, with well-defined dosage, we may be able to label these as adjuvant therapies or be given as part of a regimen to patients who are resistant to available treatment. This CML model with its transcriptomic data has opened an exciting era of identifying additional potential CML targets. There are still more upregulated genes to be screened for in the pipeline and many more taking into account the down regulated genes.

BIBLIOGRAPHY

1. Faderl, S., et al., *The biology of chronic myeloid leukemia.* New England Journal of Medicine, 1999. **341**(3): p. 164-172.
2. Kang, Z.-J., et al., *The Philadelphia chromosome in leukemogenesis.* Chinese journal of cancer, 2016. **35**(1): p. 1-15.
3. Groffen, J., et al., *Philadelphia chromosomal breakpoints are clustered within a limited region, bcr, on chromosome 22.* Cell, 1984. **36**(1): p. 93-99.
4. Hermans, A., et al., *Unique fusion of bcr and c-abl genes in Philadelphia chromosome positive acute lymphoblastic leukemia.* Cell, 1987. **51**(1): p. 33-40.
5. McWHIRTER, J.R., D.L. Galasso, and J. Wang, *A coiled-coil oligomerization domain of Bcr is essential for the transforming function of Bcr-Abl oncoproteins.* Molecular and cellular biology, 1993. **13**(12): p. 7587-7595.
6. Reuther, G.W., et al., *Association of the protein kinases c-Bcr and Bcr-Abl with proteins of the 14-3-3 family.* Science, 1994. **266**(5182): p. 129-133.
7. Apperley, J.F., *Chronic myeloid leukaemia.* The Lancet, 2015. **385**(9976): p. 1447-1459.
8. Hantschel, O., *Structure, regulation, signaling, and targeting of abl kinases in cancer.* Genes & cancer, 2012. **3**(5-6): p. 436-446.
9. Goldman, J.M. and J.V. Melo, *Chronic myeloid leukemia—advances in biology and new approaches to treatment.* New England Journal of Medicine, 2003. **349**(15): p. 1451-1464.
10. Chereda, B. and J.V. Melo, *Natural course and biology of CML.* Annals of hematology, 2015. **94**(2): p. 107-121.
11. Avelino, K.Y., et al., *Smart applications of bionanosensors for BCR/ABL fusion gene detection in leukemia.* Journal of King Saud University-Science, 2017. **29**(4): p. 413-423.
12. O'Hare, T., et al., *Targeting the BCR-ABL Signaling Pathway in Therapy-Resistant Philadelphia Chromosome-Positive LeukemiaTargeting the BCR-ABL Signaling in Ph+ Leukemia.* Clinical Cancer Research, 2011. **17**(2): p. 212-221.
13. Deininger, M.W., et al., *Chronic myeloid leukemia, version 2.2021, NCCN clinical practice guidelines in oncology.* Journal of the National Comprehensive Cancer Network, 2020. **18**(10): p. 1385-1415.
14. Goldman, J.M. and B.J. Druker, *Chronic myeloid leukemia: current treatment options.* Blood, The Journal of the American Society of Hematology, 2001. **98**(7): p. 2039-2042.
15. Champlin, R., et al., *Allogeneic stem cell transplantation for chronic myeloid leukemia resistant to tyrosine kinase inhibitors.* Clinical Lymphoma Myeloma and Leukemia, 2011. **11**: p. S96-S100.
16. Bruford, E.A., et al., *HUGO Gene Nomenclature Committee (HGNC) recommendations for the designation of gene fusions*. Leukemia, 2021. **35**(11): p. 3040-3043.
17. Schoepfer, J., et al., *Discovery of asciminib (ABL001), an allosteric inhibitor of the tyrosine kinase activity of BCR-ABL1*. 2018, ACS Publications.
18. Wylie, A.A., et al., *The allosteric inhibitor ABL001 enables dual targeting of BCR–ABL1*. Nature, 2017. **543**(7647): p. 733-737.

19. Hochhaus, A., et al., *Long-term outcomes of imatinib treatment for chronic myeloid leukemia.* New England Journal of Medicine, 2017. **376**(10): p. 917-927.
20. Cortes, J.E., et al., *Final 5-year study results of DASISION: the dasatinib versus imatinib study in treatment-naïve chronic myeloid leukemia patients trial.* Journal of Clinical Oncology, 2016. **34**(20): p. 2333.
21. Hochhaus, A., et al., *Long-term benefits and risks of frontline nilotinib vs imatinib for chronic myeloid leukemia in chronic phase: 5-year update of the randomized ENESTnd trial.* Leukemia, 2016. **30**(5): p. 1044-1054.
22. Cortes, J.E., et al., *Bosutinib versus imatinib for newly diagnosed chronic myeloid leukemia: results from the randomized BFORE trial.* Journal of Clinical Oncology, 2018. **36**(3): p. 231.
23. Soverini, S., et al., *ABL Mutations in Late-Chronic Phase Chronic Myeloid Leukemia Patients with Cytogenetic Refractoriness to Imatinib Are Associated with a Greater Likelihood of Progression to Blast Crisis and Shorter Survival. on behalf of the GIMEMA Working Party on Chronic Myeloid Leukemia*. 2004, American Society of Hematology.
24. Nicolini, F., et al., *Mutation status and clinical outcome of 89 imatinib mesylate-resistant chronic myelogenous leukemia patients: a retrospective analysis from the French intergroup of CML (Fi (ϕ)-LMC GROUP).* Leukemia, 2006. **20**(6): p. 1061-1066.
25. Soverini, S., et al., *Contribution of ABL kinase domain mutations to imatinib resistance in different subsets of Philadelphia-positive patients: by the GIMEMA Working Party on Chronic Myeloid Leukemia.* Clinical Cancer Research, 2006. **12**(24): p. 7374-7379.
26. Khorashad, J.S., et al., *Finding of kinase domain mutations in patients with chronic phase chronic myeloid leukemia responding to imatinib may identify those at high risk of disease progression.* Journal of clinical oncology, 2008. **26**(29): p. 4806-4813.
27. Branford, S., J.V. Melo, and T.P. Hughes, *Selecting optimal second-line tyrosine kinase inhibitor therapy for chronic myeloid leukemia patients after imatinib failure: does the BCR-ABL mutation status really matter?* Blood, The Journal of the American Society of Hematology, 2009. **114**(27): p. 5426-5435.
28. Druker, B.J., et al., *Efficacy and safety of a specific inhibitor of the BCR-ABL tyrosine kinase in chronic myeloid leukemia.* New England Journal of Medicine, 2001. **344**(14): p. 1031-1037.
29. Kantarjian, H., et al., *Hematologic and cytogenetic responses to imatinib mesylate in chronic myelogenous leukemia.* New England Journal of Medicine, 2002. **346**(9): p. 645-652.
30. O'Brien, S., F. Guilhot, and R. Larson, *a, Gathmann I, Baccarani M, Cervantes F, et al. Imatinib compared with interferon and low-dose cytarabine for newly diagnosed chronic-phase chronic myeloid leukemia.* N Engl J Med, 2003. **348**(11): p. 994-1004.
31. Weisberg, E. and J.D. Griffin, *Mechanism of resistance to the ABL tyrosine kinase inhibitor STI571 in BCR/ABL–transformed hematopoietic cell lines.* Blood, The Journal of the American Society of Hematology, 2000. **95**(11): p. 3498-3505.

32. Mahon, F.X., et al., *Selection and characterization of BCR-ABL positive cell lines with differential sensitivity to the tyrosine kinase inhibitor STI571: diverse mechanisms of resistance.* Blood, The Journal of the American Society of Hematology, 2000. **96**(3): p. 1070-1079.
33. White, D.L., et al., *Chronic phase chronic myeloid leukemia patients with low OCT-1 activity randomized to high-dose imatinib achieve better responses and have lower failure rates than those randomized to standard-dose imatinib.* haematologica, 2012. **97**(6): p. 907.
34. le Coutre, P., et al., *Induction of resistance to the Abelson inhibitor STI571 in human leukemic cells through gene amplification.* Blood, The Journal of the American Society of Hematology, 2000. **95**(5): p. 1758-1766.
35. Gorre, M.E., et al., *Clinical resistance to STI-571 cancer therapy caused by BCR-ABL gene mutation or amplification.* Science, 2001. **293**(5531): p. 876-880.
36. Talpaz, M., et al., *Dasatinib in imatinib-resistant Philadelphia chromosome–positive leukemias.* New England Journal of Medicine, 2006. **354**(24): p. 2531-2541.
37. Hehlmann, R., *Chronic myeloid leukemia in 2020.* Hemasphere, 2020. **4**(5).
38. Kantarjian, H., et al., *Nilotinib in imatinib-resistant CML and Philadelphia chromosome–positive ALL.* New England Journal of Medicine, 2006. **354**(24): p. 2542-2551.
39. Khoury, H.J., et al., *Bosutinib is active in chronic phase chronic myeloid leukemia after imatinib and dasatinib and/or nilotinib therapy failure.* Blood, The Journal of the American Society of Hematology, 2012. **119**(15): p. 3403-3412.
40. Gambacorti-Passerini, C., et al., *Bosutinib efficacy and safety in chronic phase chronic myeloid leukemia after imatinib resistance or intolerance: Minimum 24-month follow-up.* American journal of hematology, 2014. **89**(7): p. 732-742.
41. Jabbour, E., et al., *Characteristics and outcomes of patients with chronic myeloid leukemia and T315I mutation following failure of imatinib mesylate therapy.* Blood, The Journal of the American Society of Hematology, 2008. **112**(1): p. 53-55.
42. Nicolini, F.E., et al., *Clinical outcome of 27 imatinib mesylate-resistant chronic myelogenous leukemia patients harboring a T315I BCR-ABL mutation.* Haematologica, 2007. **92**(9): p. 1238-1241.
43. Cortes, J.E., et al., *Asciminib, a first-in-class STAMP inhibitor, provides durable molecular response in patients (pts) with chronic myeloid leukemia (CML) harboring the T315I mutation: primary efficacy and safety results from a phase 1 trial.* Blood, 2020. **136**: p. 47-50.
44. Cortes, J.E., et al., *Ponatinib efficacy and safety in Philadelphia chromosome–positive leukemia: final 5-year results of the phase 2 PACE trial.* Blood, The Journal of the American Society of Hematology, 2018. **132**(4): p. 393-404.
45. Cortes, J.E., et al., *Ponatinib in refractory Philadelphia chromosome–positive leukemias.* New England Journal of Medicine, 2012. **367**(22): p. 2075-2088.
46. Cortes, J.E., et al., *A phase 2 trial of ponatinib in Philadelphia chromosome–positive leukemias.* New England Journal of Medicine, 2013. **369**(19): p. 1783-1796.

47. Luciano, L., et al., *The multi-tyrosine kinase inhibitor ponatinib for chronic myeloid leukemia: real-world data.* European Journal of Haematology, 2020. **105**(1): p. 3-15.
48. Casavecchia, G., et al., *Early diagnosis, clinical management, and follow-up of cardiovascular events with ponatinib.* Heart Failure Reviews, 2020. **25**(3): p. 447-456.
49. Yeung, D.T., N. Shanmuganathan, and T.P. Hughes, *Asciminib: a new therapeutic option in chronic-phase CML with treatment failure.* Blood, The Journal of the American Society of Hematology, 2022. **139**(24): p. 3474-3479.
50. Eide, C.A., et al., *Combining the allosteric inhibitor asciminib with ponatinib suppresses emergence of and restores efficacy against highly resistant BCR-ABL1 mutants.* Cancer Cell, 2019. **36**(4): p. 431-443. e5.
51. Soverini, S., et al., *Implications of BCR-ABL1 kinase domain-mediated resistance in chronic myeloid leukemia.* Leukemia research, 2014. **38**(1): p. 10-20.
52. Nicolini, F.E., et al., *The BCR-ABLT315I mutation compromises survival in chronic phase chronic myelogenous leukemia patients resistant to tyrosine kinase inhibitors, in a matched pair analysis.* Haematologica, 2013. **98**(10): p. 1510.
53. Soverini, S., et al., *Philadelphia-positive patients who already harbor imatinib-resistant Bcr-Abl kinase domain mutations have a higher likelihood of developing additional mutations associated with resistance to second-or third-line tyrosine kinase inhibitors.* Blood, The Journal of the American Society of Hematology, 2009. **114**(10): p. 2168-2171.
54. Kumar, R., et al., *Specific, targetable interactions with the microenvironment influence imatinib-resistant chronic myeloid leukemia.* Leukemia, 2020. **34**(8): p. 2087-2101.
55. Skaggs, B.J., et al., *Phosphorylation of the ATP-binding loop directs oncogenicity of drug-resistant BCR-ABL mutants.* Proceedings of the National Academy of Sciences, 2006. **103**(51): p. 19466-19471.
56. Griswold, I.J., et al., *Kinase domain mutants of Bcr-Abl exhibit altered transformation potency, kinase activity, and substrate utilization, irrespective of sensitivity to imatinib.* Molecular and cellular biology, 2006. **26**(16): p. 6082-6093.
57. Roa-Espitia, A.L., et al., *Focal adhesion kinase is required for actin polymerization and remodeling of the cytoskeleton during sperm capacitation.* Biology Open, 2016. **5**(9): p. 1189-1199.
58. Fabry, B., et al., *Focal adhesion kinase stabilizes the cytoskeleton.* Biophysical journal, 2011. **101**(9): p. 2131-2138.
59. Miller, P.G., et al., *In Vivo RNAi screening identifies a leukemia-specific dependence on integrin beta 3 signaling.* Cancer cell, 2013. **24**(1): p. 45-58.
60. Ghatak, S., J. Morgner, and S.A. Wickström, *ILK: a pseudokinase with a unique function in the integrin–actin linkage.* Biochemical Society Transactions, 2013. **41**(4): p. 995-1001.
61. Guo, L. and C. Wu, *Regulation of fibronectin matrix deposition and cell proliferation by the PINCH-ILK-CH-ILKBP complex.* The FASEB Journal, 2002. **16**(10): p. 1298-1300.

62. Gagné, D., et al., *Integrin-linked kinase regulates migration and proliferation of human intestinal cells under a fibronectin-dependent mechanism.* Journal of cellular physiology, 2010. **222**(2): p. 387-400.
63. Yamaguchi, M., *Drosophila models for human diseases*. Vol. 1076. 2018: Springer.
64. Pandey, U.B. and C.D. Nichols, *Human disease models in Drosophila melanogaster and the role of the fly in therapeutic drug discovery.* Pharmacological reviews, 2011. **63**(2): p. 411-436.
65. Kaufman, T.C., *A short history and description of Drosophila melanogaster classical genetics: Chromosome aberrations, forward genetic screens, and the nature of mutations.* Genetics, 2017. **206**(2): p. 665-689.
66. Mirzoyan, Z., et al., *Drosophila melanogaster: a model organism to study cancer.* Frontiers in genetics, 2019. **10**: p. 51.
67. Ugur, B., K. Chen, and H.J. Bellen, *Drosophila tools and assays for the study of human diseases.* Disease models & mechanisms, 2016. **9**(3): p. 235-244.
68. Millburn, G.H., et al., *FlyBase portals to human disease research using Drosophila models.* Disease Models & Mechanisms, 2016. **9**(3): p. 245-252.
69. Yu, S., F. Luo, and L.H. Jin, *The Drosophila lymph gland is an ideal model for studying hematopoiesis.* Developmental & Comparative Immunology, 2018. **83**: p. 60-69.
70. Letourneau, M., et al., *Drosophila hematopoiesis under normal conditions and in response to immune stress.* FEBS letters, 2016. **590**(22): p. 4034-4051.
71. Gold, K.S. and K. Brückner, *Drosophila as a model for the two myeloid blood cell systems in vertebrates.* Experimental hematology, 2014. **42**(8): p. 717-727.
72. Amoyel, M., A.M. Anderson, and E.A. Bach. *JAK/STAT pathway dysregulation in tumors: a Drosophila perspective*. in *Seminars in cell & developmental biology*. 2014. Elsevier.
73. Sonoshita, M. and R. Cagan, *Modeling human cancers in Drosophila.* Current topics in developmental biology, 2017. **121**: p. 287-309.
74. Brand, A.H. and N. Perrimon, *Targeted gene expression as a means of altering cell fates and generating dominant phenotypes.* development, 1993. **118**(2): p. 401-415.
75. Perveen, F.K., *Drosophila melanogaster: Model for Recent Advances in Genetics and Therapeutics.* 2018.
76. Cho, K.S., S.M. Bang, and A. Toh, *Lipids and lipid signaling in Drosophila models of neurodegenerative diseases*, in *Omega-3 Fatty Acids in Brain and Neurological Health*. 2014, Elsevier. p. 327-336.
77. Blake, A.J., et al., *RNAi-based techniques for the analysis of gene function in drosophila germline stem cells*, in *RNAi and Small Regulatory RNAs in Stem Cells*. 2017, Springer. p. 161-184.
78. Hultmark, D. and I. Andó, *Hematopoietic plasticity mapped in Drosophila and other insects.* eLife, 2022. **11**: p. e78906.
79. Rizki, M., *Alterations in the haemocyte population of Drosophila melanogaster.* Journal of Morphology, 1957. **100**(3): p. 437-458.
80. Bunt, S., et al., *Hemocyte-secreted type IV collagen enhances BMP signaling to guide renal tubule morphogenesis in Drosophila.* Developmental cell, 2010. **19**(2): p. 296-306.

81. Woodcock, K.J., et al., *Macrophage-derived upd3 cytokine causes impaired glucose homeostasis and reduced lifespan in Drosophila fed a lipid-rich diet.* Immunity, 2015. **42**(1): p. 133-144.
82. Banerjee, U., et al., *Drosophila as a genetic model for hematopoiesis.* Genetics, 2019. **211**(2): p. 367-417.
83. Eleftherianos, I. and C. Revenis, *Role and importance of phenoloxidase in insect hemostasis.* Journal of innate immunity, 2011. **3**(1): p. 28-33.
84. Bidla, G., M.S. Dushay, and U. Theopold, *Crystal cell rupture after injury in Drosophila requires the JNK pathway, small GTPases and the TNF homolog Eiger.* Journal of cell science, 2007. **120**(7): p. 1209-1215.
85. Dudzic, J.P., et al., *Drosophila innate immunity: regional and functional specialization of prophenoloxidases.* BMC biology, 2015. **13**(1): p. 1-16.
86. Nam, H.J., et al., *Genetic evidence of a redox-dependent systemic wound response via Hayan protease-phenoloxidase system in Drosophila.* The EMBO journal, 2012. **31**(5): p. 1253-1265.
87. Cattenoz, P.B., et al., *Temporal specificity and heterogeneity of Drosophila immune cells.* The EMBO journal, 2020. **39**(12): p. e104486.
88. Tattikota, S.G., et al., *A single-cell survey of Drosophila blood.* Elife, 2020. **9**: p. e54818.
89. Fu, Y., et al., *Single-cell RNA sequencing identifies novel cell types in Drosophila blood.* Journal of Genetics and Genomics, 2020. **47**(4): p. 175-186.
90. Honegger, B., et al., *Imp-L2, a putative homolog of vertebrate IGF-binding protein 7, counteracts insulin signaling in Drosophila and is essential for starvation resistance.* Journal of biology, 2008. **7**(3): p. 1-11.
91. Kwon, Y., et al., *Systemic organ wasting induced by localized expression of the secreted insulin/IGF antagonist ImpL2.* Developmental cell, 2015. **33**(1): p. 36-46.
92. Torraca, V. and S. Mostowy, *Septins and bacterial infection.* Frontiers in cell and developmental biology, 2016. **4**: p. 127.
93. Holz, A., et al., *The two origins of hemocytes in Drosophila.* 2003.
94. Lanot, R., et al., *Postembryonic hematopoiesis in Drosophila.* Developmental biology, 2001. **230**(2): p. 243-257.
95. Crozatier, M., et al., *Cellular immune response to parasitization in Drosophila requires the EBF orthologue collier.* PLoS biology, 2004. **2**(8): p. e196.
96. Mandal, L., U. Banerjee, and V. Hartenstein, *Evidence for a fruit fly hemangioblast and similarities between lymph-gland hematopoiesis in fruit fly and mammal aorta-gonadal-mesonephros mesoderm.* Nature genetics, 2004. **36**(9): p. 1019-1023.
97. Jung, S.-H., et al., *The Drosophila lymph gland as a developmental model of hematopoiesis.* 2005.
98. Makhijani, K., et al., *The peripheral nervous system supports blood cell homing and survival in the Drosophila larva.* Development, 2011. **138**(24): p. 5379-5391.
99. Makhijani, K., et al., *Regulation of Drosophila hematopoietic sites by Activin-β from active sensory neurons.* Nature Communications, 2017. **8**(1): p. 1-12.
100. Bretscher, A.J., et al., *The Nimrod transmembrane receptor Eater is required for hemocyte attachment to the sessile compartment in Drosophila melanogaster.* Biology open, 2015. **4**(3): p. 355-363.

101. Csordas, G., F. Grawe, and M. Uhlirova, *Eater cooperates with Multiplexin to drive the formation of hematopoietic compartments.* Elife, 2020. **9**.
102. Kim-Jo, C., J.-L. Gatti, and M. Poirié, *Drosophila cellular immunity against parasitoid wasps: A complex and time-dependent process.* Frontiers in Physiology, 2019. **10**: p. 603.
103. Govind, S., *Innate immunity in Drosophila: Pathogens and pathways.* Insect science, 2008. **15**(1): p. 29-43.
104. Lemaitre, B. and J. Hoffmann, *The host defense of Drosophila melanogaster.* Annual review of immunology, 2007. **25**(ARTICLE): p. 697-743.
105. Martinelli, C. and J.-M. Reichhart, *Evolution and integration of innate immune systems from fruit flies to man: lessons and questions.* Journal of Endotoxin Research, 2005. **11**(4): p. 243-248.
106. Valanne, S., J.-H. Wang, and M. Rämet, *The Drosophila toll signaling pathway.* The Journal of Immunology, 2011. **186**(2): p. 649-656.
107. Myllymäki, H., S. Valanne, and M. Rämet, *The Drosophila imd signaling pathway.* The Journal of Immunology, 2014. **192**(8): p. 3455-3462.
108. Brown, S., N. Hu, and J.C.-G. Hombría, *Identification of the first invertebrate interleukin JAK/STAT receptor, the Drosophila gene domeless.* Current Biology, 2001. **11**(21): p. 1700-1705.
109. Brown, S., N. Hu, and J.C.-G. Hombría, *Novel level of signalling control in the JAK/STAT pathway revealed by in situ visualisation of protein-protein interaction during Drosophila development.* 2003.
110. Chen, H.-W., et al., *mom identifies a receptor for the Drosophila JAK/STAT signal transduction pathway and encodes a protein distantly related to the mammalian cytokine receptor family.* Genes & development, 2002. **16**(3): p. 388-398.
111. Binari, R. and N. Perrimon, *Stripe-specific regulation of pair-rule genes by hopscotch, a putative Jak family tyrosine kinase in Drosophila.* Genes & development, 1994. **8**(3): p. 300-312.
112. Hou, X.S., M.B. Melnick, and N. Perrimon, *Marelle acts downstream of the Drosophila HOP/JAK kinase and encodes a protein similar to the mammalian STATs.* Cell, 1996. **84**(3): p. 411-419.
113. Yan, R., et al., *Identification of a Stat gene that functions in Drosophila development.* Cell, 1996. **84**(3): p. 421-430.
114. Al Outa, A., et al., *Validation of a Drosophila model of wild-type and T315I mutated BCR-ABL1 in chronic myeloid leukemia: an effective platform for treatment screening.* haematologica, 2020. **105**(2): p. 387.
115. Bernardoni, R., et al., *A new BCR-ABL1 Drosophila model as a powerful tool to elucidate the pathogenesis and progression of chronic myeloid leukemia.* haematologica, 2019. **104**(4): p. 717.
116. Fogerty, F., et al., *Dominant effects of the bcr-abl oncogene on Drosophila morphogenesis.* Oncogene, 1999. **18**(1): p. 219-232.
117. Lo Iacono, M., et al., *Genetic screening for potential new targets in chronic myeloid leukemia based on drosophila transgenic for human BCR-ABL1.* Cancers, 2021. **13**(2): p. 293.
118. Messa, F., et al., *Drosophila melanogaster (Dm): a promising genetic tool for identification of candidate genes and pathways involved in CML progression and drug testing.* Cancer Research, 2008. **68**(9_Supplement): p. 391-391.

119. Stevens, T.L., et al., *Using Bcr-Abl to examine mechanisms by which abl kinase regulates morphogenesis in Drosophila.* Molecular biology of the cell, 2008. **19**(1): p. 378-393.
120. Jabbour, E. and H. Kantarjian, *Chronic myeloid leukemia: 2018 update on diagnosis, therapy and monitoring.* American journal of hematology, 2018. **93**(3): p. 442-459.
121. Nowell, P.C. and D.A. Hungerford, *Chromosome studies on normal and leukemic human leukocytes.* Journal of the National Cancer Institute, 1960. **25**(1): p. 85-109.
122. Rowley, J.D., *A new consistent chromosomal abnormality in chronic myelogenous leukaemia identified by quinacrine fluorescence and Giemsa staining.* Nature, 1973. **243**(5405): p. 290-293.
123. Lugo, T.G., et al., *Tyrosine kinase activity and transformation potency of bcr-abl oncogene products.* Science, 1990. **247**(4946): p. 1079-1082.
124. Hochhaus, A., et al., *Dasatinib induces durable cytogenetic responses in patients with chronic myelogenous leukemia in chronic phase with resistance or intolerance to imatinib.* Leukemia, 2008. **22**(6): p. 1200-1206.
125. Barouch-Bentov, R. and K. Sauer, *Mechanisms of drug resistance in kinases.* Expert opinion on investigational drugs, 2011. **20**(2): p. 153-208.
126. Chan, W.W., et al., *Conformational control inhibition of the BCR-ABL1 tyrosine kinase, including the gatekeeper T315I mutant, by the switch-control inhibitor DCC-2036.* Cancer cell, 2011. **19**(4): p. 556-568.
127. Tanaka, R., et al., *Activity of the multitargeted kinase inhibitor, AT9283, in imatinib-resistant BCR-ABL–positive leukemic cells.* Blood, The Journal of the American Society of Hematology, 2010. **116**(12): p. 2089-2095.
128. Miller, G.D., B.J. Bruno, and C.S. Lim, *Resistant mutations in CML and Ph+ ALL–role of ponatinib.* Biologics: targets & therapy, 2014. **8**: p. 243.
129. Klein, J., *Homology between immune responses in vertebrates and invertebrates: does it exist?* Scandinavian journal of immunology, 1997. **46**(6): p. 558-564.
130. Bashaw, G.J., et al., *Repulsive axon guidance: Abelson and Enabled play opposing roles downstream of the roundabout receptor.* Cell, 2000. **101**(7): p. 703-715.
131. Lanot, R., et al., *Postembryonic Hematopoiesis in Drosophila, De velop*. 2001, Biol.
132. SHRESTHA, R. and E. GATEFF, *Ultrastructure and Cytochemistry of the Cell Types in the Larval Hematopoietic Organs and Hemolymph of Drosophila Melanogaster: (drosophila/hematopoiesis/blool cells/ultrastructure/cytochemistry).* Development, Growth & Differentiation, 1982. **24**(1): p. 65-82.
133. Franc, N.C., et al., *Croquemort, a novel Drosophila hemocyte/macrophage receptor that recognizes apoptotic cells.* Immunity, 1996. **4**(5): p. 431-443.
134. Rizki, T., R.M. Rizki, and E. Grell, *A mutant affecting the crystal cells inDrosophila melanogaster.* Wilhelm Roux's archives of developmental biology, 1980. **188**(2): p. 91-99.
135. Lemaitre, B., J.-M. Reichhart, and J.A. Hoffmann, *Drosophila host defense: differential induction of antimicrobial peptide genes after infection by various*

classes of microorganisms. Proceedings of the National Academy of Sciences, 1997. **94**(26): p. 14614-14619.
136. Evans, C.J., T. Liu, and U. Banerjee, *Drosophila hematopoiesis: markers and methods for molecular genetic analysis.* Methods, 2014. **68**(1): p. 242-251.
137. Anderl, I., et al., *Transdifferentiation and proliferation in two distinct hemocyte lineages in Drosophila melanogaster larvae after wasp infection.* PLoS pathogens, 2016. **12**(7): p. e1005746.
138. Livak, K.J. and T.D. Schmittgen, *Analysis of relative gene expression data using real-time quantitative PCR and the 2− ΔΔCT method.* methods, 2001. **25**(4): p. 402-408.
139. Sinenko, S.A. and B. Mathey-Prevot, *Increased expression of Drosophila tetraspanin, Tsp68C, suppresses the abnormal proliferation of ytr-deficient and Ras/Raf-activated hemocytes.* Oncogene, 2004. **23**(56): p. 9120-9128.
140. Márkus, R., et al., *Sessile hemocytes as a hematopoietic compartment in Drosophila melanogaster.* Proceedings of the National Academy of Sciences, 2009. **106**(12): p. 4805-4809.
141. Zettervall, C.-J., et al., *A directed screen for genes involved in Drosophila blood cell activation.* Proceedings of the National Academy of Sciences, 2004. **101**(39): p. 14192-14197.
142. Baril, C., et al., *Human NUP98-HOXA9 promotes hyperplastic growth of hematopoietic tissues in Drosophila.* Developmental biology, 2017. **421**(1): p. 16-26.
143. Moreira, C.G., A. Jacinto, and S. Prag, *Drosophila integrin adhesion complexes are essential for hemocyte migration in vivo.* Biology open, 2013. **2**(8): p. 795-801.
144. Qiu, P., P.C. Pan, and S. Govind, *A role for the Drosophila Toll/Cactus pathway in larval hematopoiesis.* Development, 1998. **125**(10): p. 1909-1920.
145. Hoffmann, J.A., *The immune response of Drosophila.* Nature, 2003. **426**(6962): p. 33-38.
146. Hultmark, D., *Drosophila immunity: paths and patterns.* Current opinion in immunology, 2003. **15**(1): p. 12-19.
147. Graveley, B.R., et al., *The developmental transcriptome of Drosophila melanogaster.* Nature, 2011. **471**(7339): p. 473-479.
148. Ekengren, S. and D. Hultmark, *A family of Turandot-related genes in the humoral stress response of Drosophila.* Biochemical and biophysical research communications, 2001. **284**(4): p. 998-1003.
149. Ekengren, S., et al., *A humoral stress response in Drosophila.* Current biology, 2001. **11**(9): p. 714-718.
150. Warsch, W., C. Walz, and V. Sexl, *JAK of all trades: JAK2-STAT5 as novel therapeutic targets in BCR-ABL1+ chronic myeloid leukemia.* Blood, The Journal of the American Society of Hematology, 2013. **122**(13): p. 2167-2175.
151. Patel, A.B., T. O'Hare, and M.W. Deininger, *Mechanisms of resistance to ABL kinase inhibition in chronic myeloid leukemia and the development of next generation ABL kinase inhibitors.* Hematology/Oncology Clinics, 2017. **31**(4): p. 589-612.
152. Kim, L.K., et al., *Down-regulation of NF-κB target genes by the AP-1 and STAT complex during the innate immune response in Drosophila.* PLoS biology, 2007. **5**(9): p. e238.

153. Cortes, J., C. Pavlovsky, and S. Saußele, *Chronic myeloid leukaemia.* The Lancet, 2021. **398**(10314): p. 1914-1926.
154. Sasaki, K., et al., *Relative survival in patients with chronic-phase chronic myeloid leukaemia in the tyrosine-kinase inhibitor era: analysis of patient data from six prospective clinical trials.* The Lancet Haematology, 2015. **2**(5): p. e186-e193.
155. Bower, H., et al., *Life expectancy of patients with chronic myeloid leukemia approaches the life expectancy of the general population.* 2016.
156. Abubaker, D., et al., *Expression of chronic myeloid leukemia oncogenes BCR-ABL P210 and BCR-ABL T315I affect cellular and humoral innate immunity in Drosophila melanogaster.* Micropublication Biology, 2022. **2022**.
157. *FastQC*. 2015.
158. Kim, D., et al., *Graph-based genome alignment and genotyping with HISAT2 and HISAT-genotype.* Nature biotechnology, 2019. **37**(8): p. 907-915.
159. Danecek, P., et al., *Twelve years of SAMtools and BCFtools.* Gigascience, 2021. **10**(2): p. giab008.
160. Liao, Y., G.K. Smyth, and W. Shi, *featureCounts: an efficient general purpose program for assigning sequence reads to genomic features.* Bioinformatics, 2014. **30**(7): p. 923-930.
161. Love, M.I., W. Huber, and S. Anders, *Moderated estimation of fold change and dispersion for RNA-seq data with DESeq2.* Genome biology, 2014. **15**(12): p. 1-21.
162. Ulgen, E., O. Ozisik, and O.U. Sezerman, *pathfindR: an R package for comprehensive identification of enriched pathways in omics data through active subnetworks.* Frontiers in genetics, 2019. **10**: p. 858.
163. Youn, M., et al., *Comparison of the transcriptomic signatures in pediatric and adult CML.* Cancers, 2021. **13**(24): p. 6263.
164. Huang, C.Y., et al., *Targeting Reductive Metabolic Shifts by T315I Mutation in BCR-ABL Myeloid Leukemia for Therapy.* bioRxiv, 2022.
165. Qiu, T., et al., *Rap1GAP alters leukemia cell differentiation, apoptosis and invasion in vitro.* Oncology reports, 2012. **28**(2): p. 622-628.
166. Han, L., et al., *Protein binding and signaling properties of RIN1 suggest a unique effector function.* Proceedings of the National Academy of Sciences, 1997. **94**(10): p. 4954-4959.
167. De Luca, M., et al., *Association of a common LAMA5 variant with anthropometric and metabolic traits in an Italian cohort of healthy elderly subjects.* Experimental gerontology, 2011. **46**(1): p. 60-64.
168. Conrad, C., et al., *ADAM8 in invasive cancers: links to tumor progression, metastasis, and chemoresistance.* Clinical Science, 2019. **133**(1): p. 83-99.
169. Sumei, S., et al., *Hypermethylation of DHRS3 as a Novel Tumor Suppressor Involved in Tumor Growth and Prognosis in Gastric Cancer.* Frontiers in Cell and Developmental Biology, 2021. **9**: p. 624871.
170. Huang, X., et al., *An overview of the cytoskeleton-associated role of PDLIM5.* Frontiers in Physiology, 2020. **11**: p. 975.
171. Drysdale, R. and F. Consortium, *FlyBase.* Drosophila, 2008: p. 45-59.
172. Chen, F., et al., *Biological characterization of Drosophila Rapgap1, a GTPase activating protein for Rap1.* Proceedings of the National Academy of Sciences, 1997. **94**(23): p. 12485-12490.

173. Yang, Y., et al., *Low expression of Rap1GAP is associated with epithelial-mesenchymal transition (EMT) and poor prognosis in gastric cancer.* Oncotarget, 2017. **8**(5): p. 8057.
174. Wang, Y.-C., Z. Khan, and E.F. Wieschaus, *Distinct Rap1 activity states control the extent of epithelial invagination via α-catenin.* Developmental cell, 2013. **25**(3): p. 299-309.
175. Mitra, R.S., et al., *Rap1GAP promotes invasion via induction of matrix metalloproteinase 9 secretion, which is associated with poor survival in low N-stage squamous cell carcinoma.* Cancer research, 2008. **68**(10): p. 3959-3969.
176. Looi, C.-K., et al., *The role of Ras-associated protein 1 (Rap1) in cancer: Bad actor or good player?* Biomedicines, 2020. **8**(9): p. 334.
177. Mutvei, A.P., et al., *Rap1-GTPases control mTORC1 activity by coordinating lysosome organization with amino acid availability.* Nature communications, 2020. **11**(1): p. 1-13.
178. Goldsmith, J., B. Levine, and J. Debnath, *Autophagy and cancer metabolism.* Methods in enzymology, 2014. **542**: p. 25-57.
179. *Alliance of Genome Resources Portal: unified model organism research platform.* Nucleic acids research, 2020. **48**(D1): p. D650-D658.
180. Adams, M.K., et al., *The retinaldehyde reductase activity of DHRS3 is reciprocally activated by retinol dehydrogenase 10 to control retinoid homeostasis.* Journal of Biological Chemistry, 2014. **289**(21): p. 14868-14880.
181. Altucci, L., et al., *Retinoic acid-induced apoptosis in leukemia cells is mediated by paracrine action of tumor-selective death ligand TRAIL.* Nature medicine, 2001. **7**(6): p. 680-686.
182. Lou, S., et al., *Inhibition of retinoic acid receptor α phosphorylation represses the progression of triple-negative breast cancer via transactivating miR-3074-5p to target DHRS3.* Journal of Experimental & Clinical Cancer Research, 2021. **40**(1): p. 1-15.
183. Passon, N., et al., *Somatic amplifications and deletions in genome of papillary thyroid carcinomas.* Endocrine, 2015. **50**(2): p. 453-464.
184. Oler, G., et al., *Gene expression profiling of papillary thyroid carcinoma identifies transcripts correlated with BRAF mutational status and lymph node metastasis.* Clinical Cancer Research, 2008. **14**(15): p. 4735-4742.
185. Meyer, H., et al., *The disintegrin and metalloprotease Meltrin from Drosophila forms oligomers via its protein binding domain and is regulated by the homeobox protein VND during embryonic development.* Insect biochemistry and molecular biology, 2010. **40**(11): p. 814-823.
186. Mochizuki, S. and Y. Okada, *ADAMs in cancer cell proliferation and progression.* Cancer science, 2007. **98**(5): p. 621-628.
187. Miyauchi, M., et al., *ADAM8 is an antigen of tyrosine kinase inhibitor-resistant chronic myeloid leukemia cells identified by patient-derived induced pluripotent stem cells.* Stem cell reports, 2018. **10**(3): p. 1115-1130.
188. Li, L., et al., *Ibrutinib reverses IL-6-induced osimertinib resistance through inhibition of Laminin α5/FAK signaling.* Communications biology, 2022. **5**(1): p. 1-14.
189. Gordon-Weeks, A., et al., *Tumour-derived laminin α5 (LAMA5) promotes colorectal liver metastasis growth, branching angiogenesis and notch pathway inhibition.* Cancers, 2019. **11**(5): p. 630.

190. Szabó, K., G. Jékely, and P. Rørth, *Cloning and expression of sprint, a Drosophila homologue of RIN1.* Mechanisms of development, 2001. **101**(1-2): p. 259-262.
191. Thai, M., et al., *ABL fusion oncogene transformation and inhibitor sensitivity are mediated by the cellular regulator RIN1.* Leukemia, 2011. **25**(2): p. 290-300.
192. Afar, D.E., et al., *Regulation of the oncogenic activity of BCR-ABL by a tightly bound substrate protein RIN1.* Immunity, 1997. **6**(6): p. 773-782.
193. Liao, K.A., N. González-Morales, and F. Schöck, *Zasp52, a core Z-disc protein in Drosophila indirect flight muscles, interacts with α-actinin via an extended PDZ domain.* PLoS genetics, 2016. **12**(10): p. e1006400.
194. Liu, X., et al., *High expression of PDLIM5 facilitates cell tumorigenesis and migration by maintaining AMPK activation in prostate cancer.* Oncotarget, 2017. **8**(58): p. 98117.
195. Schlomann, U., et al., *Metalloprotease inhibitor profiles of human ADAM8 in vitro and in cell-based assays.* Biological Chemistry, 2019. **400**(6): p. 801-810.